Commission of the European Communities

NEA/NSC/DOC (94) 22
INDC (EUR) 028/G

JOINT
RESEARCH
CENTRE

ANNUAL PROGRESS REPORT ON NUCLEAR DATA 1993

INSTITUTE FOR REFERENCE MATERIALS AND MEASUREMENTS

GEEL (BELGIUM)

June 1994
EUR 15822 EN

Commission of the European Communities

NEA/NSC/DOC (94) 22

INDC (EUR) 028/G

JOINT
RESEARCH
CENTRE

ANNUAL PROGRESS REPORT ON NUCLEAR DATA 1993

INSTITUTE FOR REFERENCE MATERIALS AND MEASUREMENTS

GEEL (BELGIUM)

June 1994
EUR 15822 EN

ISBN 92-826-8432-6

CATALOGUE N° : GBNA15822ENC

TABLE OF CONTENTS

Note: For further information concerning the Project Nuclear Measurements (Nuclear Data, Nuclear Metrology), please contact A.J. Deruytter, Project Manager, IRMM, Retieseweg, B-2440 Geel, Belgium

Editor: H.H. Hansen

EXECUTIVE SUMMARY

A.J. Deruytter

In 1993, work was continued along main objectives of the project "Nuclear Measurements" in the subprojects "Nuclear Data" and "Nuclear Metrology": to improve the neutron standards data set, relative to which partial cross-sections or other quantities, important for fission and fusion technology, are determined; to study radionuclide decay data for standards applications; to develop nuclear measurement techniques for nuclear and non-nuclear applications.

The efforts for the improvement of the set of **standard neutron cross-sections** and for other quantities selected within the INDC/NEANDC Standards File continued. Work continued on octacosanol samples as hydrogeneous layers for standard cross-section ratio measurements of $^{235}U(n,f)/H(n,n)$ with Frisch gridded ionization chambers. Measurements of mass-energy-and angular distributions of fission fragments in neutron induced fission of ^{237}Np were finalized. Total cross-section measurements have been done in the framework of the NEA-NSC Collaboration on the $^{10}B(n,\alpha)$ Standard Cross Section in order to extend the energy range where this cross-section can be used as a standard.

Requests from the nuclear science community became more and more demanding and followed from deficiencies in available experimental data sets, which were detected by careful evaluation efforts in the framework of the International Evaluation Cooperation (IEC) of the NEA Nuclear Science Committee (NEA-NSC). The requests are summarized in the NEA High Priority Request List.

In the activity on **nuclear data for fission technology** very high resolution measurements were done of the total cross-section of natural iron in the neutron energy range between 0.2 and 20 MeV. In particular attention was given to the lower MeV region. Also a new type of measurements was started with the determination of the gamma-ray emission cross-sections of low-lying levels of palladium isotopes for neutron energies between 0.2 and 3.3 MeV, with the aim to obtain more precise data on the inelastic scattering cross-section for weakly absorbing fission product nuclides.

In the field of **nuclear data for fusion technology** the double differential cross-section ratio of ^{58}Ni (n,xα) to ^{27}Al(n,xα) was measured at 6.5, 8.0, 9.0 and 15.6 MeV. Deduced total alpha particle yields of the ^{58}Ni(n,xα) are compared with recent evaluations. Total neutron cross sections were measured for ^{27}Al in the range 175 keV to 25 MeV and total neutron cross-section measurements of vanadium in the same energy region were started. Vanadium is a possible candidate for the blanket material in fusion reactors and is being considered by the Engineering Design Activities of ITER.

More basic measurements linked to our nuclear data programme were performed, mainly for PhD research and using GELINA as a high resolution neutron spectrometer unique in Europe. They concern: spin assignments of ^{238}U and ^{113}Cd p-wave resonances as a contribution to parity non-conservation (PNC) studies performed at Los Alamos in the frame of the TRIPLE Collaboration; measurements of (n, charged particle) reactions on chlorine and of high resolution $^{138}Ba(n,\gamma)$ cross-sections, for their key-role in astrophysical applications.

In **radionuclide metrology** highlights were (1) the thorough study of the energy resolution of silicon detectors to alpha particles, and the measurement of the Fano factor for silicon detectors using electrons, and (2) the extreme background reduction for a low-level HP Ge detection system by working in an underground facility at SCK/CEN, Mol, Belgium, at a depth at about 225 m, corresponding to 500 m water equivalent.

The major facilities of IRMM, the Geel linear electron accelerator GELINA and the 7 MV Van de Graaff accelerator were fully operational. They were used for neutron data measurements and in the non-nuclear applications. In 1993 the refurbishment plan for GELINA remained on schedule.

At the 7 MV Van de Graaff accelerator the Nuclear Reaction Analysis (NRA) technique for the determination of light elements (boron, carbon, nitrogen, oxygen) concentrations in advanced materials continued in the frame of a HCM Network, and the Charged Particle Activation Analysis (CPAA) technique has been installed and tested.

In the frame of the radiation physics research, experiments were successfully performed at GELINA on the generation of Smith-Purcell (SP) radiation at optical wavelengths, when ultrarelativistic electrons (35 to 110 MeV) travel close to a metallic grating.

NUCLEAR DATA

NUCLEAR DATA FOR STANDARDS

The objective of the work on standard nuclear data is to improve the set of neutron data to be used in measurements consistency checks. Competing reactions, angular and kinetic energy distributions of the reaction products have to be studied to increase the reliability of the given standard cross sections. Appropriate research topics are selected from listings of the INDC/NEANDC Standards File. Complementary work is pertinent to radionuclide decay data and associated atomic data requested for calibration and reference purposes.

Neutron Data for Standards

Standard Cross Section Ratio $^{235}U(n,f)/H(n,n)$

F.-J. Hambsch, R. Vogt

Due to the importance of the investigation whether a new sample material, with a reasonably high hydrogen content, namely octacosanol, would fulfil the requirements of a precise cross section ratio determination, all the previously mentioned measurements have been repeated[1]. This was done with a careful check of the counting gas quality and the quality of the neutron producing target. Only certified gas with N50-quality 95 % Ar + 5 % CO_2 together with a new TiT-target for neutron production have been used. Not only the quality of the gas mixture is important, but also the freshness of the gas inside the ionization chamber. To assure the latter, the chamber was always rinsed after longer interruptions of the measurements and after sample changes. In addition to that not only the different octacosanol samples have been measured, but also the tristearin samples used in the previous investigation[2]. Measurements at incident neutron energies ranging from 0.3 to 2 MeV have been performed for six different octacosanol samples and four different tristearin samples.

The resulting proton recoil spectra do not show any more the aspects reported previously[1]. Now spectra for e.g. octacosanol of 136 µg/cm^2 and 137 µg/cm^2 are found to be comparable at the high energy end (Fig. 1, left). Also the comparison of octacosanol (137 µg/cm^2) and tristearin (148 µg/cm^2) (Fig. 1, right) shows within

---

(1) CBNM Annual Progress Report on Nuclear Data (1992), EUR 15155 EN

(2) H.H. Knitter, C. Budtz-Jørgensen and H. Bax, Proc. Advisory Group Meeting on Nuclear Standard Reference Data, IAEA TECDOC 335 (1985)

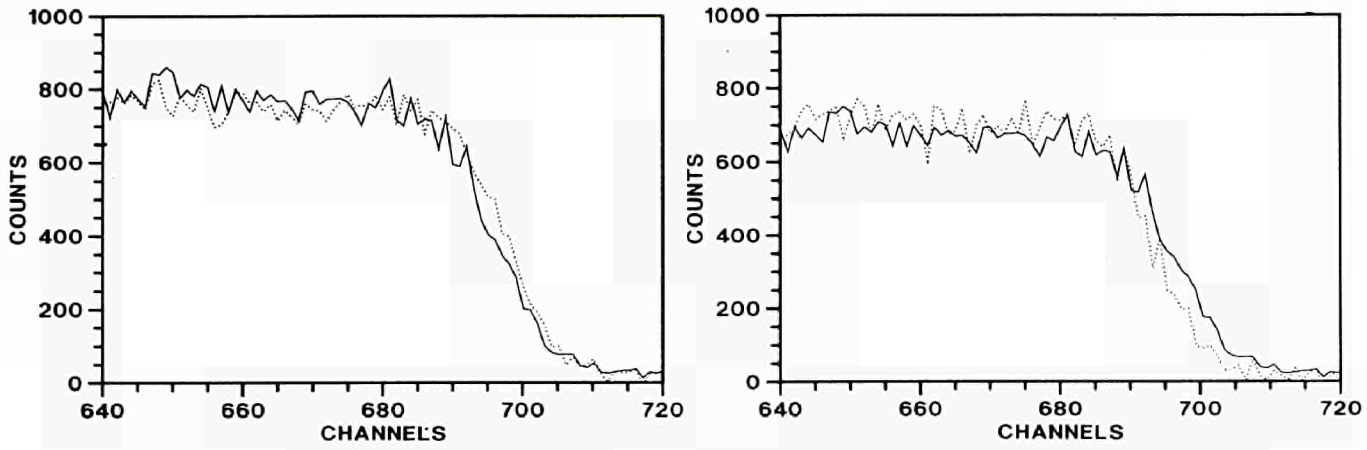

Fig. 1. *Comparison of the proton recoil spectra for about 2 MeV incident neutron energy and octacosanol sample thicknesses of 137 µg/cm^2 (solid line) and 136 µg/cm^2 (dotted line) (left part) and octacosanol sample of 137 µg/cm^2 (solid line) and tristearin sample of 148 µg/cm2 (dotted line) (right part)*

one channel the same spectrum, which is expected from energy loss calculations, based on data of Ziegler et al.[1]. From the determination of the end points of the proton recoil spectra (at half height of the spectra) it is possible to determine the stopping power and compare it to literature values. These endpoints as a function of the sample thickness are shown in Fig. 2 for octacosanol (left part) and tristearin (right part) at the incident neutron energy of about 2 MeV. It is evident that the endpoints are better approximated by a straight line for tristearin than for octacosanol. This is found also at other energies, especially the point for the thickest octacosanol sample was always off the line. From the fitted slopes some differences have been found in the stopping power as compared to the Ziegler

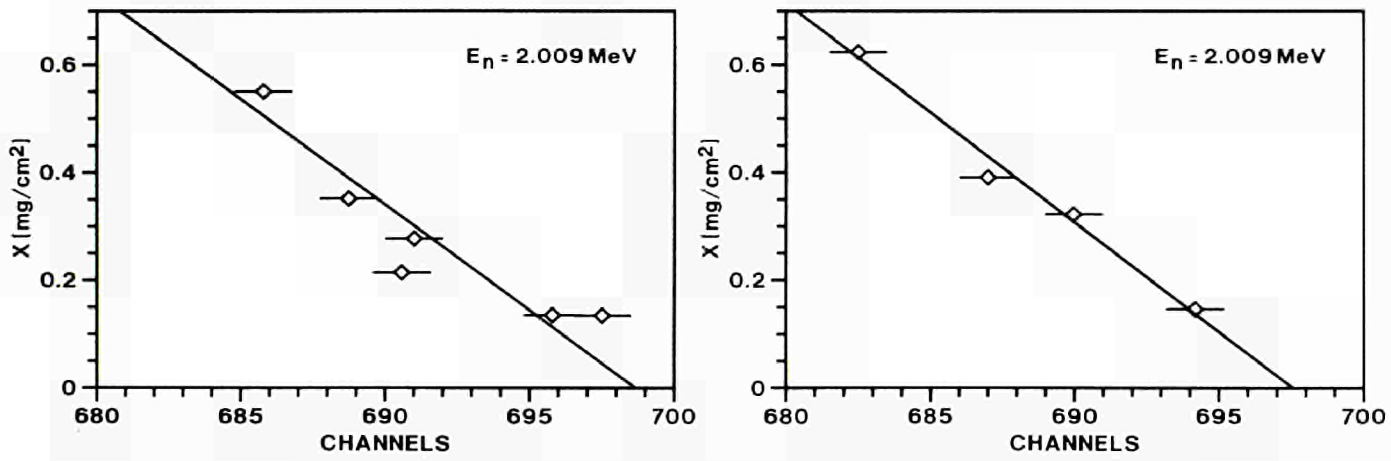

Fig. 2. *Sample thickness versus channel number at half height of the proton recoil distribution, left part: octacosanol, right part: tristearin. Straight line fit to get the stopping power at about 2 MeV incident neutron energy*

(1) J.F. Ziegler et al., The stopping and range of ions in solids, Pergamon Press, New York (1985)

data[1] (Fig. 3). However, in view of the straggling of the experimental points, the agreement is quite good. The proton recoil spectra have been compared with Monte-Carlo calculations, taking into account the TiT target thickness, the neutron emission kinematics, the n-p scattering law, the stopping power for the samples and the electronic resolution. In Fig. 4 this comparison is shown, for the thinnest and thickest octacosanol and tristearin samples, respectively. It is evident that in three of the four cases a surplus of the experimental spectra compared to the Monte-Carlo simulation is found. In the fourth case the difference is not so evident. This was the tristeorin target for which the previous investigation[2] had resulted in a significant difference between Monte-Carlo simulation and experiment. Thus, the previous conclusion[2], that the homogeneity of the sample was not good enough can no longer be maintained. Reasons may be found in the experimental procedure.

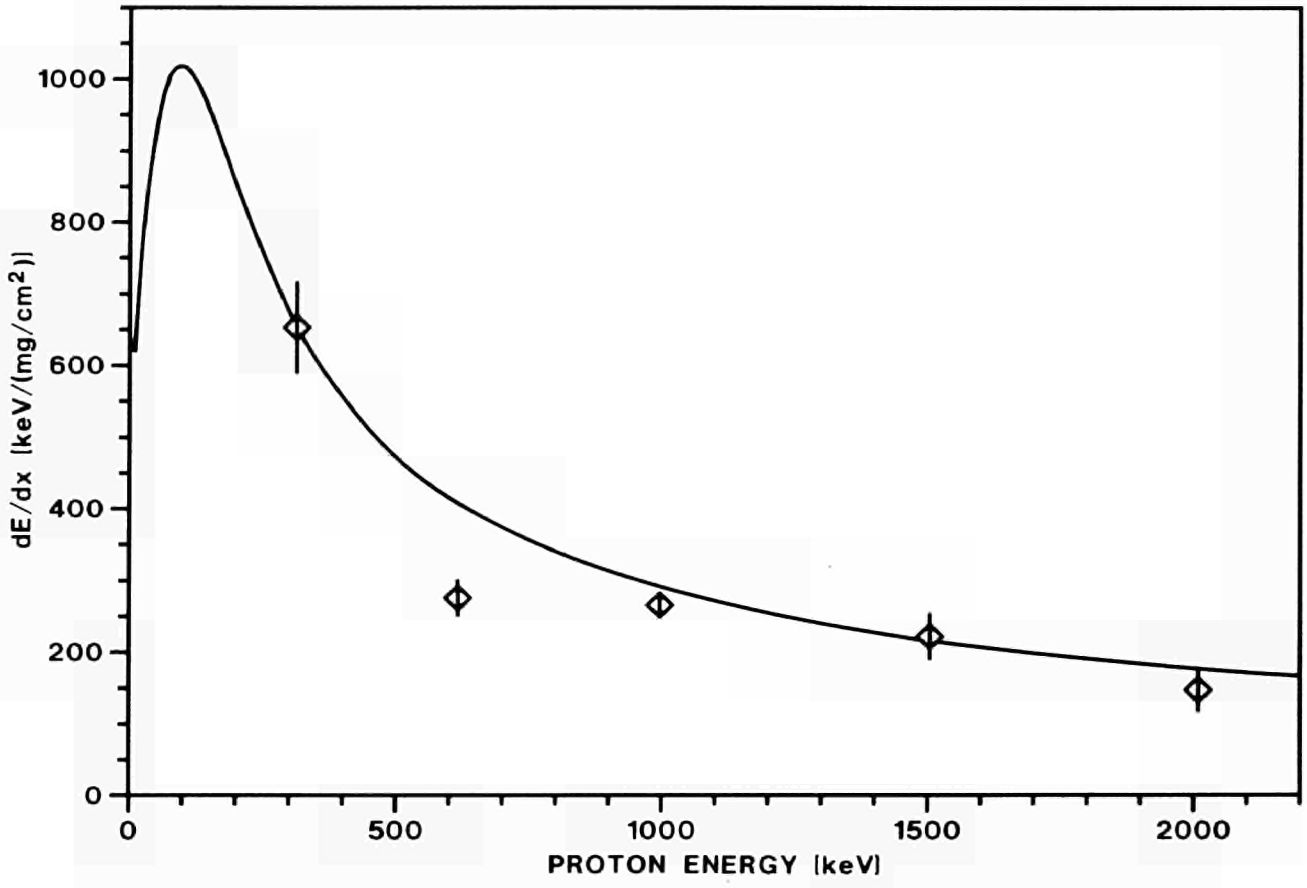

Fig. 3. Stopping power values.of ref. (1) (solid line) compared to the measured ones of octacosanol

(1) J.F. Ziegler et al., The stopping and range of ions in solids, Pergamon Press, New York (1985)

(2) H.H. Knitter, C. Budtz-Jorgensen and H. Bax, Proc. Advisory Group Meeting on Nuclear Standard Reference Data, IAEA TECDOC335 (1985)

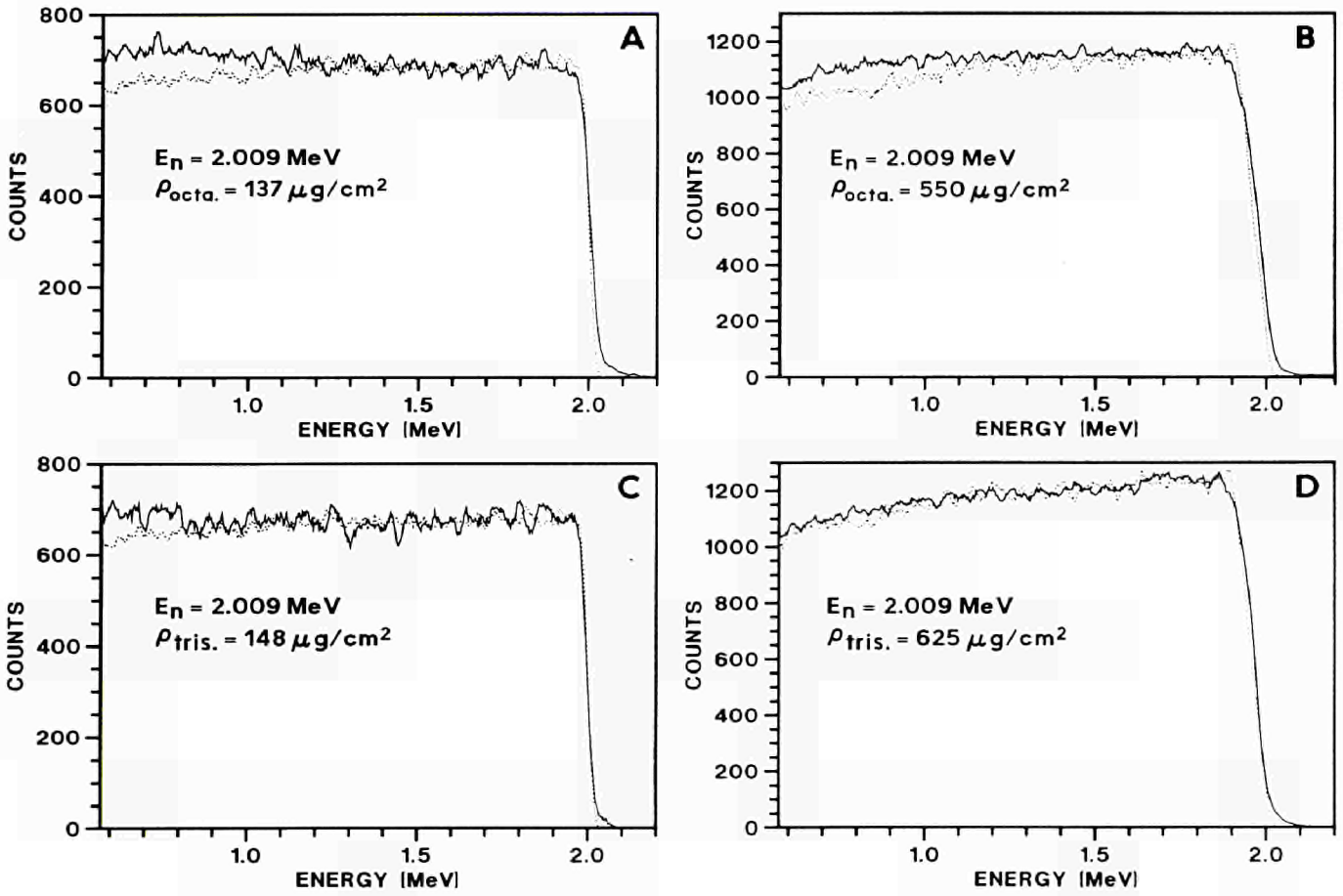

Fig. 4. ***Comparison of the proton recoil spectra calculated with the Monte-Carlo method (dotted line) and the experiment (solid line): (A) thinnest octacosanol sample, (B) thickest octacosanol sample, (C) thinnest tristearin sample and (D) thickest tristearin sample, all at about 2 MeV incident neutron energy***

Improving the Knowledge about the $^{252}Cf(sf)$ Standard; Peculiarities Found by using Different Counting Gases

F.-J. Hambsch, J. van Aarle and R. Vogt

Recent measurements of the spontaneous fission of ^{252}Cf using a twin ionization chamber with Frisch grids and methane as counting gas, revealed inconsist encies in the determination of the absolute energy scale. At the pressure of $0.6 \cdot 10^5$ Pa, used in the measurements, it is very difficult to make an absolute energy calibration with the α-activity of the ^{252}Cf sample. This is due to the fact that the α-particles are not stopped within the active counter volume between cathode and grid. Another point, which still is unclear, is the correction of the pulse height defect. It is claimed that in methane the pulse height defect is negligible[1]. However, without any pulse height defect corrections the fission fragment mass distribution calculated from the measured data yields masses

(1) G. Simon, J. Trochon, F. Brisard and C. Signarbieux, Nucl. Inst. Methods A286 (1990) 220

around 107 and 145 and widths σ_A of about 7.5. Compared to literature values[1] these results are too asymmetric and too broad, respectively.

Measurements have been repeated with the counting gas 90 % Ar + 10 % CH_4, using the same setup and the same pressure of $0.6 \cdot 10^5$ Pa. The pulse height in 90 % Ar + 10 % CH_4 is larger by about 15 % than in pure methane. Other measurements were done with the same setup and both counting gases at an increased pressure of $1.2 \cdot 10^5$ Pa. In these cases it is assured that the α-particles are stopped in the active counting volume between cathode and grid. For 90 % Ar + 10 % CH_4 only a very small decrease in pulse height was observed at the higher pressure, whereas, for methane again a drastic pressure dependency of the pulse height is observed (Fig. 5).

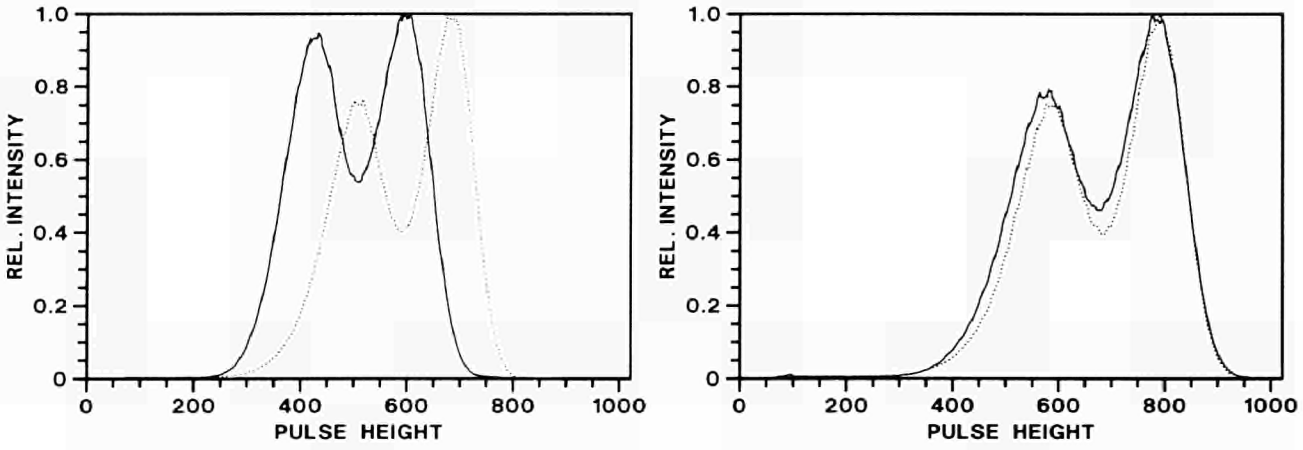

Fig. 5. ***Comparison of raw spectra measured at different pressure. Left part: methane $1.2 \cdot 10^5$ Pa (solid line), $0.6 \cdot 10^5$ Pa (dotted line) and right part: 90 % Ar + 10 % CH_4 $1.2 \cdot 10^5$ Pa (solid line), $0.6 \cdot 10^5$ Pa (dotted line)***

Further analysis of the raw spectra, taking into account the energy calibration, electronic instability, calculation of angular distribution and finally the correction for energy loss as function of angle revealed another peculiarity. Also the energy loss correction as function of angle was different for the different gases and pressures. For 90 % Ar + 10 % CH_4, the slope changed between $0.6 \cdot 10^5$ Pa and $1.2 \cdot 10^5$ Pa, pretending a thicker target at higher pressure. For methane this effect was even worse, making it impossible to find a good energy loss correction for the higher pressure.

The final preneutron mass distributions were calculated using ν-data as function of mass[2]. Introducing the known pulse height defect for 90 % Ar + 10 % CH_4 resulted in a good agreement of the mass distribution parameters (mean mass and variance) with respect to previous results[3]. A difference in the calculated mass

(1) R. Schmidt and H. Henschel, Nucl. Phys. A395 (1983) 15
(2) C. Budtz-Jorgensen and H.-H. Knitter, Nucl. Phys. A490 (1988) 307
(3) R. Schmidt and H. Henschel, Nucl. Phys. A395 (1983) 15

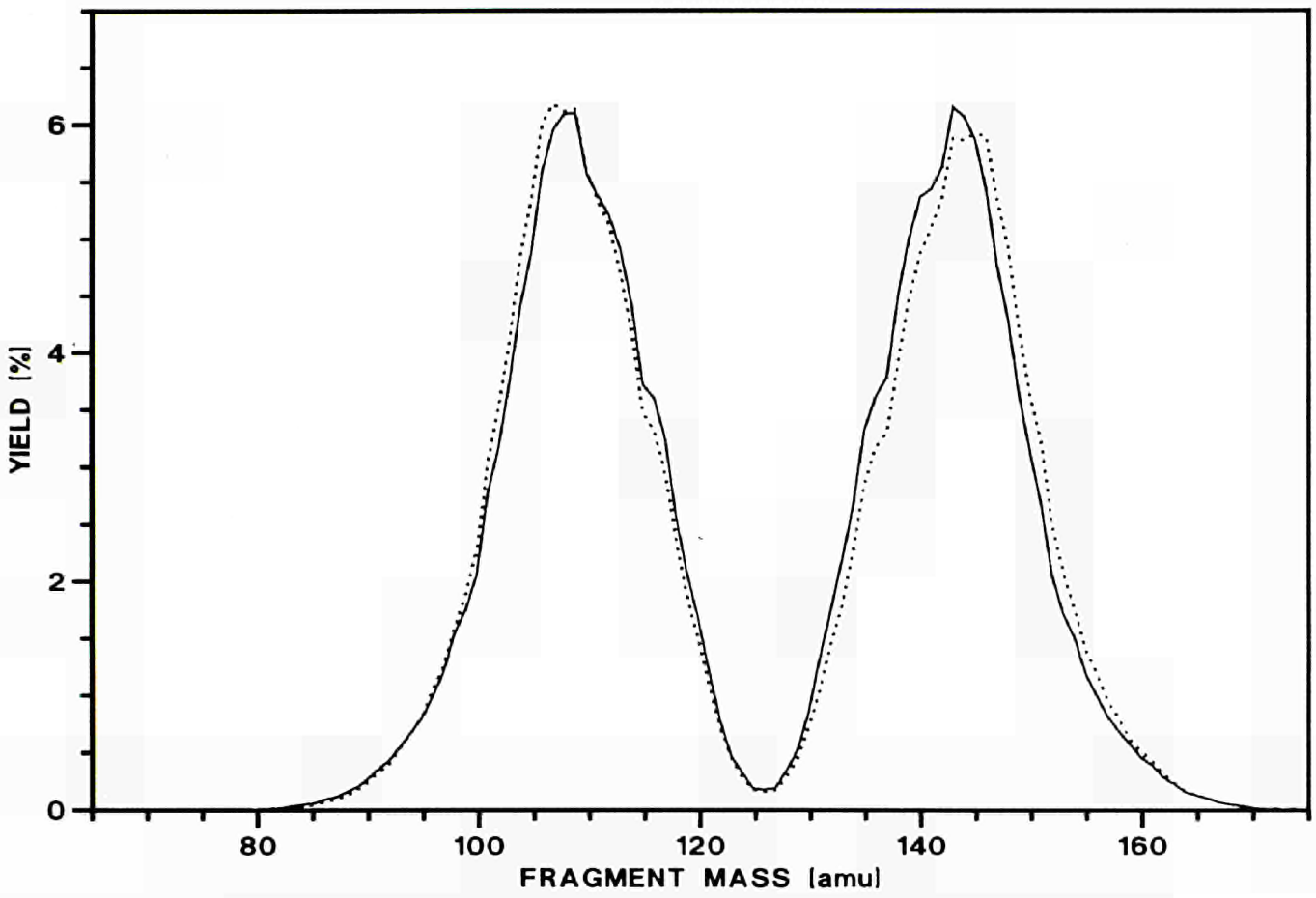

Fig. 6. *Comparison of the preneutron mass distribution for methane at different pressure $1.2 \cdot 10^5$ Pa (dotted line), $0.6 \cdot 10^5$ Pa (solid line)*

distribution has been found comparing those measured with methane at 0.6 and $1.2 \cdot 10^5$ Pa, as shown in Fig. 6. This is most probably due to the changed shape of the raw energy spectra.

At the moment the absolute calibration remains unresolved. In case of 90 % Ar + 10 % CH_4 the total kinetic energy has a value of 180.7 MeV with a probable error in the α-peak position of (1-2) % and for methane 157.5 MeV. The first value is not far of the recommended literature value of (184.1 ± 1.3) MeV[1].

The Total Neutron Cross Section of ^{10}B from 80 eV to 100 keV

A. Brusegan, E. Macavero, C. Van der Vorst

Transmission measurements have been done in the framework of the NEANSC collaboration on the $^{10}B(n,\alpha)$ Standard Cross Sections in order to extend the energy range along which this cross section can be used as a standard. Three well characterized samples of boron carbide enriched to 93.38 % in ^{10}B were available.

(1) C. Budtz-Jorgensen and H.-H. Knitter, Nucl. Phys. A490 (1988) 307

Their thicknesses range from 0.024 up to 0.109 at/barn of ^{10}B, i.e. 0.183 at/barn in total. Samples of carbon and of enriched ^{11}B (> 97 %, boron carbide) have been or will be measured, respectively as a test of the accuracy of the data and in order to correct for the ^{11}B cross section.

The detector, a 0.6 cm thick Li-glass (NE 912), was placed at 50 m flight distance from the neutron source of GELINA, which was running at 800 Hz and with 1 ns electron burst width. The background was determined with the black resonance technique.

Tests with a 0.14 at/barn thick carbon sample show that its transmission could be measured within 0.5 % below 5 keV and within 2.5 % up to 100 keV.

These larger spreads at the high energy seem to arise from dead time effects and from the collimation. In the new series of measurement the dead time has been reduced from 2.4 μs to 0.8 μs and the collimation has been improved.

NUCLEAR DATA FOR FISSION TECHNOLOGY

The objective of the work on nuclear data for fission technology is to reach a more accurate knowledge of data requested in fission research and in fission technology. Measurements cover actinide fission cross section data as well as structural material neutron interaction data. Research topics are taken to fulfil European demands collected in the NEA High Priority Request List.

Neutron Data of Actinides

Search for the Fission Modes in ^{252}Cf

J. van Aarle*, F.-J. Hambsch

In addition to the search for fission modes of the compound nucleus ^{238}Np, the same calculations based on the multi-modal random neck-rupture model of Brosa, Grossmann and Müller[1] have been started also for ^{252}Cf. From an experimental point of view there is evidence that the mass distribution can only be fitted reasonably if at least three Gaussian distributions are taken into account for the asymmetric masses. However, Brosa and coworkers have found only one standard mode which is attributed to the asymmetric masses. In terms of Brosa modes that would mean a splitting of the standard mode into three submodes in case of ^{252}Cf too, as already found for ^{238}Np. The first results are shown in Fig. 7. Indeed a

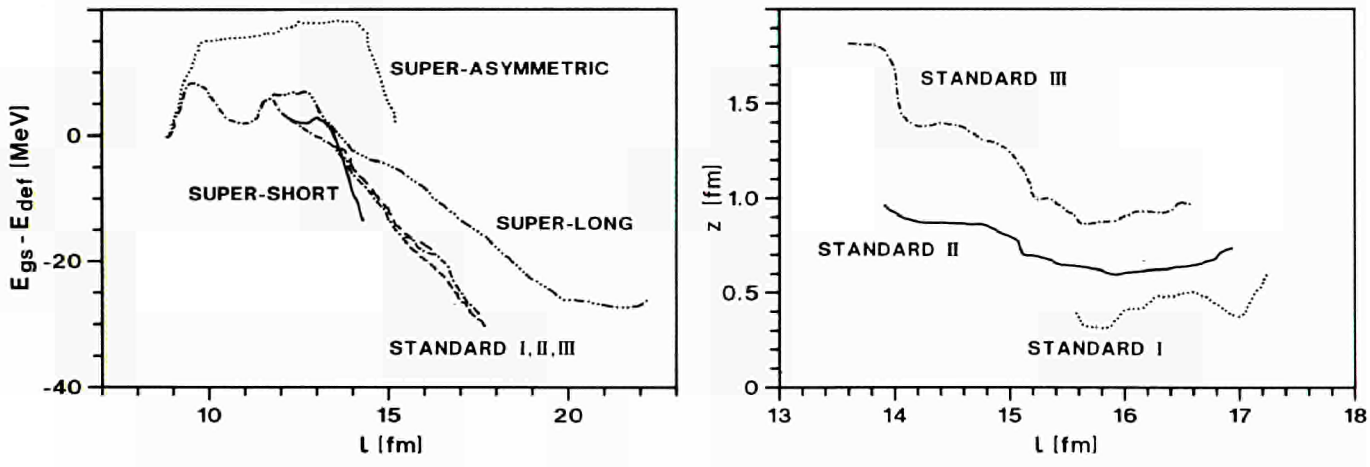

Fig. 7. ***Fission modes in ^{252}Cf. Left part: Potential energy $E_{gs}-E_{def}$ of the deformed nucleus for the different fission modes as function of the elongation parameter l. Right part: Asymmetry parameter z versus elongation parameter l, shown zoomed in l between 13 fm and 18 fm to make the subspliting into the three standard modes better visible***

---

* EC Fellow from University of Marburg, Germany

(1) U. Brosa, S. Grossmann and A. Müller, Phys. Rep. 197 (1990) 167

splitting of the standard mode into the three submodes standard I, II and III has been found, however, they are very much overlapping. Only the asymmetry parameter z (right part of Fig. 14) reveals significant distance between the three submodes and thus, could be used to distinguish between the modes taking into account the known experimental positions of the three Gaussians in the mass distribution. In addition to the three standard modes, the already known super-long, super-short and super-asymmetric modes have been found too. The problem to establish the bifurcation points, however, remains still open.

Neutron Induced Fission of ^{237}Np

P. Siegler*, F.-J. Hambsch, R. Vogt

The fission fragment properties of the reaction $^{237}Np(n,f)$ have been investigated for incident neutron energies from 0.3 MeV up to 5.5 MeV covering the range below and above the fission threshold.
The neutrons were obtained at the 7 MV Van de Graaff accelerator from the $D(d,n)^3He$, $T(p,n)^3He$ and the $^7Li(p,n)^7Be$ reactions.
For the detection of the fission fragments a double Frisch gridded ionization chamber with a 60 µg/cm^2 thick ^{237}Np target was used to measure the mass-, energy- and angular distributions.
For all neutron energies except at 0.3, 0.5 MeV and 0.7 MeV, about $2 \cdot 10^5$ events have been accumulated. The low fission cross-section below the fission threshold at 0.7 MeV was the limiting factor, e.g. at 0.3 MeV only 3600 events in 100 hour beamtime could be registered. For the measurement at 0.3 MeV and 0.5 MeV, thin lithium-metal targets were used to reduce the uncertainty of the neutron energy. The energy spread was 16 keV and therefore small enough to guarantee that the measurement was performed at the correct neutron energy in view of the steep rise of the cross section. For the calibration of the detector system the thermal neutron induced fission of ^{235}U was used.
The ^{235}U-target has had similar dimensions as the ^{237}Np target and all obtained information served as a reference for the analysis of the neptunium experiment. Taking into account a pulse height defect for the Ar-CH_4 counting gas as well as $\upsilon(A,\bar{T}\bar{K}\bar{E})$ values based on data from Wahl et al.[1], the mass and energy distributions have been found in good agreement with previously published data for $^{235}U(n_{th},f)$[2,3].

---

* EC Fellow from Technical University of Darmstadt, Germany

(1) A.C. Wahl et al., Atom. Data Nucl. Data Tab. 39 (1988) 1
(2) F.-J. Hambsch et al., Nucl.Phys. A491 (1989) 56
(3) R. Müller et al., KfK Report 3220 Karlsruhe 1981

The raw data analysis has been finalized. For all measured neutron energies, complete data sets for the mass-, energy- and angular distribution of the fission fragments are available. The experimental data were carefully checked for electronic drifts and corrected for the energy loss in the target, grid inefficiency and pulse-height defect. The impact of the incident neutron on the nucleus as well as the neutron evaporation as function of mass and kinetic energy were considered.

For the neutron evaporation, the only available data of Müller et al.[1] have been interpolated, assuming the same structure for $\bar{\nu}$ as in the case of $^{235}U(n_{th},f)$.

As a result of the refined analysis described above, in Fig. 8 the mean total kinetic energy ($\overline{TKE}$) as function of the incident neutron energy is shown.

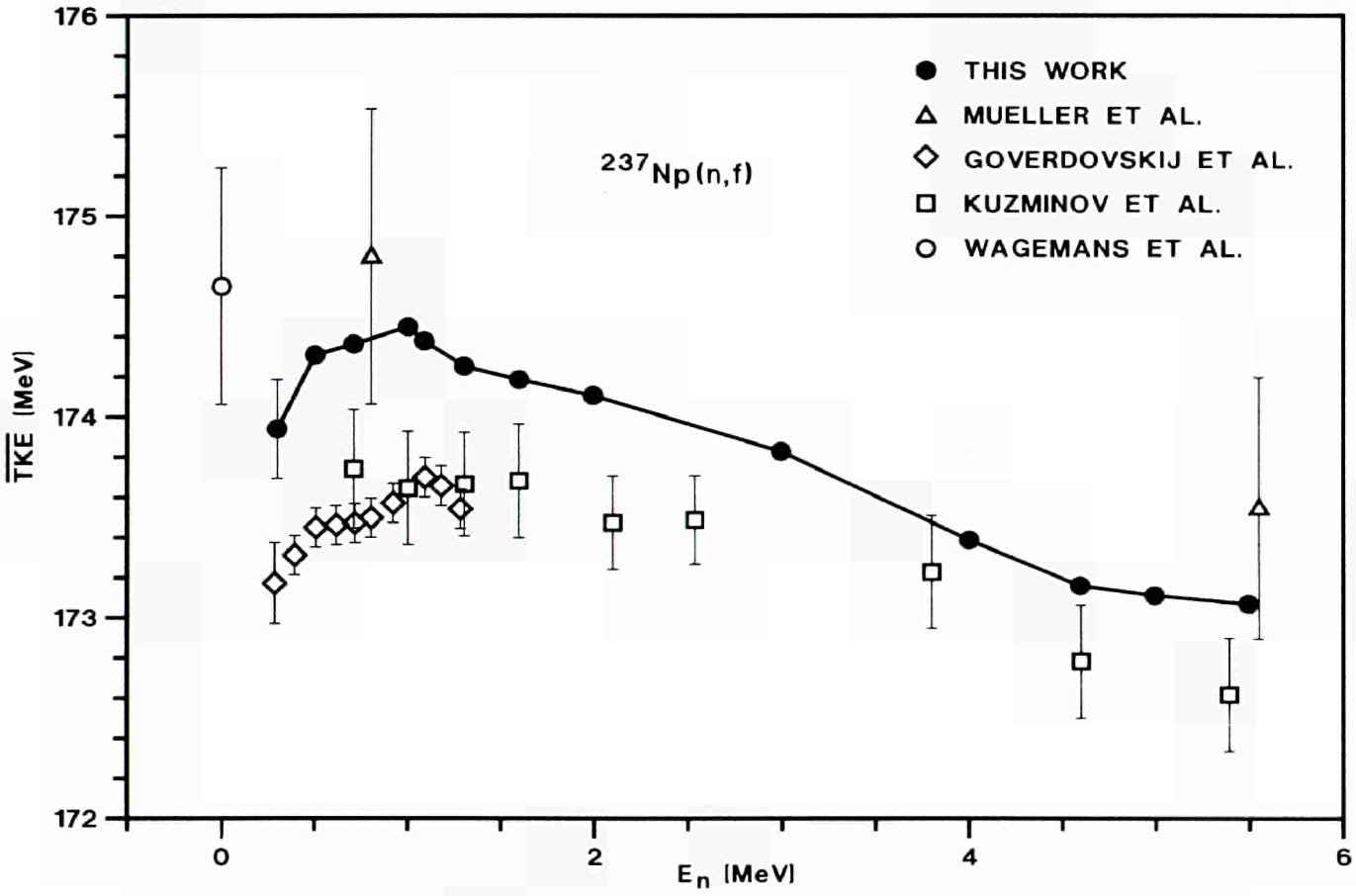

Fig. 8. Average $\overline{TKE}$ as function of the incident neutron energy

Included in the picture are results of other authors[2-5] for the reaction $^{237}Np(n,f)$. All data are normalized to the same mean $\overline{TKE}$ of 170.5 MeV of $^{235}U(n_{th},f)$. The present measurement and those of Kuzminov et al.[3] and Goverdovskij et al.[4],

(1) R. Müller et al., KfK Report 3220 Karlsruhe 1981
(2) R. Müller et al., KfK Report 3220 Karlsruhe 1981
(3) B.D. Kuzminov et al., Sov. J. Nucl. Phys. 11 (1970) 166
(4) A.A. Goverdovskij et al., Sov. J. Nucl. Phys. 55 (1992) 9
(5) C. Wagemans et al., Nucl. Phys. A369 (1981) 1

show a similar structure and especially the maximum around 1 MeV is confirmed. Whether the increase of the $\overline{TKE}$ up to 1 MeV and the decrease for higher neutron energies is a result of changing contributions of the so called fission modes will be subject of further investigations. In Fig. 9, left part, the differences between the $\overline{TKE}$ as function of the heavy mass for 1.0 MeV neutron energy and 0.5 MeV are plotted. Over the most abundant mass range A = 130 to A = 150 the $\overline{TKE}$(A) at E_n = 1.0 MeV shows constantly higher values than at E_n = 0.5 MeV. Contrary to this behaviour the difference between 1.0 MeV and 5.5 MeV shows an enhanced change for the heavy masses around A = 132 (Fig. 9, right part). This is an indication that for higher neutron energies the changing abundancies of the fission modes become the dominating effects.

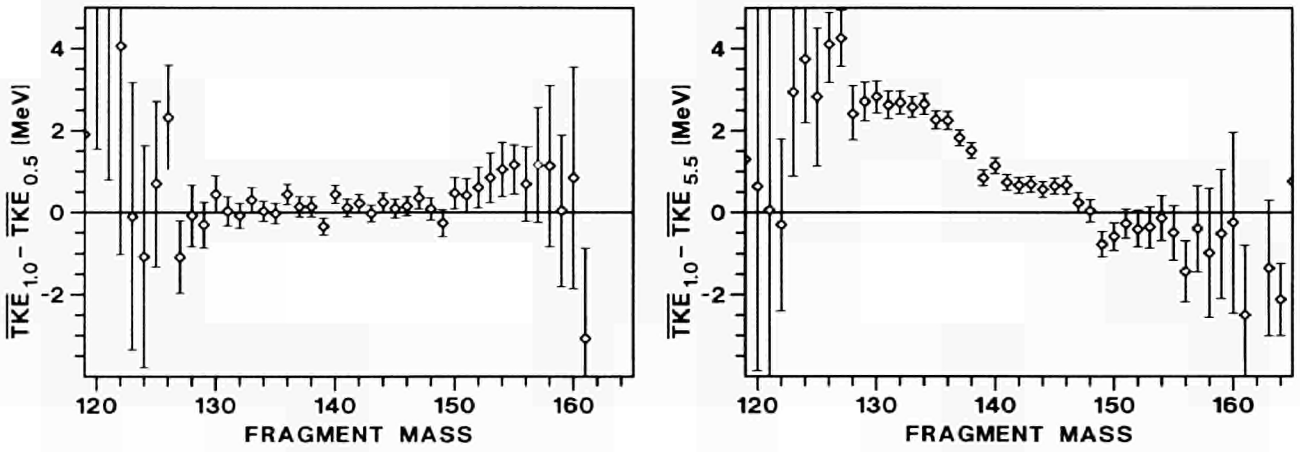

Fig. 9. ***Difference of the $\overline{TKE}$ as function of the heavy fragment mass at E_n = 1.0 MeV and E_n = 0.5 MeV (left part) and at E_n = 1.0 MeV and E_n = 5.5 MeV (right part)***

A fast Method of Calculating Fission Modes

S. Oberstedt* , F.-J. Hambsch, P. Siegler**

The calculation of fission properties based on the multi-modal random neck-rupture model of Brosa, Grossmann and Müller[1] is being used to calculate fission fragment properties for the ^{237}Np(n,f)-reaction[2] as well as for the spontaneous fission of ^{252}Cf. In the frame of this model the nucleus is parametrized in the five-dimensional coordinate-space of the generalized Lawrence shapes. The complete calculations of the search for the different fission modes existing in the investigated nuclear system and of the experimental observables are, however,

* SCK-CEN, Mol, Belgium
** EC Fellow from Technical University of Darmstadt, Germany
(1) U. Brosa, S. Grossmann and A. Müller, Phys. Rev. 197 (1990) 167
(2) CBNM Annual Progress Report on Nuclear Data (1991), EUR 14514 EN and CBNM Annual Report 91, EUR 14374 EN

very time consuming, especially since it is not known a priori, how many fission modes do exist in the nucleus under study.

With a new survey of the nuclear energy (RAYLSCAN) in a three-dimensional subspace of the five dimensional Lawrence parametrization with respect to the asymmetry parameter z and the neck radius r an immediate detection of the existing fission modes is possible[1] and the associated fission paths may be calculated much faster. A complete fission-mode calculation basically consists now of performing the RAYLSCAN calculations for different parameters with a succeeding analysis of the respective energy landscapes (see Fig. 10). The reduction of computer processing time is at least a factor of four.

In about the same time as the fission modes were calculated for the nucleus ^{238}Np, the new method allowed to calculate the fission modes in ^{236}U, ^{238}U, ^{237}Np and ^{246}Cf.

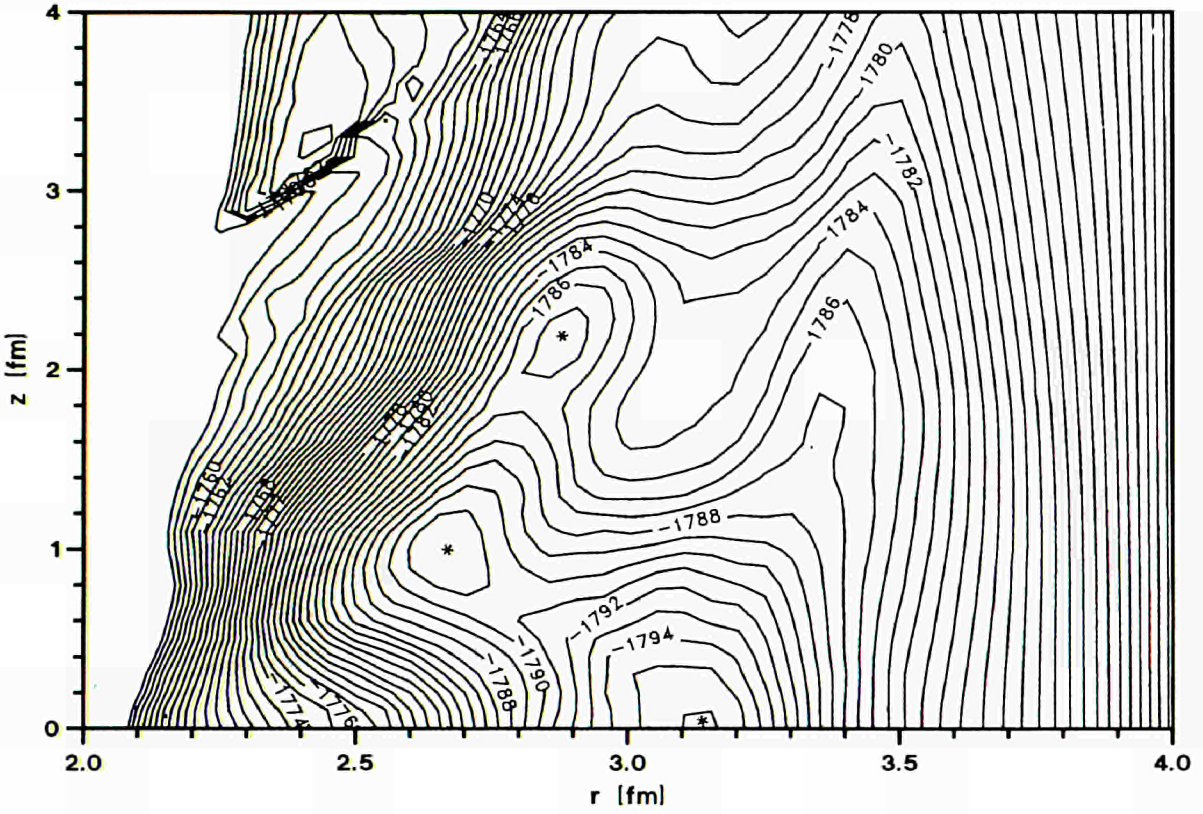

Fig. 10. ***Typical energy landscape in the new RAYLSCAN representation. The different fission modes are indicated by stars***

First results on groundstates, barrier heights and mean mass-splits of the respective fission modes are presented in Table 1. With this refined method of fission mode calculations it will now be possible to systematically investigate fission properties over a wide range of nuclei in a reasonable time.

---

(1) S. Oberstedt, IRMM Internal Report GE/R/VG/77/93

Table 1. First results obtained with the new fission mode calculations for different actinide nuclei. All energies, E, are in MeV. For the characteristic mass-split, A, of each fission mode the heavy fragment mass number is given

	E_{II}	E_A	E_B	E_{sI}	E_{sIII}	A_{std}	A_{sI}	A_{sIII}
^{236}U	2.4	6.3	9.5	10.9	7.5	140	120	(155)
^{238}U	2.6	6.2	10.1	11.2	7.8	139	120	(155)
^{237}Np	2.7	5.2	7.2	11.0	7.2	138	120	(155)
^{246}Cf	2.0	6.2	6.0	7.0	-	(140)	134	-

Investigation of the Fission Fragments' Mass and Energy Distributions for Several Plutonium-Isotopes

L. Dematté*, C. Wagemans**, P. D'hondt***, S. Pommé****, A. Deruytter, R. Barthélémy, J. Van Gils

In the frame of a systematic study of the mass and energy distributions (and their correlations) of the spontaneously fissioning plutonium isotopes, about 30.000 ^{242}Pu(SF) and 14.000 ^{244}Pu (SF) events have been recorded. The measurements were performed with the double energy detection method and relative to the well-known $^{239}Pu(n_{th},f)$ reaction, for which purpose a thermal neutron beam of the BR1 reactor (SCK/CEN, Mol, B) was used. The ^{244}Pu(SF) data taking is still being continued.

During the analysis of the data, great care was given to the choice of the $^{239}Pu(n_{th},f)$ neutron emission data $<\nu>(m_i^*)$, m_i^* being the fission fragment mass before neutron emission. As shown in Fig. 11, three sets of data are available: experimental data from Apalin et al.[1] and Milton and Fraser[2] and evaluated data from Wahl[3]. In order to select the best set of $<\nu>(m_i^*)$ data, the $^{239}Pu(n_{th},f)$ post-neutron emission mass distribution was calculated from our experimental data in combination with each of the three different $<\nu>(m_i^*)$ data sets from the literature. The best agreement is obtained by comparing these distributions with the radiochemical data of Wahl[3] (Fig. 11).

---

* EC Fellow from University of Bologna, Italy
** University of Gent, Belgium
*** SCK/CEN, Mol, Belgium
**** EC Fellow from University of Gent, Belgium

(1) V. Apalin et al, Nucl. Phys 71 (1965) 553
(2) J.C.D. Milton and J.S. Fraser, Ann. Rev. Nucl. Sci. 16 (1966) 1146
(3) A.C. Wahl, Atom. Data and Nucl. Data Tables 39 (1988) 1

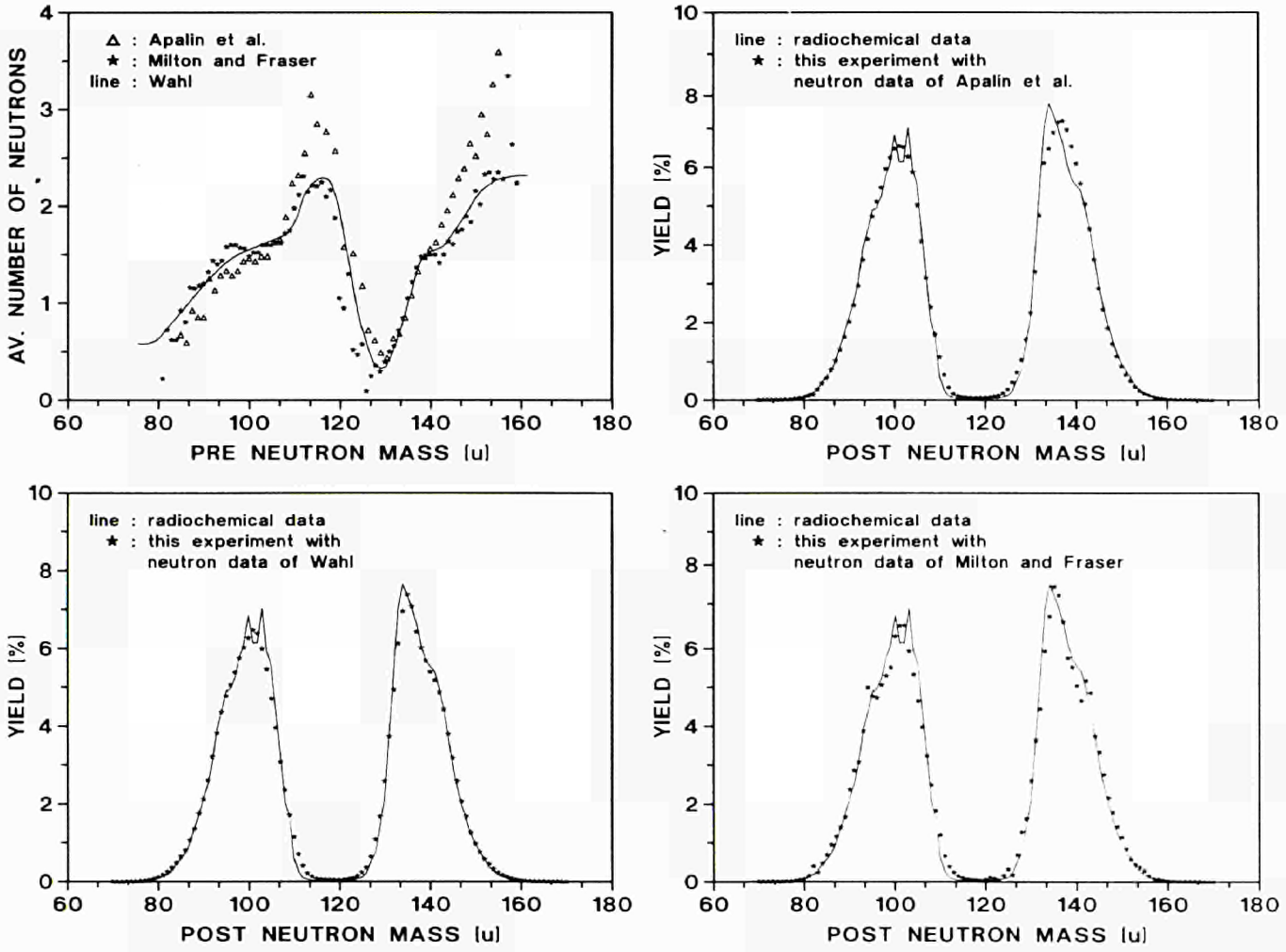

Fig. 11. *$\langle\nu\rangle(mi^*)$ data for ^{239}Pu (n_{th},f) used in the correction procedure (upper left). The corresponding post-neutron mass distributions are compared with the radiochemical data compiled by Wahl*

The above mentioned evaluated data were used for the neutron emission correction of the ^{242}Pu(SF) and ^{244}Pu(SF) measurements, after normalizing them to the average number of neutrons emitted in ^{242}Pu(SF) and ^{244}Pu(SF), respectively. The pre-neutron emission mass distributions obtained in this way are shown in Fig. 12 and compared with similar results previously obtained for ^{236}Pu(SF), ^{238}Pu(SF) and ^{240}Pu(SF)[1]. It is apparent that ^{242}Pu forms a kind of a "turning point": up to A = 242, the mass yield around $m_h \approx 135$ increases with increasing values of A, whilst the mass yield around $m_h \approx 142$ correspondingly decreases.

For A = 244 however, the mass yield around $m_h \approx 135$ decreases as compared to A = 242, whilst the mass yield around $m_h \approx 142$ stabilizes. This behaviour can be understood by the interplay of the standard I and standard II fission modes (or the corresponding shells) together with the conservation of the N/Z ratio of the fissioning nucleus during the fission process.

(1) C. Wagemans et al, Nucl. Phys. A502 (1989) 287c

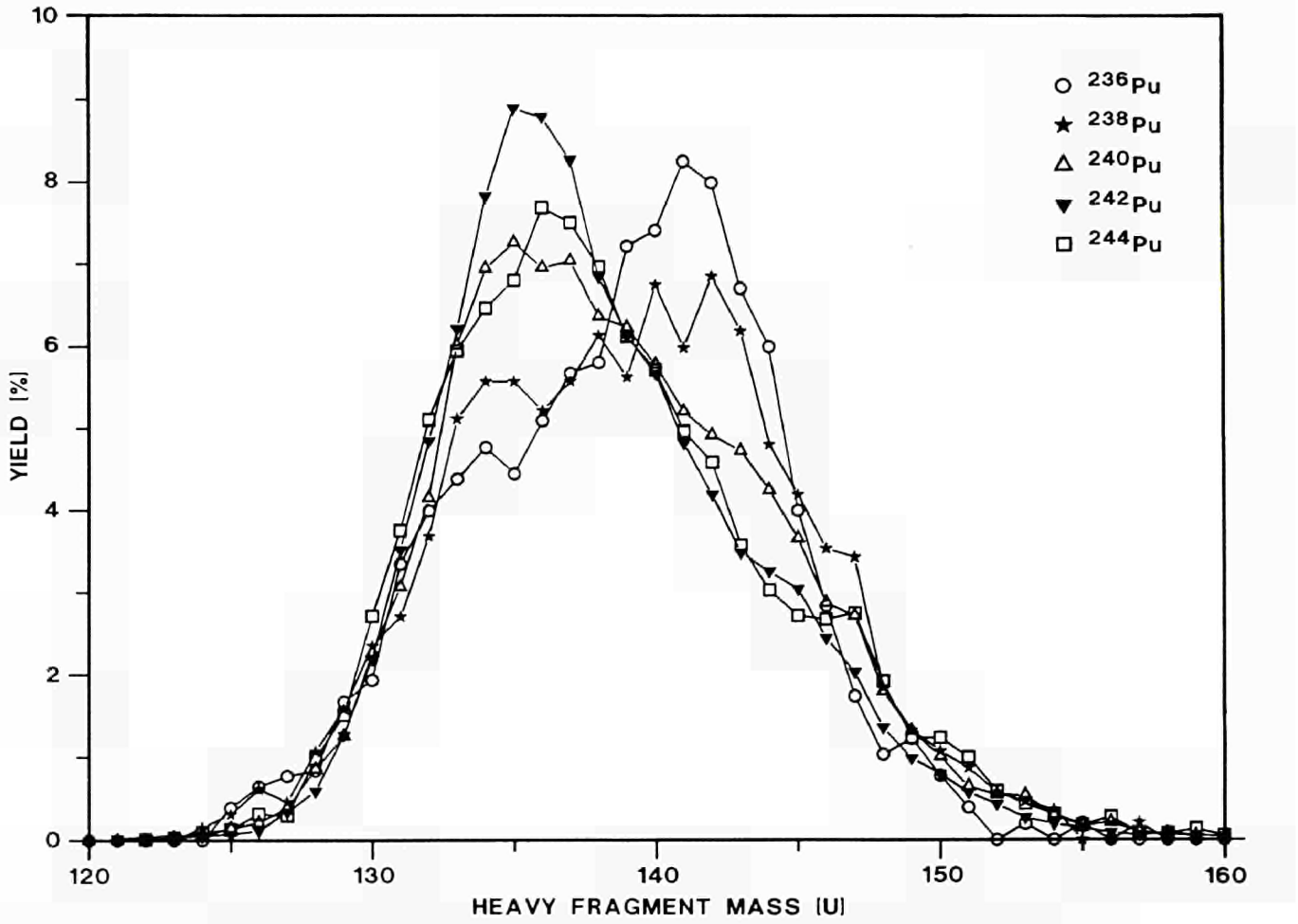

Fig. 12. Comparison of the pre-neutron emission mass distributions for ^{236,238,240,242,244}Pu(S.F.))

Ternary Fission in ^{235}U(n,f) Resonances

S. Pommé*, C. Wagemans**, S. Druyts***, J. Van Gils, R. Barthélémy

During the ternary fission process, an energetic light charged particle (mostly an α-particle or a triton) is emitted together with the - so-called binary - fission fragments. This occurs roughly once every 500 fission events.

The aim of this experiment is to study the ternary α-particle and triton yields in the resonances and to correlate them with other fission observables such as the resonance spin and the fission modes. Later on, the t/α-ratio will be investigated at higher neutron energies to verify an earlier observed doubling of this ratio above 200 keV as compared to thermal fission, which would lead to a significant enhancement of the tritium production in fast reactors.

For this experiment we constructed a convenient detection set-up and tested two new data acquisition systems (partially) developed at the IRMM: an apec - 1064

* EC Fellow from University of Gent, Belgium
** University of Gent, Belgium
*** EC Fellow from KU Leuven, Belgium; now at University of Gent, Belgium

system (from Aero-Physics) connected to an IBM/PC (DOS 6.00) and a system with Transputer Multiplexer Modules connected to a micro-VAX (VMS).
Both systems worked reliably. The measurements are currently continued on the apec system.
Ternary fission experiments are dealing with low counting rates and need a critical tuning of the detector set-up to measure both tritons and α-particles adequately. They have to provide the kinetic energy of the ternary particles, the energy (or time-of-flight) of the neutrons which induce the fission reaction, a clear identification of the particles and background and a large solid angle for statistical reasons. It has been opted for an asymmetric, double ΔE-E detection system consisting of a methane filled twin ionisation chamber acting as ΔE-sections and on both sides of the common cathode a surface barrier detector (SBD) inside the chamber to collect the remaining energy. The ^{235}U-target is situated in the center of the cathode. At one side of the cathode, the distance between the target and the SBD was kept small (15 mm) to get a good geometry factor and low losses of α-particles. At the other side a thicker ΔE-section was chosen to obtain a better distinction between the (low) ΔE ionization signal of the tritons and background signals. For this reason also the gas pressure was increased to 3 bar. The gain in counting rates with these compact configurations is still paid with some loss of identification power, since the broad angular distributions give rise to a spread on the possible ΔE-E combinations. Fission fragments and natural α-particles are stopped with a 30 μm Al target shielding. The anode is partly transparent to allow the passage of the outgoing ternary particles.
From the rather complex combination of the various detector information first experimental results are collated in Fig. 13.

Neutron Data of Structural Materials

Very High Resolution Measurements of the Total Cross-Section of Natural Iron

K. Berthold*, C. Nazareth, G. Rohr, H. Weigmann

High resolution cross section data are especially important for shielding problems. This has been realized since long for the "resolved resonance region". In the case of structural materials strong fluctuations of the cross-section are present and important also in the lower MeV region. The insufficient knowledge of these fluctuations is a possible reason for the observed discrepancies between shielding benchmark experiments and calculations.

---

* EC Fellow from Technical University of Darmstadt, Germany

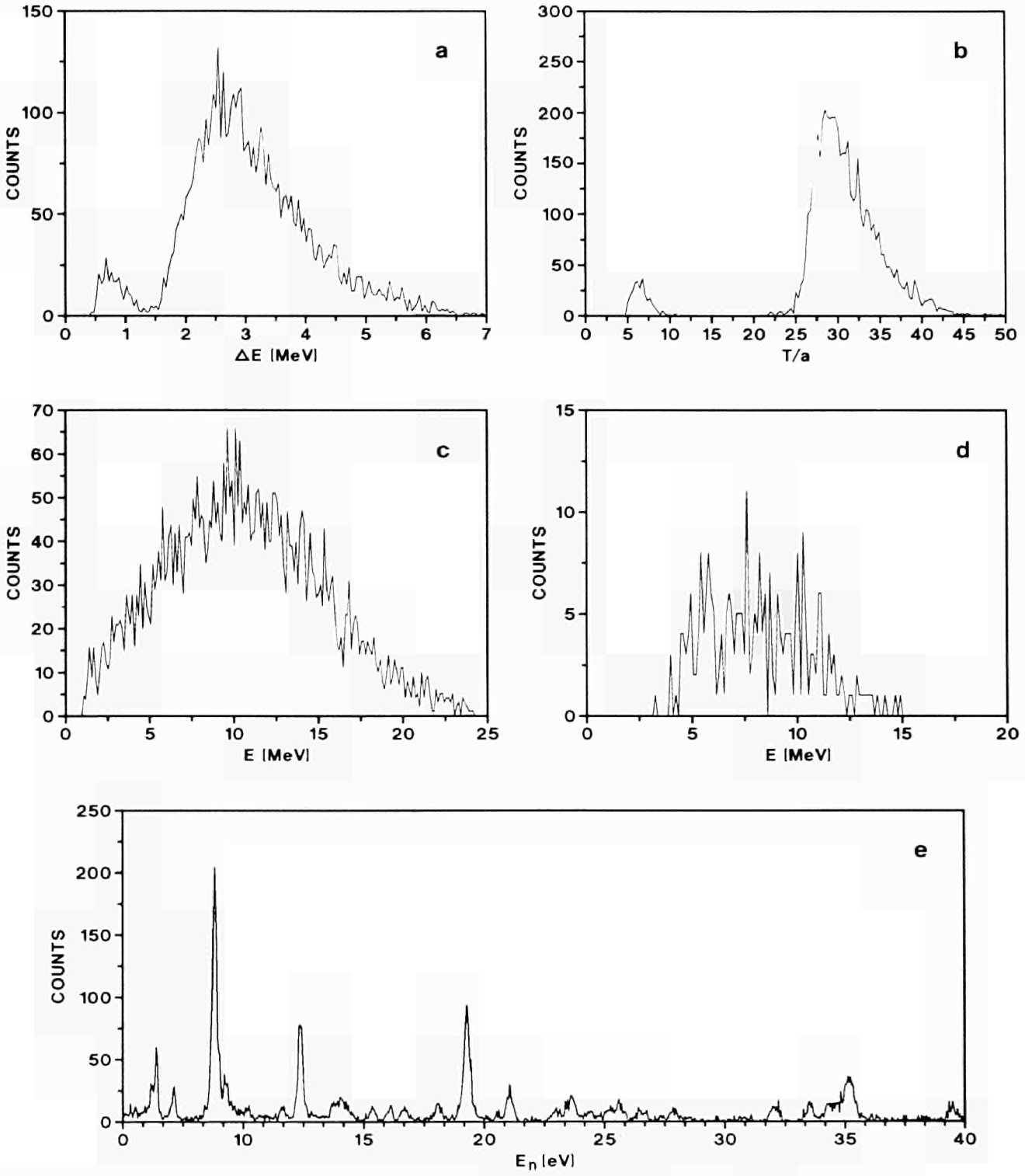

Fig. 13. Measurements on ternary fission in $^{235}U(n,f)$.(a)ΔE-spectrum of α-particles and tritons (b) identification spectrum of the ternary particles $T/a=(E-\Delta E)^{1.73}-(E)^{1.73}$, (c) energy deposited in the surface barrier detector by the α-particles, (d) E-spectrum of the tritons, (e) ternary fission cross-section of ^{235}U as a function of the incident neutron energy

The outstanding characteristic of GELINA's pulsed neutron source is its excellent time of flight resolution of nominal 2.5 ps/m. This facility is thus particularly

suited for high resolution measurements of materials used in shielding applications.
The total cross-section of natural iron has recently been remeasured at GELINA in the neutron energy range between 0.2 and 20 MeV. Measurements have been performed on three samples of different thicknesses including one with an average transmission of 0.1, in order to check for consistency and remaining resolution effects. The cross sections in the "unresolved resonance region" still show rather strong fluctuations. The resonance region data will be analysed by an R-matrix routine and the parameters compared to existing compilations.

Very High Resolution Transmission Measurements and Resonance Parameters of ^{58}Ni and ^{60}Ni

A. Brusegan, G. Rohr, R. Shelley, E. Macavero, C. Van der Vorst, F. Poortmans*, L. Mewissen*, G. Vanpraet**

The nickel isotopes have a closed proton shell (Z = 28) and are therefore of interest for fundamental nuclear physics. Furthermore they are important structural materials for fast reactors and for shielding in fusion installations.
The total cross section has been measured in the neutron energy range from 14 eV up to 30 MeV at GELINA with the time-of-flight technique. Four flight path distances (50, 100, 200 and 400 m), 1 ns electron burst width, up to three enriched samples of different thicknesses for each isotope and four different types of detectors have been used to optimize the measurements. The neutron beam was moderated, except for the 400 m measurements.
Compared with the previous version of this work[1],the analysis has been extended up to about 831 keV and the R-Matrix code Multi has been modified to include the resolution functions of the detectors (Li-glass and ^{10}B slab) and of the moderated and unmoderated neutron beam, respectively.
The extension of the measurements to very low energy allows a better determination of the effective potential scattering radius together with the resonance parameters of the negative energy s-wave resonances; the potential scattering radii for p- and d-wave resonances have been estimated from the interference minima occurring at about 400 keV and above 800 keV respectively.
For 378 resonances of ^{58}Ni and 367 of ^{60}Ni the resonance parameters E_0, g, J and l have, where possible, been determined. Some spin values in ^{58}Ni were taken from the scattering experiments of Perey et al.[2].

---

* SCK/CEN, Mol, Belgium
** University of Antwerpen, Belgium
(1) A. Brusegan et al., Intern. Conf. Nucl. Data for Sci. and Techn., Jülich, Germany (1991)
(2) C.M. Perey et al., Report ORNL/TM-10841 (1988); Phys. Rev. C47 (1993) 1143

In Table 2, the s-wave strength functions and level spacings are quoted together with the s-, p- and d-wave radii for the two isotopes. The 2.2 keV resonance of ^{60}Ni deserves particular attention for its relevance in the normalization of capture cross section data with the pulse height weighting method.

Table 2. Some resonance parameters of ^{58}Ni and ^{60}Ni

	^{58}Ni	^{60}Ni
N. of resonances	61	58
<Do> (keV)	13.41 ± 0.90	13.78 ± 0.94
So(10000)	3.32 ± 0.60	3.10 ± 0.58
Ro(fm)	7.1 ± 0.3	6.7 ± 0.3
R1(fm)	4.0 ± 0.3	4.0 ± 0.3
R2(fm)	7.1 ± 0.3	6.7 ± 0.3

Neutron capture gamma ray spectra in ^{58}Ni resonances

A. Brusegan, C. Coceva*, E. Macavero, C. Van der Vorst

A program on the determination of the electric and magnetic dipole radiative strength was started. A germanium detector, with an anti-Compton shield, is used to detect gamma-ray spectra emitted after neutron capture in different ^{58}Ni resonances selected by time of flight. The measurements are carried out at GELINA, with sample and detector placed at 25 m flight distance. Neutron energies are explored between 320 eV and 103 keV.

* ENEA, Bologna, Italy

NUCLEAR DATA FOR FUSION TECHNOLOGY

The objective of the work on nuclear data for fusion technology is to contribute to an improved knowledge of data for neutron transport calculation in the blanket and for an estimate of the gas production. Measurements are presently done in three areas: (1) double-differential neutron emission cross sections; (2) double-differential charged particle emission cross sections and (3) total and radiative capture cross sections of structural materials; since the latter are related to fission as well as to fusion technology, they are described in the section on fission technology.

The Neutron Spectrum of a Thick Be Li Target Bombarded with Protons of 4 and 5.5 MeV

A. Meister*, W. Schubert, E. Wattecamps

A 1 mm thick lithium target with a 0.05 mm beryllium entrance window is used at the 7 MV Van de Graaff to generate a "white" neutron spectrum with neutron energies ranging from some keV to some MeV. The high energy limit is determined by the energy of the incident protons. To prepare and optimise the experimental set up for (n,n' γ) cross-section measurements, e.g. on palladium, the source neutron spectrum was measured with a thin organic scintillator (5 mm thick PILOT U scintillator). The measurements are done by neutron time-of-flight technique with 400 ps/m resolution for proton energies E_p = 4 MeV and 5.5 MeV in a collimated neutron beam line in forward direction. Fig. 14 shows a time-of-flight spectrum for E_p = 4 MeV. The detection efficiency of the scintillation detector has been calculated on the basis of the H(n,n)H scattering and considering the effects of neutron multiple scattering[2].

The neutron source spectra for 4 and 5.5 MeV proton energy are shown in Fig. 15. Measured data are crosses or dots connected by a continuous line. The small neutron yield in the higher energy part of the spectrum is produced by the ^{9}Be(p,n) reaction in the beryllium window, whereas the bulk of the spectrum below the second steep edge is produced by the ^{7}Li(p,n)^{7}Be reaction. The lowest energy part of the spectrum, near and below the detector bias, is calculated (histogram) by target reaction kinematics relying on the cross-section of the ^{7}Li(p,n)^{7}Be reaction and the stopping power for protons in lithium metal. The

---

* Visiting Scientist from Technical University of Dresden, Germany

(1) K. Seidel et al., Yad. Fiz. 42 (1985) 1041

(2) M. Drosg, Nucl. Instr. Meth. 105 (1972) 573

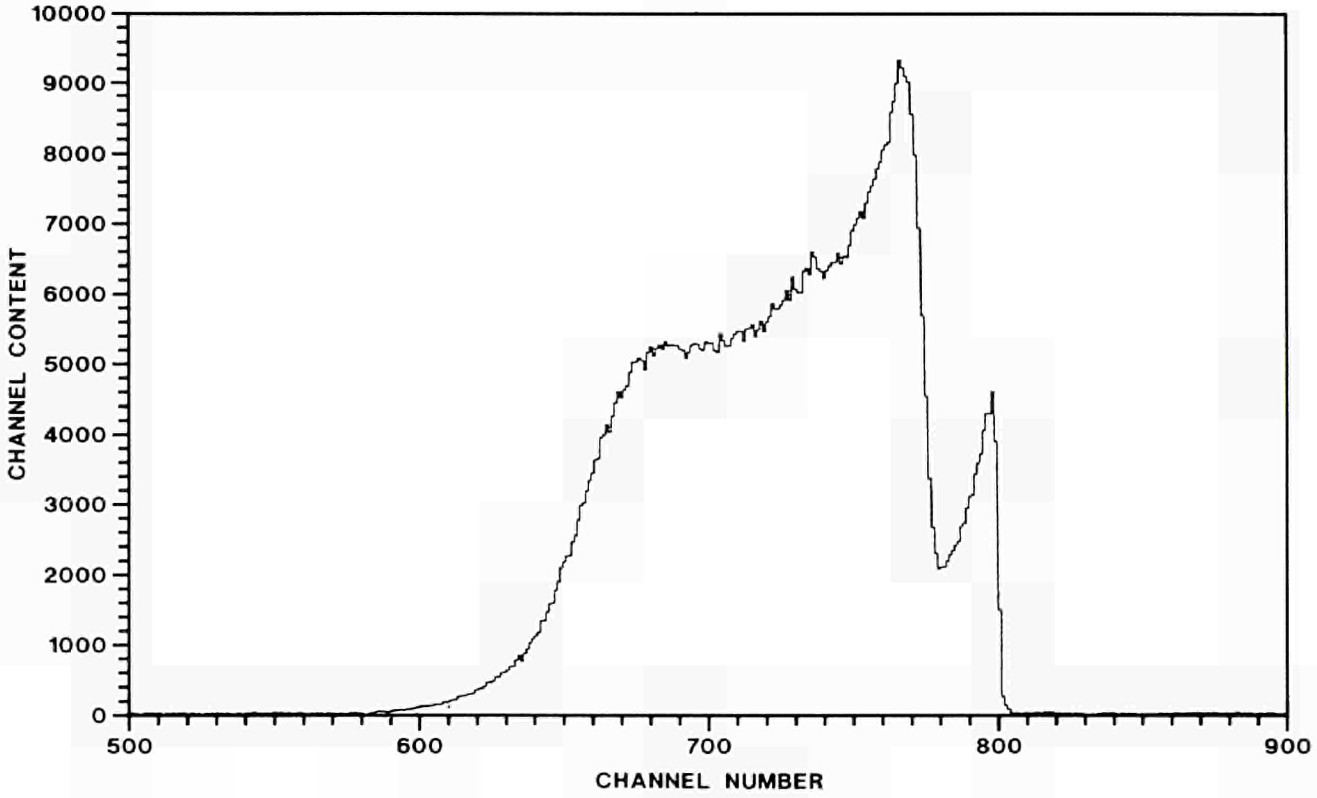

Fig. 14. *Neutron time-of-flight spectrum for E_p = 4 MeV, 4.318 m flight path and 1.56 ns time channel width (large time-of-flight at small channel number)*

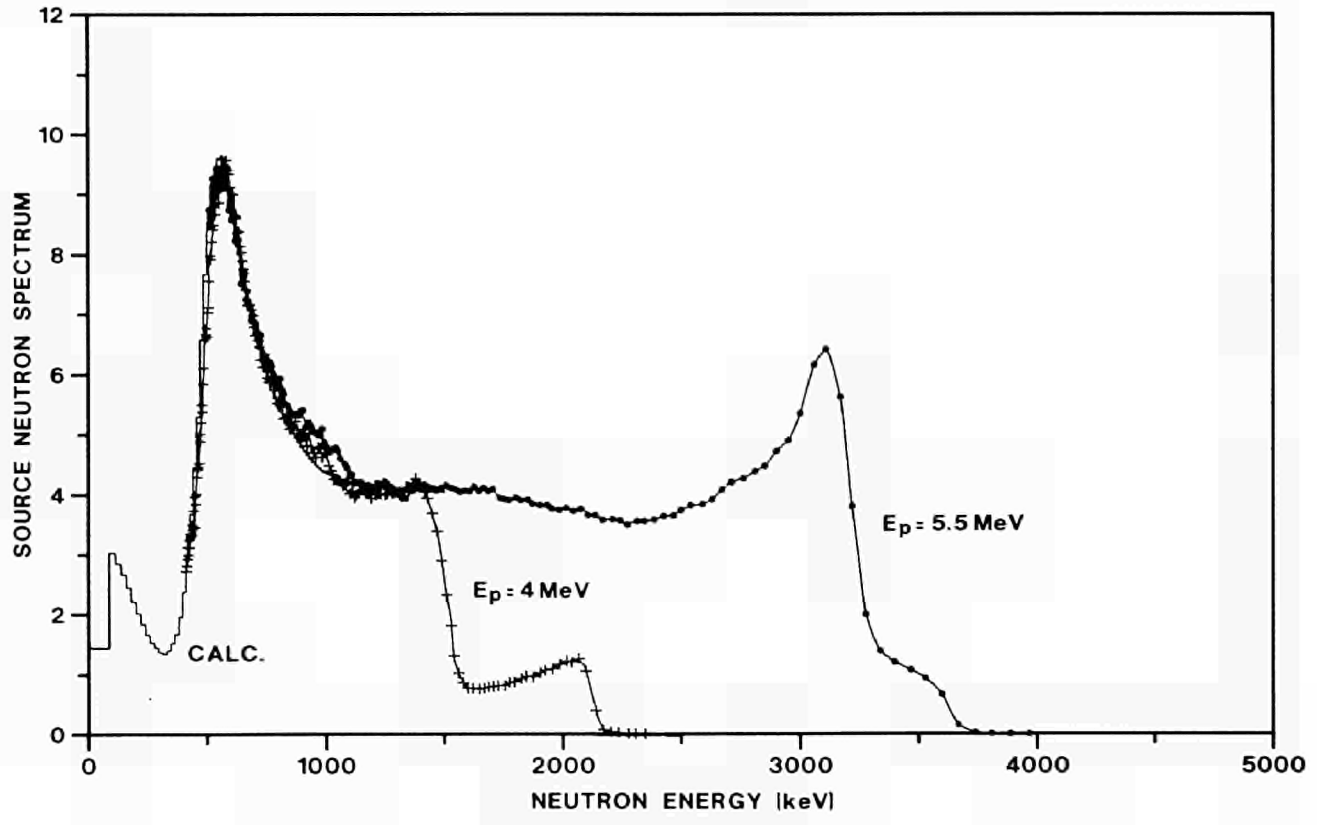

Fig. 15. *Thick target neutron energy spectra for E_p = 4 MeV and 5.5 MeV. The ordinate is in arbitrary units*

cross-section and the stopping power data were taken from the literature[1, 2]. Measured and calculated spectra agree well in the region of expected overlap.

Neutron Total Cross-Section Measurements of ^{12}C, ^{232}Th and ^{10}B from 1.5 to 18 MeV

A. Crametz, W. Schubert, E. Wattecamps

A time of flight facility for neutron total cross section measurements with 60 ps/m resolution is operational at the Van de Graaff. The neutron target is a lithium metal slab of 1 mm thickness covered with a sheet of 0.1 mm beryllium. Neutrons are produced simultaneously by ^{7}Be(d,n) and ^{7}Li(d,n). Deuterons of 6.5 MeV and a burst width of 1.4 ns at 625 kHz impinge on the target. The flight path lenght is 2296.5 cm and the neutron detector is a NE213 liquid scintillator of 12.38 cm diameter and 3.22 cm thickness with a time resolution of 0.8 ns. Preliminary results were presented at the International Workshop on Nuclear Data for Fusion Technology, held in San Diego, USA. At that stage the measurement technique had reached an accuracy level of approximately 5 %. Since then the accuracy and especially the reproduciblity of the measurements have been considerably improved by

- replacing the beryllium cover of the target of 0.05 mm by one of 0.1 mm thickness to reduce steep structures in the source spectrum;
- using three independent fluence monitors and requiring systematic agreement among them, within the statistical accuracy;
- installing, programming and testing an automatic new sample changer for four samples. The positioning is made to within 0.1 mm, the sample control is linked with the time-of-flight data acquisition system;
- determining correction factors for dead time losses and small differences between sample positions.

A large number of runs was made recently with three samples. The analysis of the test case with ^{12}C measurements gives fine agreement with the ENDF/B6 evaluated data file. The analysis for ^{232}Th and ^{10}B is in progress.

Total Neutron Cross Section Measurement of ^{27}Al at High Energy

R. Shelley, G. Rohr, C. Nazareth, M. Moxon*

A study of the neutron cross section of ^{27}Al is relevant to the structural material data required for reactor and fusion studies and to recent progress made with the

---

* Visiting Scientist from AEE, Harwell, United Kingdom

(1) H. Liskien and A. Paulsen, Atom. Data Nucl. Data Tables 15 (1975) 57

(2) H.H. Andersen and J.F. Ziegler, Hydrogen Stopping Powers and Ranges in all Elements, Pergamon, New York (1977)

investigation of resonance spacings and their distribution. For this isotope no new data has become available for almost two decades and, with the present very high resolution capabilities of GELINA, the energy resolution compared to earlier measurements has now been improved by an order of magnitude.

This has been achieved by measuring, at a distance of 400 m, the transmission of the neutron beam from the linac uranium target using the time-of-flight (TOF) technique. With the 1 ns pulsed linac operating at 800 Hz, the transmission through a 99.5 % pure aluminium sample (0.19293 at/b thick) was detected by a NE110 plastic scintillator viewed by four RCA photomultipliers. The resultant TOF spectra were stored in 64 k channels of 1ns width and covered a neutron energy range from 175 keV to 25 MeV. Data from a second measurement with a thinner sample (0.05373 at/b) has been incorporated to facilitate the resonance analysis.

Fig. 16 shows the complexity of the resonance structure observed in the cross section. The transmission data shown has been fitted up to 680 keV with two R-Matrix multi-level formalism codes, MULTI and REFIT. The improved

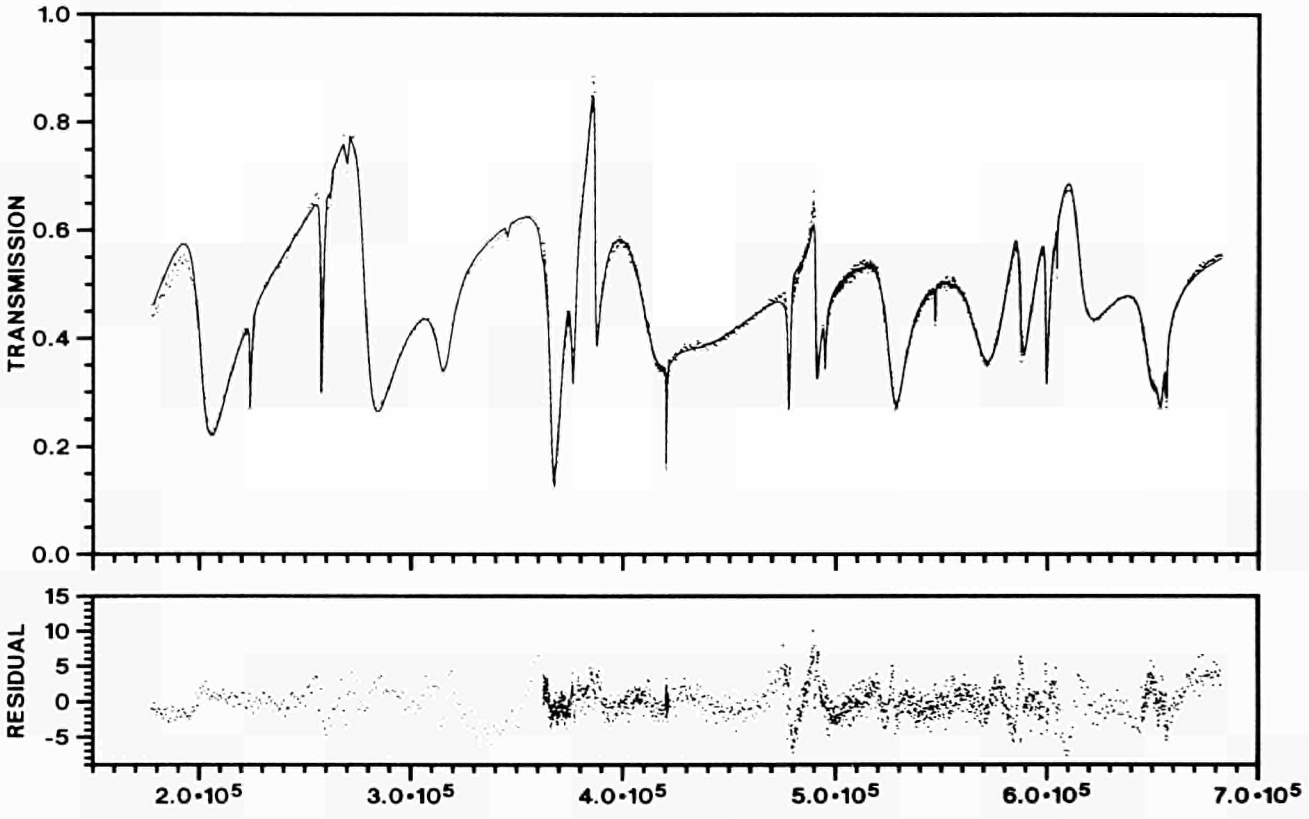

Fig. 16. REFIT fit (continuous line) to the neutron transmission through 0.19293 at/b of aluminium in the energy range 180 to 680 keV

resolution has shown the resonance structure to be substantially more complex than previously reported and 20 % more levels are seen. The resonance parameters E_0, Γ_n, J and l have been assigned for 35 levels in the energy range

170 keV to 680 keV and future analysis should extend this to the inelastic threshold at 844 keV and improve the fit. Regular spacings of s-wave neutron resonances, independent of their compound spin, are observed.

Total Neutron Cross Section Measurement of Vanadium
R. Shelley, G. Rohr, C. Nazareth

Vanadium is a possible candidate for the blanket material in fusion reactors and is presently being considered by the Engineering Design Activities (EDA) of the International Thermonuclear Experimental Reactor (ITER). A thorough study of the total neutron cross section has been initiated at GELINA and the first measurement with natural vanadium of 99.8 % purity started in November 1993. Time of flight transmission data through a 28 mm thick sample are presently being taken in the neutron energy range (0.175 - 25) MeV utilising the highest resolution possible at GELINA (400 m flightpath, 1 ns pulsewidth and 800 Hz). A series of measurements with different sample thicknesses and energy ranges is planned.

The Measurement of the Cross-Section Ratio of $^{58}Ni(n,x\alpha)$ to $^{27}Al(n,x\alpha)$
C. Tsabaris*, G. Rollin, E. Wattecamps

The accuracy of the cross section for alpha particle production by neutrons in ^{58}Ni is poor. Therefore this cross-section has been re-measured with the multi-telescope at the Van de Graaff relative to the cross section of ^{27}Al(n,xα). Though the cross section of the latter is well established from activation measurements, however, neither the angular distribution, nor the energy spectrum of the alpha particles from ^{27}Al were known except for neutron energies at 14 MeV. Thus, for the first time the angular yield distribution of the ^{27}Al(n,xα) reaction and a new measurement of ^{58}Ni(n,xα) to ^{27}Al(n,xα) reaction rate ratio of total alpha particle yields have been determined for neutron energies below 14 MeV.
The multi-telescope device was described elsewhere[1]. Preliminary results of ^{58}Ni(n,xα) to ^{27}Al(n,xα) cross section ratios were presented at the International Workshop on Nuclear Data for Fusion Technology, held in San Diego, USA.
The double differential cross section ratios were measured at 6.5, 8.0, 9.0 and 15.6 MeV. The angular distributions measured for ^{27}Al and ^{58}Ni are shown in Fig. 17, together with a fit by Legendre polynomials, which in case of ^{27}Al is defined to yield the total alpha particle production cross section as recommended by

---

* EC Fellow from University of Athens, Greece

(1) E. Wattecamps, Intern. Conf. Nucl. Data for Sci. and Techn., Jülich, Germany (1991)

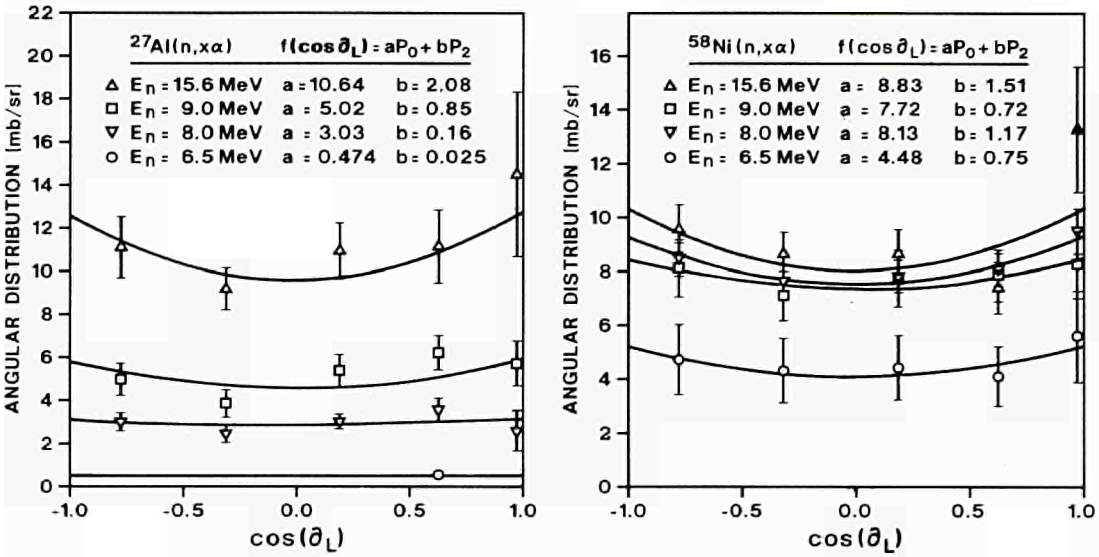

Fig. 17. Measured angular distributions and analytical fit of the $^{27}Al(n,x\alpha)$ reaction (left). Measured angular distributions and analytical fit of the $^{58}Ni(n,x\alpha)$ reaction (right)

H.Vonach[1]. Typical differential cross sections per MeV energy interval of the alpha particles for ^{27}Al and for ^{58}Ni were deduced from integration over 4π (Fig. 18). Total alpha particle yields are shown in Fig. 19 together with data available in literature. At 6.5 MeV the accuracy is poor because the $^{27}Al(n,x\alpha)$ reference cross section and the alpha particle energy of the $^{27}Al(n,x\alpha)$ reaction are small.

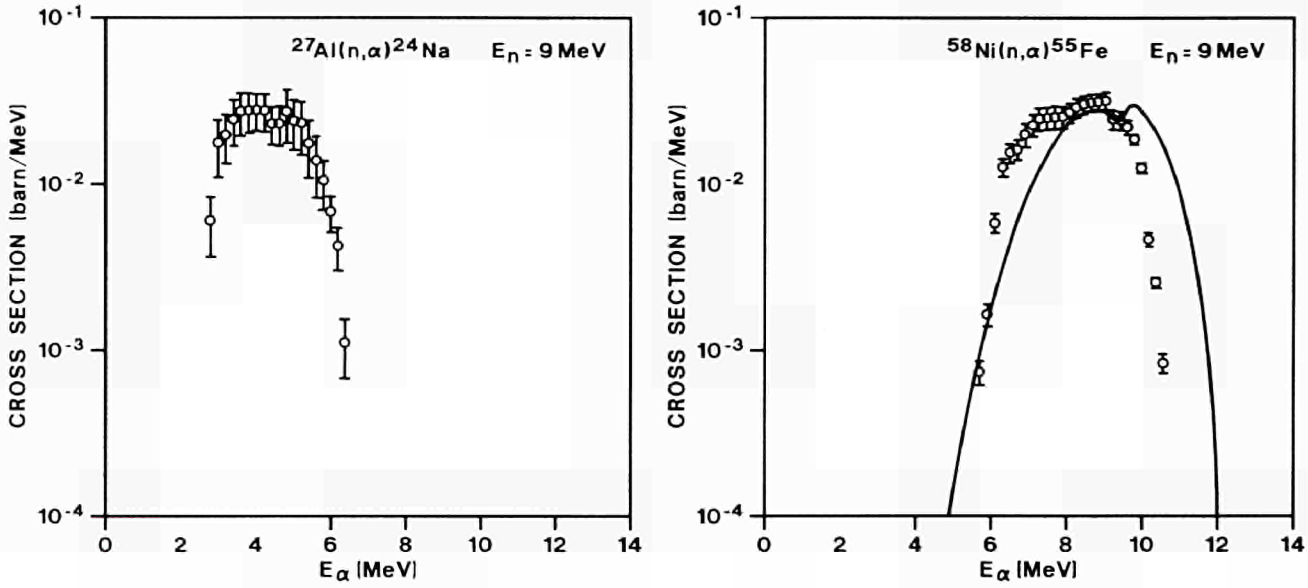

Fig. 18. The alpha particle energy spectrum for the $^{27}Al(n,x\alpha)$ reaction at E_n = 9 MeV (left). The alpha particle energy spectrum for the $^{58}Ni(n,x\alpha)$ reaction at E_n = 9 MeV and a calculated spectrum (STAPRE) (right)

(1) H. Vonach, Nucl. Standards for Nuclear Measurements, Techn. Rep. 227, IAEA, Vienna (1983)

Additional measurements by similar techniques were performed recently with the multi-telescope for ^{58}Ni(n,xα) relative to ^{58}Ni(n,xp) at 5.0, 6.5, 7.5 and 8.5 MeV. The analysis of the measurements is in progress as well as a calculation of these double differential data by the STAPRE code.

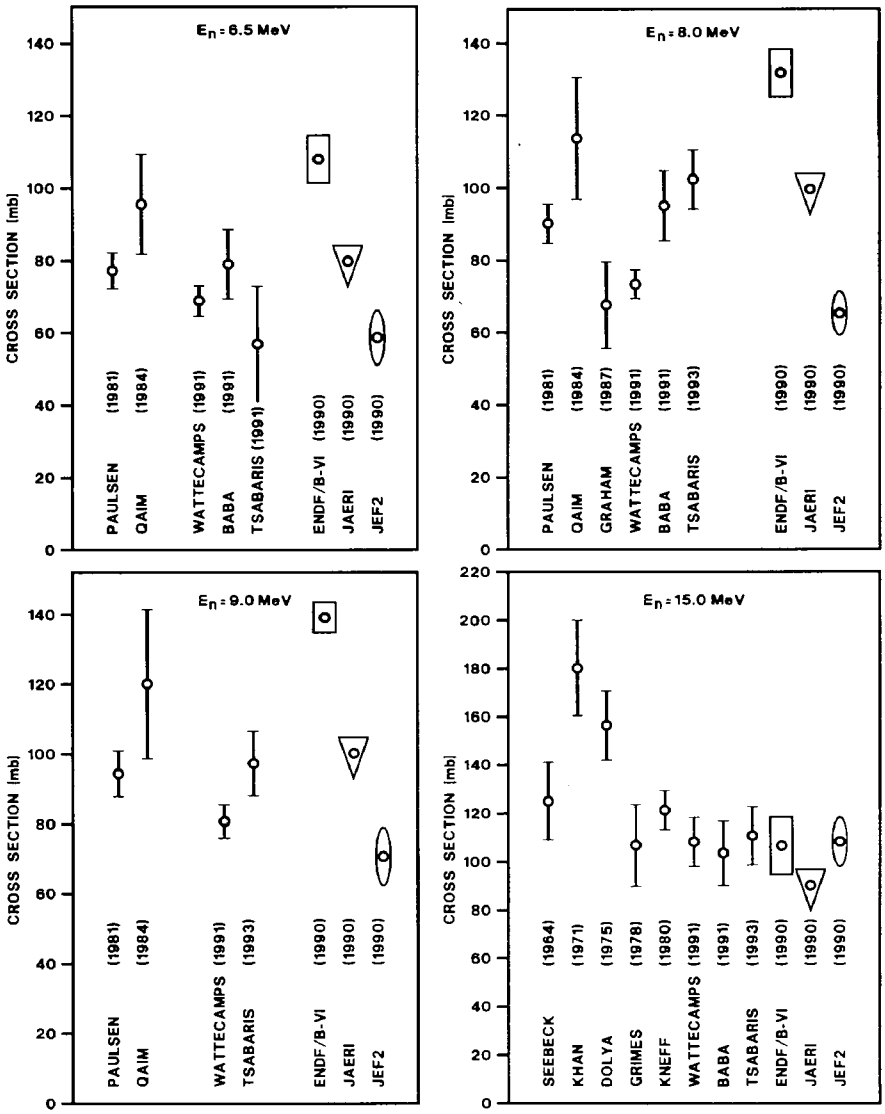

Fig. 19. Summary of total alpha particle yields of the ^{58}Ni(n,xα) reaction at various neutron energies

Cross-Section Ratio Measurements of ^{63}Cu(n,xp) to ^{58}Ni(n,xp)

C. Tsabaris*, G. Rollin, E. Wattecamps

At the IAEA's second research co-ordination meeting on activation cross sections (San Diego, USA, 1993), it was recommended to perform measurements of the ^{63}Cu(n,p) cross section by prompt detection techniques, such as the multi-telescope which is operational at IRMM. The feasibility of such measurements

* EC Fellow from University of Athens, Greece

was investigated recently with 8.0 MeV neutrons by measuring at five angles the (n,xp) reaction rate ratios of ^{63}Cu to ^{58}Ni. The latter reaction has a large and well known cross section and is used as a reference. The measuring conditions remain unchanged for $^{63}Cu(n,xp)$ and the reference ^{58}Ni reactions. The foreground to background ratio and the counting rate of the foreground are suited to proceed with the measurements. A detailed analysis for five angles at 8.0 MeV is in progress and additional measurements were performed very recently at 7 energies between 2.0 and 15.2 MeV.

SPECIAL STUDIES

A series of special measurements linked to the data programme has been performed. These research topics concerned PhD work as well as extended international collaboration making use of the unique features of GELINA as a high energy-resolution machine for neutron measurements.

Spin Assignment of ^{238}U Neutron p-Wave Resonances

F. Gunsing*, F. Corvi, K. Athanasopulos, H. Postma**

The aim of this experiment is to contribute to parity-non-conservation (PNC) studies performed at Los Alamos in the frame of the TRIPLE collaboration. Reasons for and preliminary results of this long-lasting measurement were already presented earlier[1].

The 12 gigabyte of listmode data from the $^{238}U(n,\gamma)$ reaction were sorted out into gamma-ray spectra corresponding to about 80 time-of-flight intervals, associated with s-wave, p-wave and background regions. In order to obtain the pure capture yield of a given resonance, the gamma-spectrum corresponding to nearby background regions was subtracted from the raw data after proper normalization. A limited energy region of two of these spectra for p-waves having different spin is shown in Fig. 20. The ratio of the areas of the peaks around 539 and 553 keV is quite different. The values of this ratio, plotted versus the resonance energy in Fig. 21, appear to split into two groups corresponding to spin and parity $J^\pi = 3/2^-$ and $1/2^-$, respectively.

High-energy gamma-ray spectra were also investigated in p-waves and several primary transitions leading to $J^\pi = 5/2^+$ states, were observed in some of them. If these transitions are visible, they are assumed to be E1 and therefore the resonance has $J^\pi = 3/2^-$. If a transition to a $J^\pi = 5/2^+$ state does not occur, nothing can be said about the spin because of Porter-Thomas fluctuations.

The spin assignments derived from the ratio of the low-energy gamma rays and from the observation of primary gamma rays are summarized in Table 3 for a total of 19 p-wave resonances. The two sets are consistent and by combining them a set of adopted spin values can be obtained.

---

* EC Fellow from Technical University of Delft, The Netherlands

** Visiting Scientist from Technical University of Delft, The Netherlands

(1) CBNM Annual Report 91, EUR 14374 EN; CBNM Annual Report 92, EUR 15029 EN

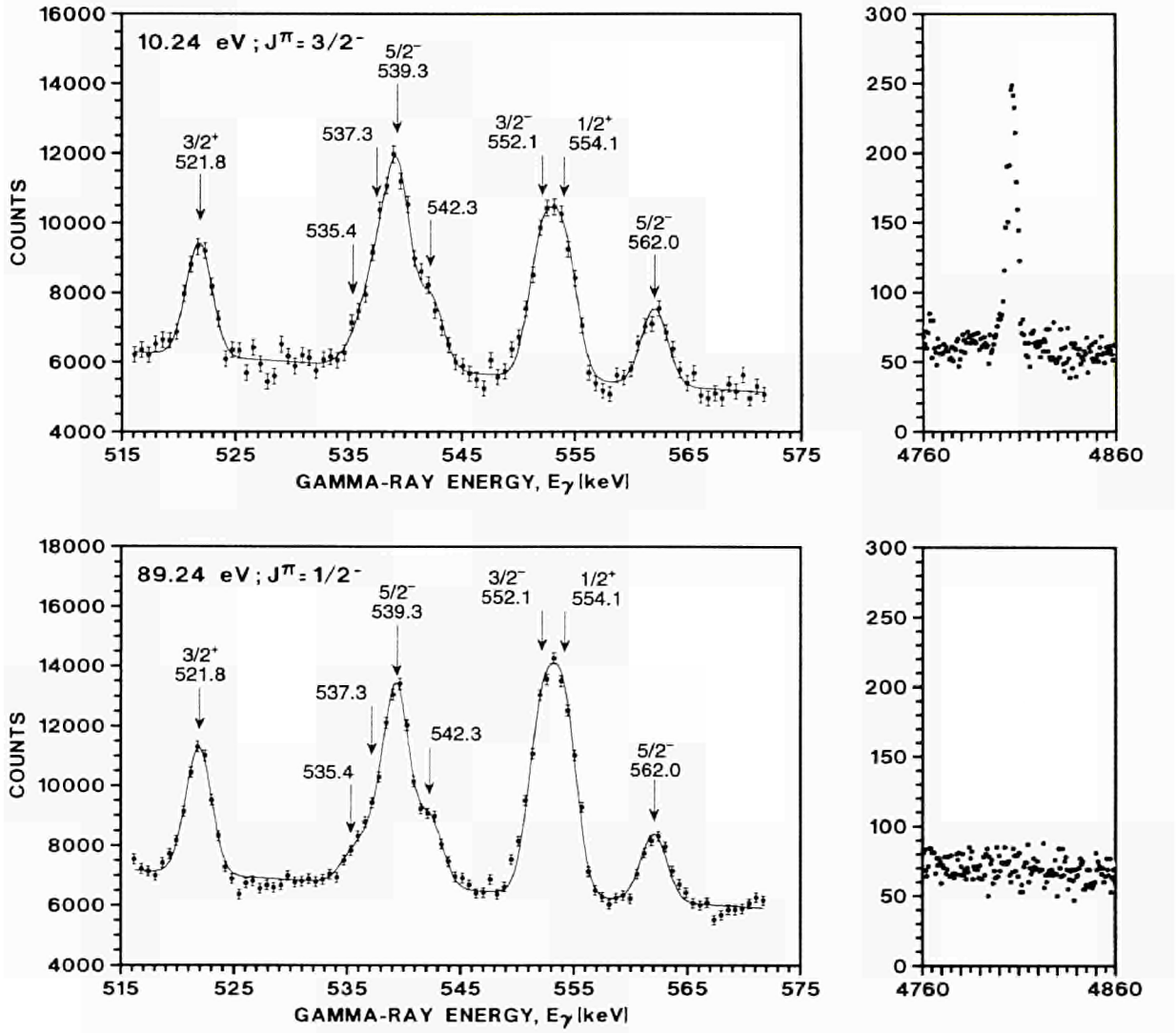

Fig. 20. *Two examples of a fit of the capture gamma-ray spectrum in the 515 - 575 keV energy region for two p-waves of different spin. On the right is shown the region around the 4806 keV transition to the $5/2^+$ ground state, observed only in the p 3/2 resonance*

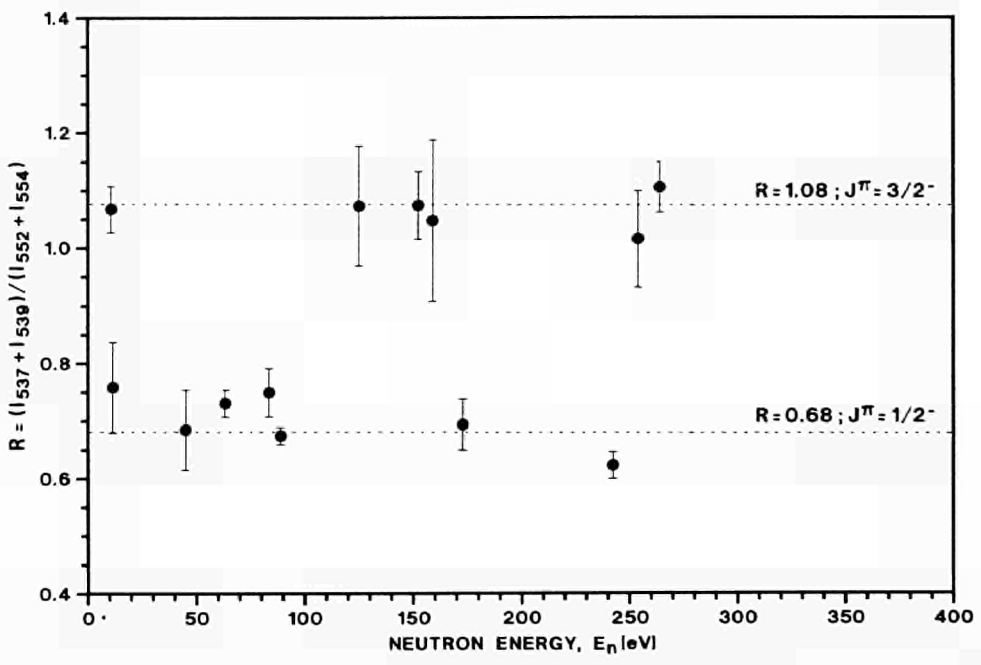

Fig. 21. *The ratios R between the sums of the intensities of the relevant lines plotted versus the resonance energy for 14 p-waves*

Using only the sample of seven assigned $J = 1/2$ resonances, the best estimate of the root-mean-square parity-violating matrix element M can be calculated by following a maximum likelihood procedure:

$$M = 0.56 \quad {}^{+\ 0.32}_{-\ 0.20} \quad \text{meV}.$$

This value confirms the maximum likelihood value of Zhu et al.[1]:

$$M = 0.56 \quad {}^{+\ 0.41}_{-\ 0.20} \quad \text{meV}.$$

The present result, however, has a better confidence interval.

Table 3. List of the present spin assignments for ^{238}U neutron p-waves

E_0[eV]	low level	prim.	adopted	E_0[eV]	low level	prim.	adopted
10.24	3/2	3/2	3/2	152.42	3/2		3/2
11.31	1/2		1/2	158.98	3/2		3/2
19.53		3/2	3/2	173.18	1/2		1/2
45.17	1/2		1/2	242.73	1/2		1/2
63.52	1/2		1/2	253.90	3/2	3/2	3/2
83.68	1/2		1/2	263.94	3/2	3/2	3/2
89.24	1/2		1/2	282.46		3/2	3/2
93.14	3/2	3/2	3/2	351.86		3/2	3/2
98.20		3/2	3/2	439.75		3/2	3/2
124.97	3/2		3/2				

Spin Assignment of Neutron p-Wave Resonances in ^{113}Cd

F. Gunsing*, F. Corvi, K. Athanassopulos, H. Postma**, Yu. Popov***, E.I. Sharapov***

In the search for parity-non-conservation (PNC) in compound nuclei, remarkable results have been obtained in the nuclei ^{238}U and ^{232}Th recently at Los Alamos. It is important to study these effects also for nuclei belonging to other mass regions. A good candidate for a new PNC experiment is ^{113}Cd, which exhibits several low-energy p-wave resonances.

For the target nucleus ^{113}Cd with $J^\pi = 1/2^+$ the situation is more complicated than for the even-even nuclei ^{238}U and ^{232}Th with $J^\pi = 0^+$. In this case, p-waves may take the spin and parity values $J^\pi = 0^-, 1^-$ and 2^- while s-waves can have $J^\pi = 0^+, 1^+$. Moreover, PNC effects can only occur if resonances of opposite parity have both the resonance spin and the channel spin in common. Therefore only resonances with $J^\pi = 1^-$ may produce the effect.

---

* EC Fellow from the Technical University of Delft, The Netherlands
** Visiting Scientist from the Technical University of Delft, The Netherlands
*** Visiting Scientist from the Joint Institute for Nuclear Research, Dubna, Russia

(1) X. Zhu et al., Phys. Rev. C46 (1992) 768

We have performed a $^{113}Cd(n,\gamma)$ experiment in collaboration with JINR, Dubna, to determine the resonance spins, using a cadmium sample of about 100g weight, enriched to 93 % ^{113}Cd. The low-level population method of spin assignment is used. Additional information can be obtained from primary gamma-ray transitions: if a transition to a $J^{\pi} = 0^+$ final state is observed, the corresponding p-wave must have $J^{\pi} = 1^-$. About 20 gigabyte of listmode data have been collected, sorted out into about 200 gamma-ray spectra. Analysis of these data is in progress.

To check the experimental data for the low-level population, Monte-Carlo simulations have been performed on the gamma-ray spectra following the decay of the compound nucleus. A first result shown in Fig. 22 is the ratio of two

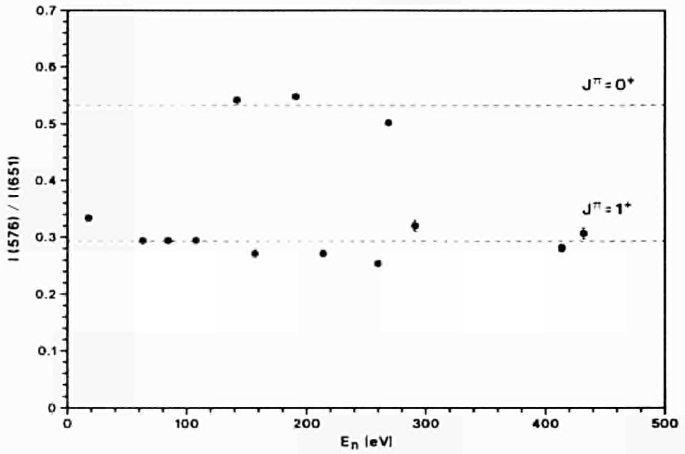

Fig. 22. ***The ratio of two suitable transitions, splitting up into two groups according to the spin. The error bars are within the plot symbols***

appropriate transitions in the case of s-waves, which have much better counting statistics than p-waves. The ratio values are split into two groups, corresponding to spin 0 and 1. Some of the spins of the s-waves are known already from literature and they agree with these measurements.

Resonance Parameters of ^{138}Ba+n from High Resolution Transmission Measurements

A. Brusegan, E. Macavero, C. Van der Vorst

High resolution transmission measurements of ^{138}Ba were performed at 50 m flight distance of Gelina's (1 ns electron burst width) pulsed neutron source.

^{138}Ba plays an important role in the stellar neutron capture rate of the s-process[1]. The measurements were carried out with an enriched (99.2 %, 0.0175 at/b thick)

(1) H. Beer, F. Corvi, A. Mauri, K. Athanassopulos, Intern. Symp. on Nuclear Astrophysics, Karlsruhe, Germany (1992)

barium carbonate sample in order to provide neutron resonance parameters, as resonance energies, neutron widths, spin and parities, of those resonances lying in the energy range from 80 eV up to 200 keV.
The analysis of about 40 resonances was performed with the R-matrix code REFIT[1] including an accurate resolution function of the spectrometer and the 0.6 cm thick Li-glass detector (NE 912) used in these measurements. Due to the extension of the energy range to low energy, the effective potential scattering radius of ^{138}Ba and the presence of negative energy s-wave resonances were investigated.
For the 14 resonances defined as s-wave, the calculated average level spacing and strength function are (15.6 ± 2.3) keV and (0.8 ± 0.3)·10^{-4} respectively.

High Resolution ^{138}Ba(n,γ) Measurements

F. Corvi, H. Beer*, K. Athanassopulos

The stellar neutron capture rate of the isotope ^{138}Ba, with magic neutron number 82, plays a key role in the theory of s-process nucleosynthesis. After a preliminary run[1] covering the energy range up to 100 keV, a second measurement was performed in 1993 at a 58.6 m flight path with a sample thickness N = 0.00486 at/b of barium enriched to 99.8 % ^{138}Ba. The improvement in time-of-flight resolution and sample mass by a factor of two allowed to extend the analysis up to 200 keV. The data were analysed with the code FANAC and values of the capture areas were derived for 138 resonances. The Maxwellian-averaged capture cross section $<\sigma>$ calculated from these results is listed in Table 4 as a function of stellar temperature kT and compared to previous values produced at the ORELA accelerator[3].
The values of Table 14 as well as all other known cross sections and solar s-process abundances were introduced as input of a parametrized s-process model calculation from which the mean neutron exposure τ_0 and the s-process abundances N(136) and N(138) were derived for the two stellar temperatures kT = 12 and 25 keV, respectively. These results are listed in Table 5 together with those calculated from the other data[2]. The ratio of N(138) to the solar abundance N_0(138) of ^{138}Ba is of particular interest: The present value of 0.92 for kT = 12 keV is consistent with a 10 % r-process contribution to the solar abundance, as expected from r-process systematics. Similarly, only the kT = 12 keV value for

---

* Visiting scientist from KfK, Karlsruhe, Germany
(1) M.C. Moxon, AEA-InTec-0470
(1) CBNM Annual Report 92, EUR 15029 EN
(3) A.R. Musgrove et al., Aust. J. Phys. 32 (1979) 213

the s-process ratio N(138)/N(136) agrees with the equivalent ratio measured in various SiC grains found in meteorites[1,2].

Table 4. Values of the Maxwellian-averaged capture cross section from the present work compared to those calculated from the ORELA data

kT [keV]	<σ> [mb] Present work	ORELA	kT [keV]	<σ> [mb] Present work	ORELA
5	13.57 ± 0.47	5.78 ± 1.19	30	4.07 ± 0.20	3.90 ± 0.80
7	10.43 ± 0.38		35	3.78 ± 0.19	3.60 ± 0.74
10	7.99 ± 0.31	5.28 ± 1.08	40	3.55 ± 0.18	3.33 ± 0.68
12	7.01 ± 0.29	5.12 ± 1.04	50	3.20 ± 0.17	2.90 ± 0.59
15	6.03 ± 0.26	4.89 ± 1.00	60	2.94 ± 0.18	2.59 ± 0.53
17	5.56 ± 0.25		70	2.73 ± 0.19	
20	5.04 ± 0.23	4.57 ± 0.94	80	2.56 ± 0.21	
25	4.46 ± 0.21	4.23 ± 0.87	100	2.27 ± 0.26	

Table 5. s-process model calculations

	Present data		ORELA data[1]	
kT [keV]	12	25	12	25
τ_0 [mbarn^{-1})]	0.175 ± 0.006	0.277 ± 0.010	0.194 ± 0.007	0.282 ± 0.010
$\frac{N(138)}{N_0(138)}$	0.92 ± 0.07	1.07 ± 0.09	1.18 ± 0.26	1.12 ± 0.24
$\frac{N(138)}{N(136)}$	6.8 ± 1.1	7.7 ± 0.3	8.4 ± 1.7	8.0 ± 0.9
N(138)/N(136)	6.48 ± 0.59[2]		SiC grain R1CPF	
	6.22 ± 0.08[3]		" KJ	
	6.22 ± 0.08[3]		" KJC	
	6.11 ± 0.09[3]		" KJD	
	5.95 ± 0.09[3]		" KJE	

Both these findings support the assumption that the major neutron source responsible for s-process nucleosynthesis is the reaction $^{13}C(\alpha,n)$ igniting at 12 keV rather than $^{22}Ne(\alpha,n)$ igniting at 25 keV.

(1) U. Ott and F. Begemann, Ap. J. 353 (1990) L 57
(2) C.A. Prombo et al., Ap. J. 410 (1993) 393

Measurement of (n,n'γ) Cross-Sections for Low-Lying Levels of Palladium Isotopes

A. Meister*, G. Rollin, W. Schubert, E. Wattecamps

The gamma ray emission cross-section of low-lying levels of palladium isotopes is measured for neutron energies from 0.2 to 3.3 MeV. The aim of this measurement is to get more precise data on the inelastic scattering cross-section for weakly absorbing fission product nuclides. The inelastic neutron scattering data of these nuclides may yield an important contribution to the nuclear reactor reactivity, but the experimental data base for evaluation of the inelastic scattering cross-section is very poor[1].

The measurements are carried out at the 7 MV Van de Graaff accelerator with a pulsed "white" neutron source utilising the ^{7}Li(p,n) reaction with a thick target. The neutron spectroscopy is done by time-of-flight technique with a 3.871 m flight path. To detect the gamma rays from inelastic scattering a HPGe detector is used covering a broad solid angle (50° full angle aperture at 90° scattering angle). The time resolution is about 10 ns (FWHM) providing an energy resolution of 7 % at 1 MeV and 12 % at 3 MeV.

A ^{10}B disk, almost as large as the palladium disk sample, is located just behind the palladium sample. The ^{10}B(n,αγ) reaction rate is registered simultaneously with the palladium gamma ray emission-rate to convert reaction ratios into a cross-section. A second reference reaction rate measurement relies on hydrogen elastic scattering by measuring with a thin organic scintillation detector (Pilot U) in the collimated beam at about 4.3 m distance from the neutron target. This reference cross section is especially suited above 1 MeV where the ^{10}B(n,αγ) cross-section is small and inaccurate.

Two series of measurements were carried out: one for a neutron energy range up to 2 MeV and another one for neutron energies up to about 3.3 MeV. The measurements are performed in single runs of about 5 h periods during a total data acquisition time of about 100 h. They are processed separately to deduce the 374 keV gamma ray emission cross-section. The normalisation is done with the ^{10}B(n,αγ) cross-section. Part of the single measurements is carried out with inverted sequence of palladium and ^{10}B samples to check the reliability of correction procedures related with gamma-ray detection efficiency.

Fig. 23 shows a gamma ray spectrum recorded within a single run for a time-of-flight window corresponding to 0.5 MeV to 2.1 MeV neutron energy. Most of the lines belong to palladium isotopes. The count rate of the 374 keV line of ^{110}Pd versus neutron energy is shown in Fig. 24. The emission cross-section of this gamma line, shown in Fig. 25, is calibrated with the ^{10}B(n,αγ) cross-section[2]. This curve is the superposition of all excited ^{110}Pd levels decaying by gamma-

(1) H. Gruppelaar, A. Hogenbirk, Report ECN-RX-92-040, ECN Petten (1992)
(2) R.A. Schrack et al., Nucl. Sci. Eng. 114 (1993) 352

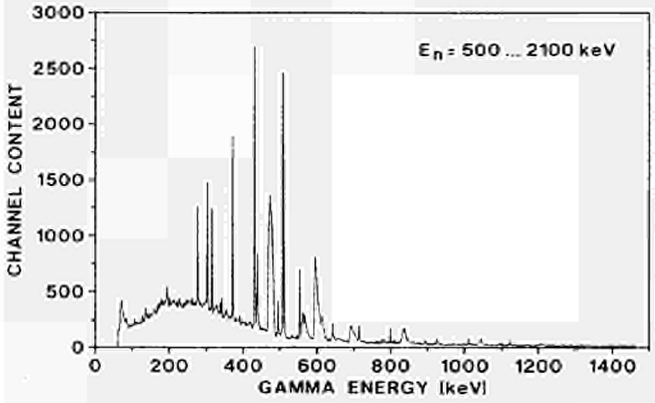

Fig. 23 Gamma-ray spectrum from the palladium sample detected within a time-of-flight window corresponding to 0.5 MeV to 2.1 MeV neutron energy

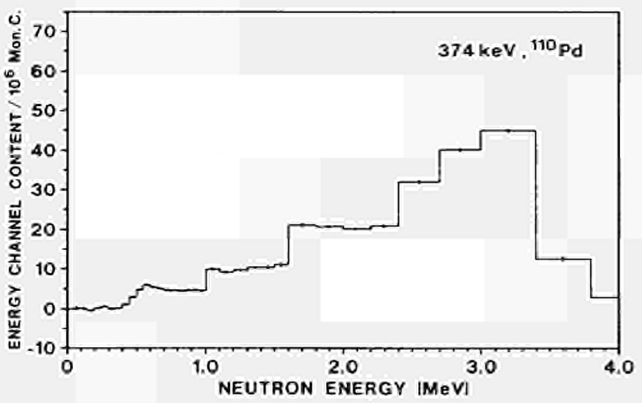

Fig. 24 Count rate of the 374 keV line of ^{110}Pd versus neutron energy. Data are the sum of eight single measurements

ray cascade via the first level at 374 keV. The analysis of separate excitation functions for individual levels is in progress.

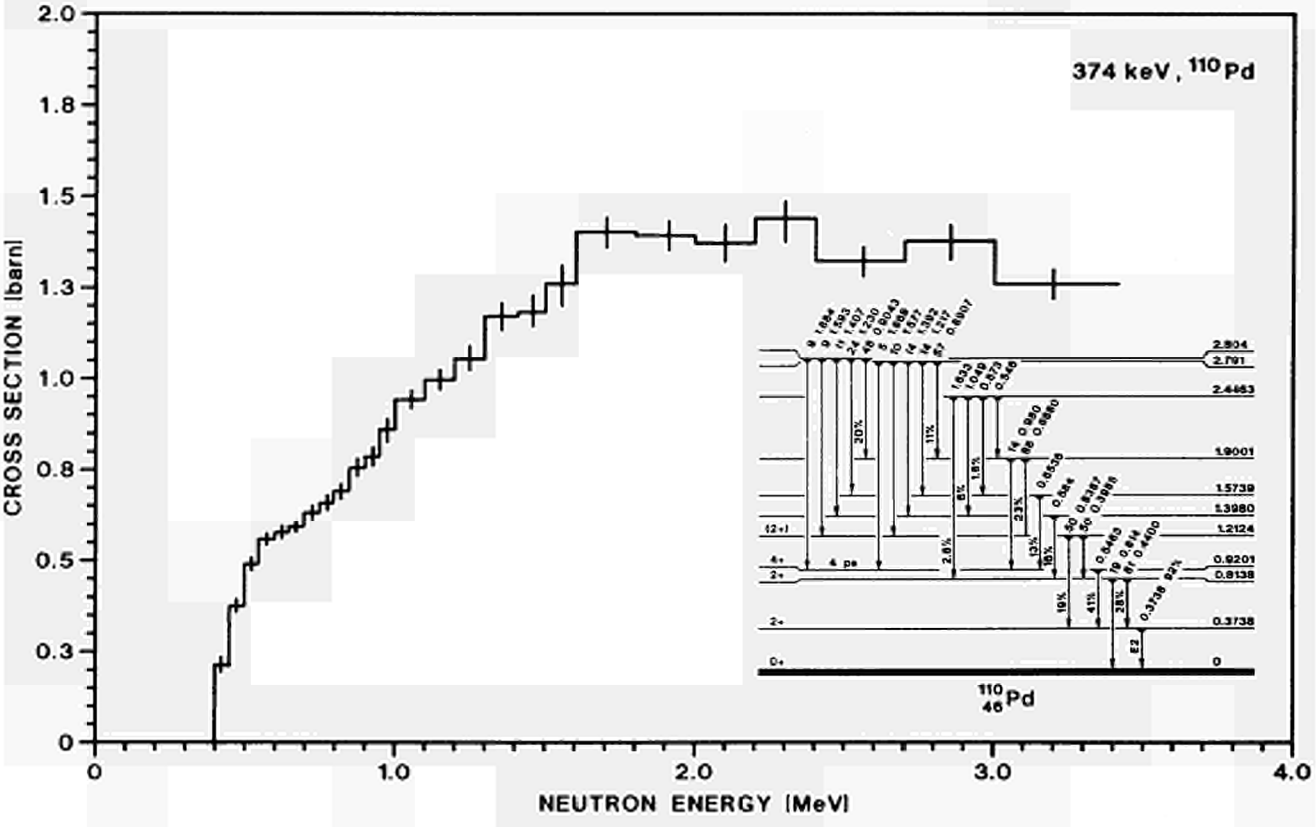

Fig. 25. Gamma ray emission cross section of the 374 keV line of ^{110}Pd calibrated with the ^{10}B(n,αγ) cross-section. Error bars drawn refer to the statistical error only

Calculations on Lattice Vibration Effects in the Doppler Broadening of the 0.18eV Cd Neutron Resonance Cross Section

A. Meister*

A gas model of target nuclei is commonly used to describe the thermal motion of atoms in a solid, but in reality a target atom is surrounded by a medium, whose degrees of freedom can be excited. Lamb[1] found for a target atom bonded in a crystal lattice, that in the limit of weak lattice binding the Doppler broadening can be approximated by a gas model with an effective temperature instead of the real sample temperature. But the question remains, how large the inaccuracy of this approximation can be. This is especially of interest when measurements with high precision exist and when applications require a high accuracy.

For the low-energy uranium resonances measured with oxide samples, where the weak bindinglimit is not satisfied very well, the gas model approach leaves systematic inaccuracies at a level of some per cent at room temperature[2].

A case where the weak binding limit should be satisfied very well is the 0.18 eV resonance of ^{113}Cd in a metallic sample. But there is no information on the size of remaining lattice effects. Therefore an estimate of the possible size of such effects for cadmium has been done. Calculations are carried out for the capture cross section in the vicinity of the 0.18 eV resonance with a model for Doppler broadening in ideal gases and with a model for a crystalline sample. The results of both models are compared.

A single peaked lattice frequency spectrum (Einstein model) with $\hbar\omega_0 = 10$ meV for cadmium metal has been used as well as a more refined representation with three vibration frequencies taking its pattern from the Debye model. The frequencies are deduced from specific heat data. Both representations give the same mean vibrational energy of 1.012*kT per degree of freedom at 300K.

Fig. 26 shows the Doppler broadened capture cross-section in the vicinity of the 0.18 eV resonance. The difference between lattice model and gas model predictions is shown in Fig. 27. The differences between the Doppler broadenings in both models are less than 100 barn. This is about 0.2 % of the maximum resonance cross-section. The differences do not vanish with increasing temperature. The use of an effective temperature instead of the sample temperature has little influence on the difference curves.

For checking the reliability and correctness of the calculations the temperature shifts of neutron resonances experimentally determined elsewhere[2] are used as a benchmark, they are reproduced within the experimental error limits.

---

* Visiting Scientist from Technical University of Dresden, Gemany

(1) W.E. Lamb, Phys. Rev., 55 (1939) 190

(2) A. Meister et al., Nucl. Data for Sci. and Techn., Antwerpen, Belgium (1982)

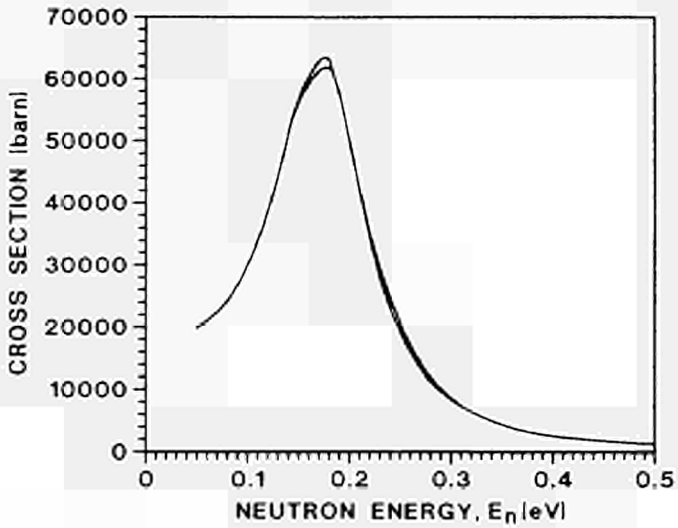

Fig. 26. The capture cross-section in the vicinity of the 0.18 eV resonance of ^{113}Cd as given by the Breit-Wigner formula and accounting for Doppler broadening at 300K

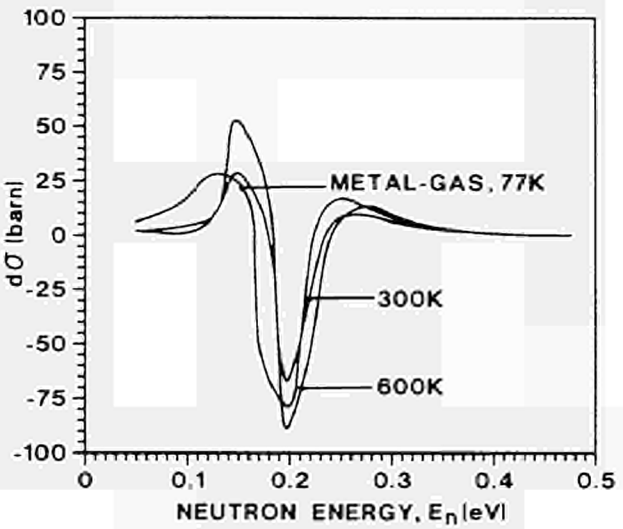

Fig. 27. Differences in the capture cross-section in the vicinity of the 0.18 eV resonance of ^{113}Cd for the Doppler broadening in Cd metal and a gas, with temperatures 77, 300 and 600K

The $^{35}Cl(n,p)^{35}S$, $^{36}Cl(n,p)^{36}S$ and $^{36}Cl(n,\alpha)^{33}P$ Reactions and their Astrophysical Implications

S. Druyts*, C. Wagemans**, R. Barthélémy, J. Van Gils

The $^{35}Cl(n,p)^{35}S$ reaction has been measured up to 100 keV neutron energy, using a gridded ionization chamber. These data were then transformed into stellar reaction rates $N_A<\sigma v>$ as a function of the stellar temperature, as shown in Fig. 28. This figure also gives a comparison with similar data obtained by P. Koehler[1]. Both data sets agree below about 2×10^7 K, but a significant discrepancy can be observed above 10^8K, which is exactly the temperature region of importance for nucleosynthesis processes.

After some preparatory experiments with poorly enriched samples, $^{36}Cl(n,p)^{36}S$ and $^{36}Cl(n,\alpha)^{33}P$ measurements are being performed now on a AgCl sample with an enrichment in ^{36}Cl of 41.7 %. A first series of experiments is taking place at a short flight-path (8 m) using a gridded ionization chamber, which also enables to measure the angular distribution of the protons. A partial time-of-flight spectrum in the neutron energy region from 0.5 to 30 keV is shown in Fig. 29.

---

* EC Fellow from KU Leuven, Belgium; now at University of Gent, Belgium
** University of Gent, Belgium

(1) P. Koehler, Phys. Rev. C44 (1991) 1675

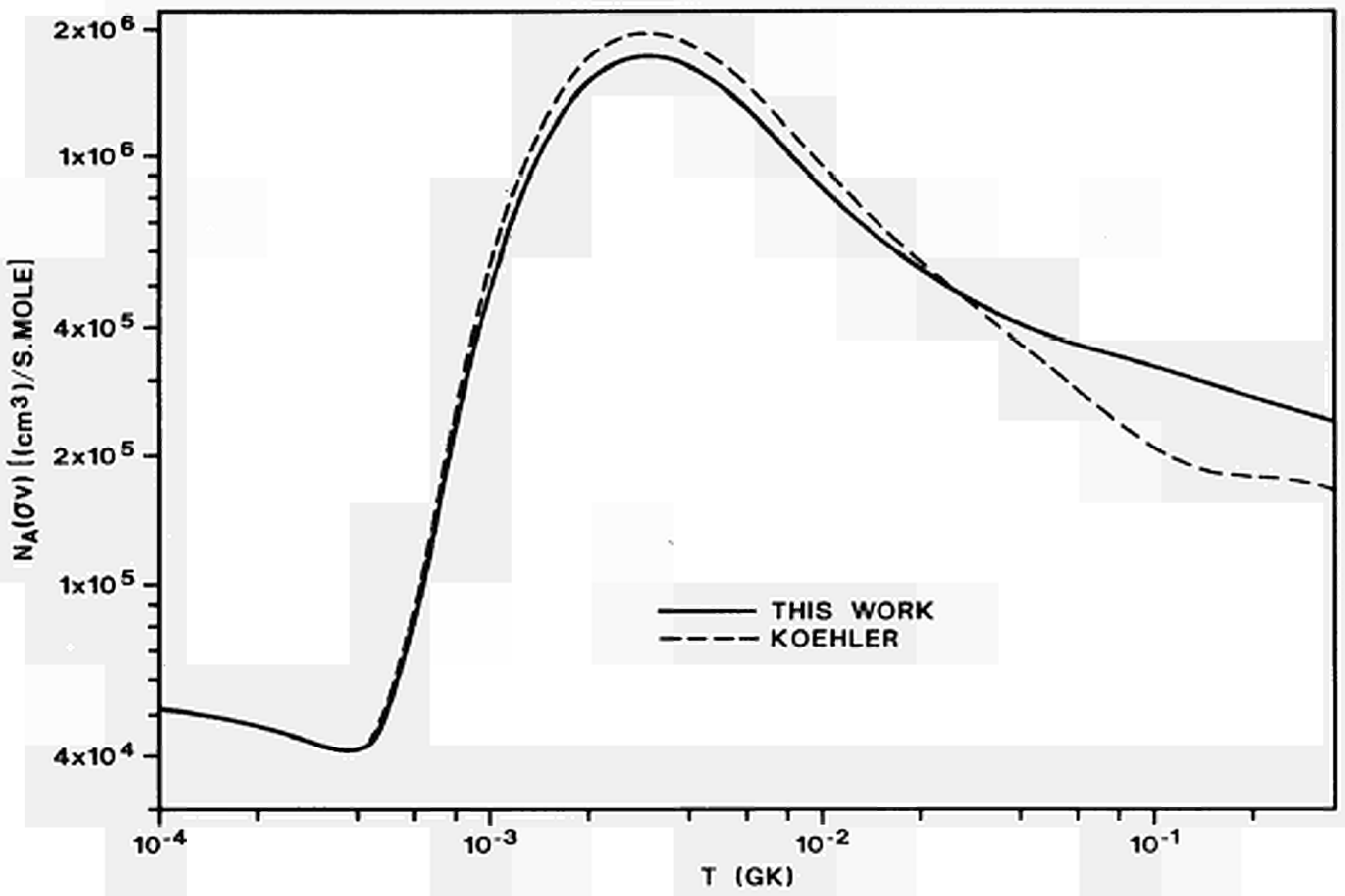

Fig. 28. Comparison of the stellar reaction rates calculated from Koehler's renormalized data and the present work, as a function of the stellar temperature

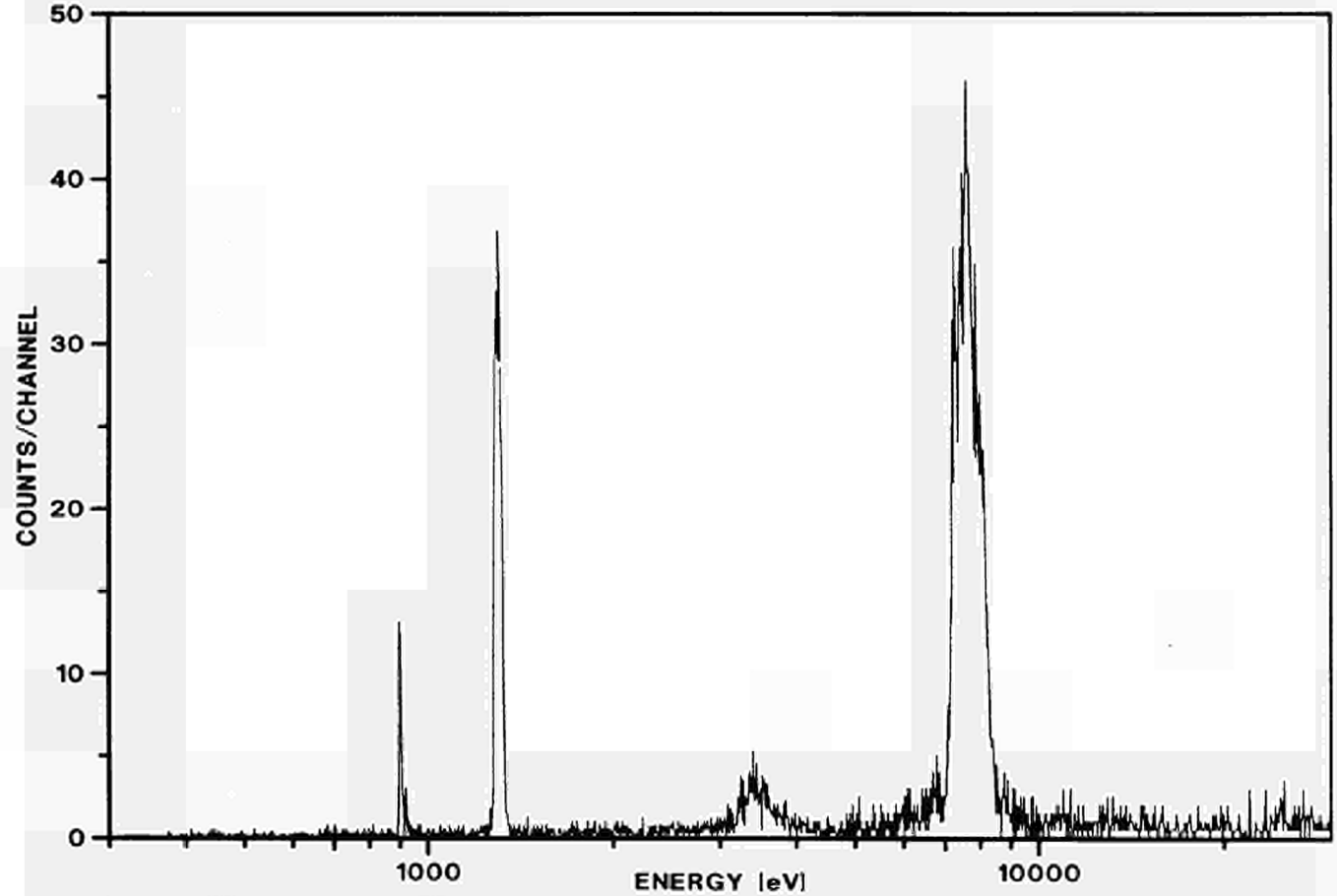

Fig. 29. $^{36}Cl(n,p)$ and $^{36}Cl(n,\alpha)$ resonances in the neutron energy region from 0.5 to 30 keV

Study of the $^{41}Ca(n,x)$ Reactions

C. Wagemans*, S. Druyts**, H. Weigmann, R. Barthélémy, J. Van Gils

After capture of an s-wave neutron in ^{41}Ca, the excited compound nucleus ^{42}Ca can decay by proton and α-particle emission as illustrated schematically in Fig. 30. The dominant $^{41}Ca(n,\alpha_0)^{38}Ar$ reaction has been studied previously using a large surface barrier detector, revealing the occurrence of a large series of strong resonances between 1 keV and 1 MeV. At present, the less prominent $^{41}Ca(n,\alpha_1)^{38}Ar$, $^{41}Ca(n,\gamma\alpha)^{38}Ar$ and $^{41}Ca(n,p)^{41}K$ reactions are being investigated with a gridded ionization chamber.

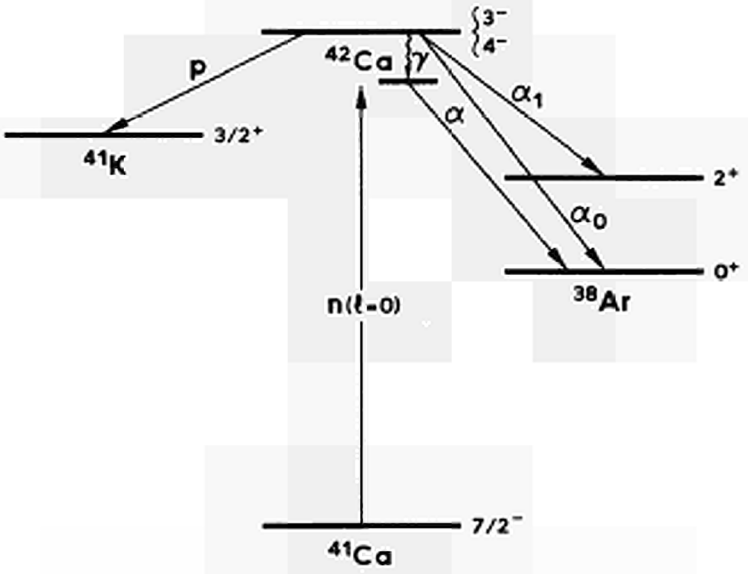

Fig. 30. Schematic representation of the proton and α-decays of the compound nucleus ^{42}Ca formed after (s-wave) neutron capture in ^{41}Ca

* University of Gent, Belgium
** EC Fellow from KU Leuven, Belgium; now at University of Gent, Belgium

NUCLEAR METROLOGY

RADIONUCLIDE METROLOGY

The objective of the work on radionuclide metrology is to advance the experimental know-how in the field of radioactivity. This is done in four major areas: the determination of decay-scheme data, the improvement and development of measurement techniques, the preparation of particular standard and reference samples and the participation in international comparisons and evaluations.

Absolute counting of Alpha-Particle Emitting Samples

B. Denecke

In the frame of an IRMM-NIST intercomparison to measure the α-particle emission rates of three ^{233}U samples, IRMM results with uncertainties of 0.1 % were communicated to the coordinator. The final evaluation is to follow when all results are available.

EUROMET Project: Metrology of ^{192}Ir Brachytherapy Sources

D.F.G. Reher

The EUROMET project concerning the metrology of ^{192}Ir brachytherapy sources has been closed. It was an international co-operation between laboratories (IRMM, JAERI, LPRI, NIRP, NMI, NPL, NRC, NRPA, RUG) and comprised two comparisons of air-kerma rate and activity measurements of ^{192}Ir wires, the calibration of several ionization chambers, the determination of a new value of the half life of ^{192}Ir, a re-evaluation of the decay scheme, and the measurement of the inhomogeneity of ^{192}Ir wires. Ten publications resulted from the work done in this project.

Standardization of a 5 MBq Extended Area Source of ^{56}Co

T. Altzitzoglou, D.F.G. Reher, B. Denecke, G. Grosse

A ^{56}Co solution has been standardized and an extended area source has been prepared out of the same solution. The ^{56}Co solution had been supplied by the SCK/CEN, Mol, Belgium, in the form of $CoCl_2$ in 0.1 N HCl and its activity

concentration was certified as well as the activity of the ^{57}Co and ^{58}Co impurities. The extended area source was intended for the calibration of a detection system, employed in the very high resolution transmission measurements of $^{58}Ni + n$ and $^{60}Ni + n$ at GELINA.

It was prepared by quantitative deposition of drops of the radioactive solution in a homogeneous pattern on a 0.5 mm thick membrane filter (Sartorius 13400, 73 mm diameter). After drying, the source was backed with a Kapton and a polyethylene foil and then sealed between two aluminium discs of 80 mm diameter and 0.5 mm thickness.

For the standardization of the solution at IRMM, more than 20 quantitative sources were prepared from the original solution and measurements were carried out employing γ-ray spectrometry, $4\pi\gamma$-counting, and $4\pi\beta$-γ-coincidence counting. All three methods gave coherent results with uncertainties below 1.5 %. However, the weighted average of the results is about 8 % lower than the certified value quoted by the supplier.

Low-Energy X-ray Standard Sources

B. Denecke, G. Grosse

Three ^{55}Fe excitation sources were assembled and sealed with thin beryllium foils forming a closed source type. Ten sets of fluorescence targets containing the elements aluminium, silicon, sulfur, phosphorus, calcium and titanium are finished. The standardisation of the sources is in progress. A prototype of the storage container and the necessary tools are ready.

The windowless Si(Li) spectrometer was repaired by the manufacturer and the detector was galvanically isolated from the UHV system to reduce noise.

Absolute Activity Measurements with the Windowless 4π-CsI(Tl)-Sandwich Spectrometer

B. Denecke

A report on the performance of the 4π-CsI(Tl)-sandwich spectrometer in the standardization of ^{57}Co, ^{109}Cd, ^{125}I, ^{152}Eu and ^{192}Ir is being prepared. This spectrometer is particularly useful when measuring absolute activity of radionuclide samples having a complex decay scheme. The windowless scintillation crystals have nearly 100 % detection efficiency for photons and charged particles. Accuracies of better than 0.3 % were reached.

Energy Resolution of Si Detectors to Alpha Particles

E. Steinbauer*, G. Bortels

The response of particle implanted passivated silicon (PIPS) detectors to alpha particles, emitted perpendicularly from the surface of a thin layer of radionuclides, was studied with respect to the statistical processes involved. Measurements were done using a 50 mm^2 PIPS detector with dead layer thickness of (48 ± 5) nm and a thin vacuum-sublimed source of ^{148}Gd, ^{238}Pu and ^{244}Cm. The thin source introduces energy straggling and a small asymmetry in the energy distribution, f_{src}, of the emitted alpha particles.

In the detector's dead layer, alpha particles produce electronic energy-loss straggling which has a Gaussian probability density function (PDF), $G_{d,s}$. It is energy independent for energies of a few MeV. Nuclear stopping in a thin dead layer can be neglected. Variations in the dead layer thickness will broaden the response function.

In the sensitive volume of the detector, the kinetic energy of the alpha particle goes into two processes: - electronic excitation and ionization (electronic stopping of projectile and recoils) and - crystal damage and lattice vibrations (non-electronic losses). The first type of random process was simulated using a Monte Carlo code to calculate its asymmetric PDF, $f_{s,e}$. It is responsible for the asymmetry of the alpha peaks. The process subsequently ends up in an electron-hole pair creation which has a Gaussian PDF, $G_{s,p}$. Trapping and recombination of charge carriers are negligible. In the charge detection process, a Gaussian amplifier noise function, G_{amp}, is introduced.

The detector response function is the convolution of $G_{d,s}$, $G_{s,p}$, G_{amp} and $f_{s,e}$. The latter function $f_{s,e}$ can be fitted by a Gaussian convulated with a sum of exponentials. The calculated response is in full agreement with the experimental alpha peak obtained for an ultra thin source and low measurement solid angle.

Results are given in Table 6. In the limit of a detector with zero dead layer thickness and a cryogenic preamplifier (0.5 keV noise FWHM) the calculated ultimate energy resolutions indicate that the gain in resolution is not substantial.

Measurement of the Fano factor

E. Steinbauer*, G. Bortels

The Fano factor was introduced to bridge the gap between the energy resolution, calculated from electron-hole pair statistics, and experiment. The model which describes the response of silicon detectors to alpha particles can also be applied to

* University of Linz, Austria

Table 6. Contribution of various random processes, associated with the detection of alpha particles, to resolution (FWHM in keV) of the alpha peak. ΔE_{tot} and ΔE_{mea} are the calculated and measured FWHM, respectively. Due to the asymmetry of $f_{s,e}$, ΔE^2_{tot} is not equal to the sum of squares of its components

Ion	Energy [keV]	f_{src}	$G_{d,s}$	$f_{s,e}$	$G_{s,p}$	G_{amp}	ΔE_{tot}	ΔE_{mea}	Ultimate
$^4He^{++}$	3183	2.0	4.2	3.4	2.9	2.8	7.9	7.6	6.1
	5499	1.6	4.2	3.8	3.8	2.8	8.5	8.5	6.9
	5808	1.3	4.2	3.8	3.9	2.8	8.6	8.5	7.0

electrons. In that case several processes are negligibly small: energy loss and straggling in the dead layer of the detector, non-electronic losses (small electron mass), and trapping and recombination losses of charge carriers when the detector bias is set for saturation. The complete electron energy ends up in electronic losses. The detector response function therefore contains only two components which are both Gaussian: charge carrier statistics and amplifier noise. The variance of the response function is given by

$$\sigma^2 = w E_e F + \sigma^2_{amp}$$

with E_e the electron energy, w = 3.81 eV per electron-hole pair at liquid nitrogen temperature and F the Fano factor. Electron backscattering and bremsstrahlung produce some spectrum deformation and have to be considered in the peak fitting. In the measurements a 50 mm^2 PIPS detector with a depletion layer of approximately 900 µm thickness was used. Monoenergetic K-shell conversion electrons from thin layers of ^{133}Ba (320.0 keV), ^{137}Cs (624.2 keV) and ^{207}Bi (481.6 and 975.6 keV) were measured. The detector and preamplifier were kept at liquid nitrogen temperature. No effect from incomplete charge collection was observed for a bias from 90 to 180 V, and no peak shift was observed when tilting the sources by 60°. The electron peaks were fitted with the convolution function of a Gaussian and the function

$$f(u) = B_1 + B_2\,\theta(-u) + B_3 e^{\frac{u}{\tau}}\,\theta(-u)$$

with constants B_i and step function $\theta(u) = 0$ for $u < 0$ and 1 for $u \geq 0$.
The first two terms care for a constant background and electron backscattering, and the third term accounts for bremsstrahlung. Fig. 31 shows the measured response function for 975.6 keV K-shell conversion electrons in the decay of ^{207}Bi. The Fano factor, F = 0.134 ± 0.007, was obtained from the Gaussian component after subtracting the electronic noise which was 800 eV at FWHM.

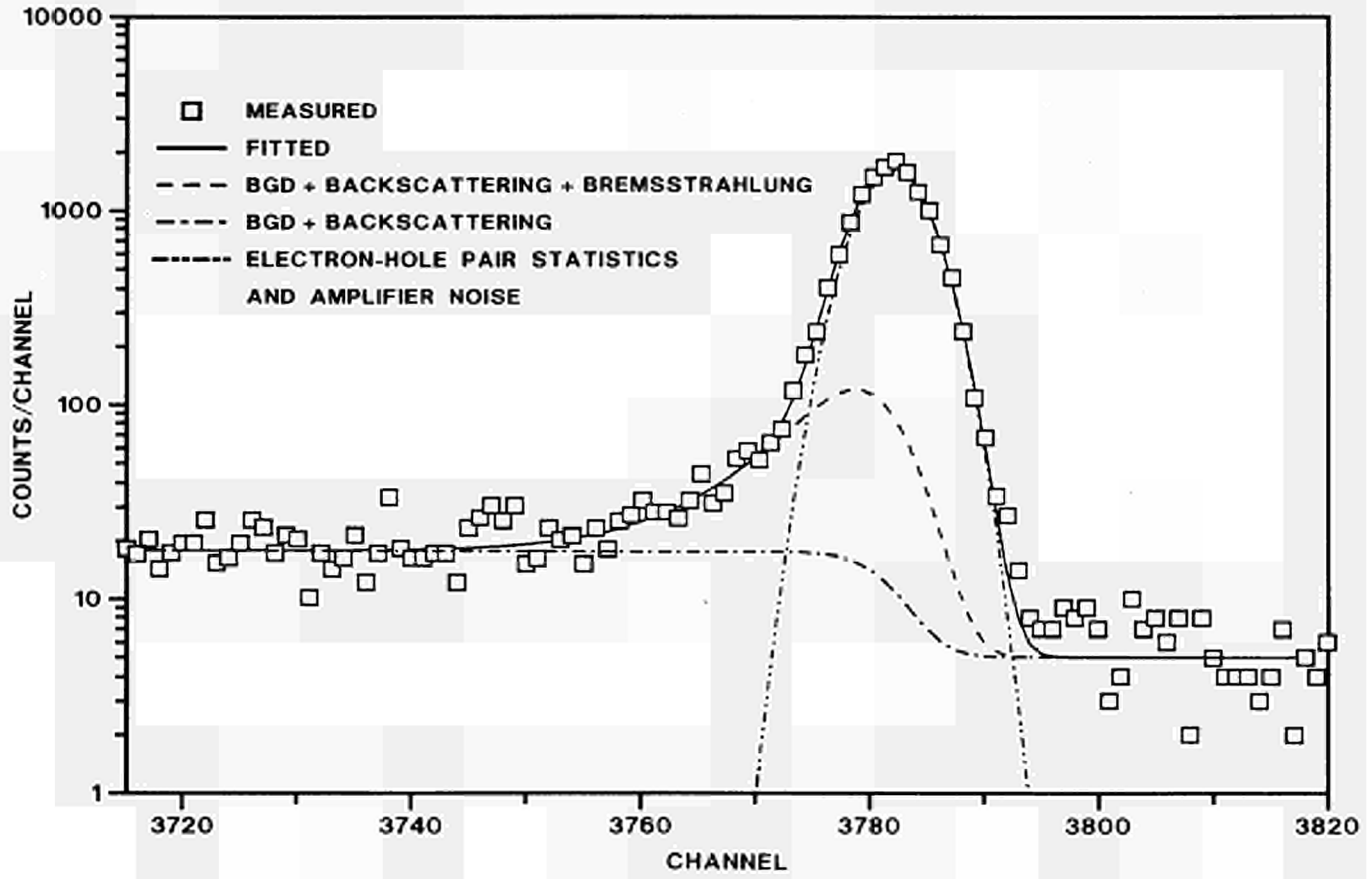

Fig. 31. Response function of a 50 mm^2 PIPS detector for K-shell conversion electrons from the ^{207}Bi decay at 975.6 keV

Investigation of the Natural Radioactivity in Volcanic Rock Samples using a Low Background γ-ray Spectrometer

R. Wordel, D. Mouchel, V.A. Solé*, J. Hoogewerff**, J. Hertogen***

A low-level HPGe detection system, operated at ground level, was used to investigate samples originating from the Eastern Sunda Volcanic Arc in Eastern Indonesia, where the subduction of the Australian plate under the Asian plate takes place and where the depth of the Australian plate varies from 100 to 300 km. The powdered rock samples were in cylindrical containers and varied from about 20 to 200 cm^3. An efficiency calibration of the detection system was performed with a powdered solid source, spiked with suitable radionuclides and having a chemical composition close to that of the investigated samples. Efficiency calculations were also done by a Monte Carlo simulation to calculate detector efficiencies for cylindrical sources. To obtain the full-energy-peak efficiency, ε_γ, for the different measured samples corrections for the actual geometry, self-absorption and absorption have been applied in this Monte Carlo program.

* University of Valencia, Spain
** University of Utrecht, The Netherlands
*** KU Leuven, Belgium

The concentrations and disequilibria of radionuclides from the natural decay chains in the samples were compared to those in a well known reference sample. A correlation between some of the radionuclide concentrations and the subducting depth under the volcanoes was observed (Table 7).

Table 7. Decay rates for ^{226}Ra measured by low level γ-ray spectrometry using the 295 keV γ-ray peak (second column), and ^{238}U determined by Instrumental Neutron Activation Analysis (third column). The fourth column shows the decay rate ratios of these two nuclides. In secular equilibirum this ratio should be 1. The value for sample one clearly shows breaking of equilibrium. In this case an anomalous enrichment of ^{226}Ra is observed. In the last column is shown the subducting depth of the Australian plate under the Asian one

Sample	Disintegration rate ^{226}Ra γ-spectr. [Bq/kg]	Disintegration rate ^{238}U INAA [Bq/kg]	$\frac{N_0(^{226}Ra)}{N_0(^{238}U)}$	Depth of plate [km] ± 10 km
1 Werung	9.5 ± 1.0	2.24 ± 0.05	4.2 ± 0.5	120
2 Lewotolo	72 ± 5	58 ± 1	1.2 ± 0.1	160
3a Batu Tara	39 ± 3	36.1 ± 0.8	1.1 ± 0.1	220
3b Batu Tara	49 ± 4	49 ± 1	1.0 ± 0.1	220
Reference	17 ± 1	18.6 ± 0.4	0.91 ± 0.09	--

Measurement of Low-Level Radioactivity in Archaeological Ceramics

R. Wordel, D. Mouchel, U. Wagner*

On request by and in collaboration with the Technical University of München, measurements of low-level radioactivity in archaeological ceramics of Celtic origin, using a low-level HPGe γ-ray detection system were done. The samples were excavated at a site close to Manching (Germany). The aim of the measurements is to characterize the clay from which the pottery was made by looking for a possible disequilibrium in the natural decay series.

Investigation of Natural and Anthropogenic Radionuclides in Soil and River Sediment

D. Mouchel, R. Wordel

Low-level radioactivity originating from natural and anthropogenic radionuclides was measured in sandy soils, river sediments and a few biological samples. Some samples were collected at an old industrial site, others were taken from a

* Technical University of München, Germany

supposedly undisturbed region. Seventeen samples, measured at sea level using a low-background HPGe detector and Marinelli beaker geometry, were analysed. Nuclides from the Chernobyl fall-out were observed in the various surface samples as well as cosmogenic (^{7}Be) and natural (^{40}K) radionuclides. Concentrations of ^{232}Th in the various samples were in a narrow range around 8 Bq/kg. Variations up to a factor 100 were observed for the ^{226}Ra concentrations in the soils; about 12 Bq at 7 m depth, up to 1100 Bq in a contaminated river sediment. Detection limits of the measurement system are: about 1 µg/g for thorium and uranium, and of the order of 0.1 Bq/kg for ^{137}Cs.

Low Level Gamma-ray Measurements in a 225 m Deep Underground Laboratory

R. Wordel, D. Mouchel, A. Bonne*, P. Meynendonckx*, H. Vanmarcke*

The background of a low-level HP Ge detection system has been reduced by placing it into an underground research facility at SCK/CEN, Mol, Belgium, at a depth of about 225 m, which corresponds to approximately 500 m water equivalent.

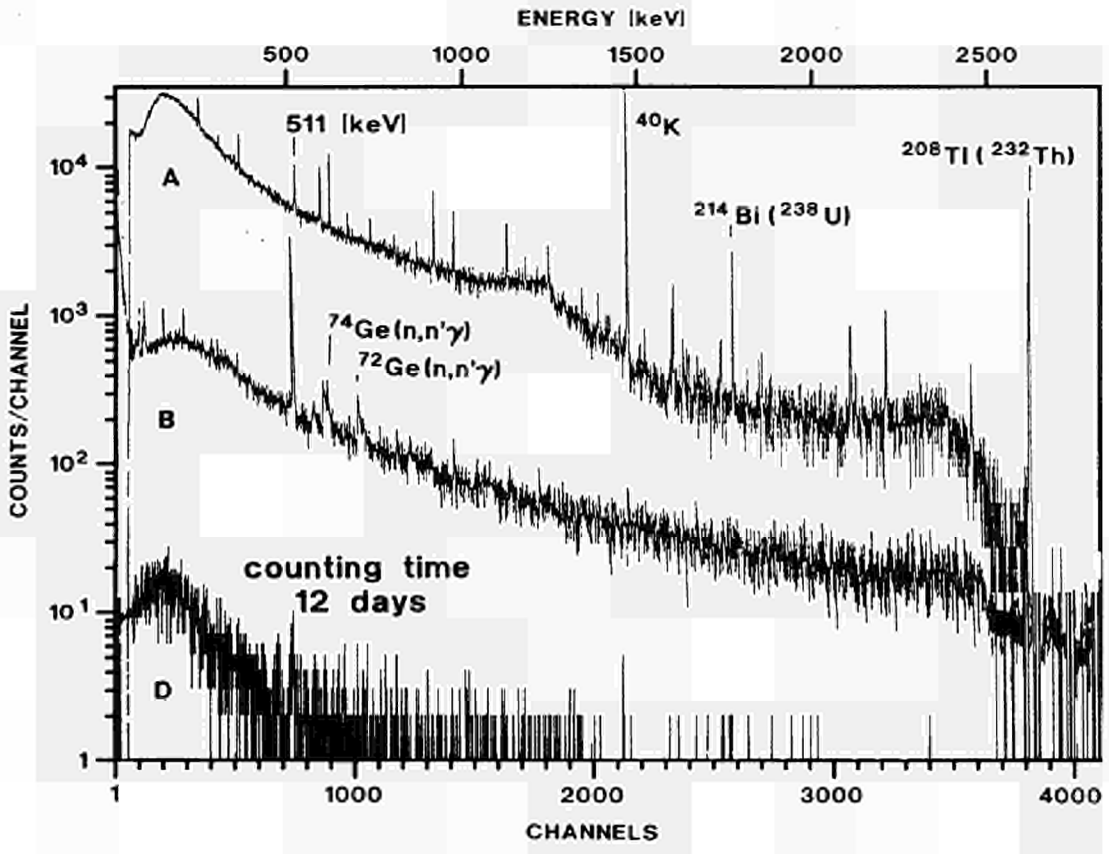

Fig. 32. ***Background spectra: A: recorded at underground laboratory without shielding. B: background at ground level with the shielding. C: identical shielding at the underground laboratory with additional copper for radon removal***

At ground level two lead shields, one of which with 1 Bq/kg intrinsic activity, surrounded the 100 cm^3 germanium crystal and reduced the background radioactivity, within the energy interval 3 to 2800 keV, by a factor of 100. The remaining count rate was mainly attributable to the influence of cosmic rays.
In the underground laboratory empty space in the system was filled up with electrolytic copper to eliminate the influence of radon. Thus, the count rate of $(0.00666 \pm 0.00006)\ s^{-1}$ within the above mentioned energy interval represents an additional reduction factor of 90 of the background, again mainly attributable to the elimination of the cosmic rays (Fig. 32).
Background count rates for selected energy regions are given in Table 8, for comparison of different germanium detection systems. They demonstrate the reduction of neutron activation peaks and the improvement of the sensitivity to particular radionuclides.

Table 8. Background of the germanium detection system at two locations

Ground level (IRMM, 24 days counting time, spectrum B in Fig. 39)		
count rate/energy interval at 150 keV	(2.73 ± 0.03)	[counts/keV·h]
count rate/energy interval at 1 MeV	(0.462 ± 0.012)	[counts/keV·h]
count rate/energy interval at 2.75 MeV	(0.102 ± 0.006)	[counts/keV·h]
count rate 511 keV peak	(38.9 ± 0.9)	[counts/h]
Underground (12 days counting time, spectrum C in Fig. 39)		
count rate/energy interval at 150 keV	(0.0822 ± 0.0066)	[counts/keV·h]
count rate/energy interval at 1 MeV	(0.0018 ± 0.0009)	[counts/keV·h]
count rate 511 keV peak	(0.2 ± 0.1)	[counts/h]

* SCK/CEN, Mol, Belgium

TECHNICAL APPENDIX

Electron Linear Accelerator

J.-M. Salomé

The GELINA electron beam was available during 2787 hours for physics experiments.

Neutrons are produced in a rotary uranium target via (γ,n) and (γ,f) reactions. According to the requested neutron energies, various moderators are placed on both sides of the target. Twelve flight paths are equipped for neutron time-of-flight experiments. On the average, 6.4 neutron beams were used simultaneously when GELINA was operated at very short bursts and 5.2 of them when operated in other conditions.

On the direct beam line, some experiments of optical transition radiation (OTR) and Smith-Purcell effect were achieved. OTR is a very useful method to measure on line various parameters of the electron beam. This system will be routinely used when the beam will be available for radiation physics experiments. Although the quality of the beam is rather poor, Smith-Purcell radiation at optical wavelengths was observed using beams of electrons with energies between 35 and 110 MeV.

The operation of the accelerator was interrupted in April during about two weeks to replace the O-rings of the compression magnet. Due to the very bad conditions of focussing coils along the accelerating sections, the electron beam is rather large and grazes the vacuum chamber at several positions. The γ-n radiation induces hardening of the organic O-rings which reduces the tightness of the vessel. Special metallic rings have been ordered and should be placed next year to solve this problem.

The measurement programme had also to be interrupted during more than one month to allow the construction of the new radiation physics laboratory.

The refurbishment of the Linac ordered end of 1992 and which consists essentially in the replacement of two sections and all the focussing coils is progressing normally. The present Linac will be operated up to August 1994. A shut down of six months is scheduled for the installation of the new sections and corresponding equipment.

Radiation Physics Laboratory
J.-M. Salomé, P. Rullhusen

Planning and construction of the new radiation physics laboratory (RPL) outside the neutron target hall is progressing on schedule. The experimental room has been built. A provisional beamline has been installed at 0°. Radiation-level measurements for a series of different absorbers have been carried out while the neutron-production programme was running. As a result two radiation beam shutters in vacuum are being designed to protect users working in the RPL. The beam transport system capable to switch from neutron production inside the neutron target hall to photon production in the RPL has been designed and the relevant parts have been ordered. This system includes also a modification of the current moderators.
A field mapping of an old 120° dipole has been performed. At present computer simulations are run in order to see if the pole pieces can be modified in a way suitable to dump a 200 MeV electron beam with rather large energy dispersion and moderate emittance into the beam catcher of the RPL.
For the general layout of the interlock system the health physics service of ESRF has been contacted and a new system including the accelerator, the neutron target hall and the RPL is being designed.

Radiation Physics
R. Cools, O. Haeberlé*, N. Maene**, F. Poortmans**, H. Riemenschneider, P. Rullhusen, J-M. Salomé, F. Van Reeth

Optical Transition Radiation

The system for beam diagnostics using optical transition radiation (OTR) has been improved. On the direct beamline of GELINA a remotely controlled sample changer has been installed which allows to use different types of foils for OTR measurements. It uses stepping motors controlled by a commercial microprocessor interface designed for CAM/CNC applications. The interface is linked via a serial line to a Macintosh computer. The user software - adapted to the special needs of OTR measurements - was developed in-house and is written using the LabView platform. The OTR light is observed with two CCD cameras in a separate room about 8 m away from the beamline using a system of radiation resistant lenses and mirrors. The signals are captured and analyzed on the same Macintosh computer using a self-written software package based on routines from the public-

---

* EC Fellow from University of Strasbourg, France
** VITO, Mol, Belgium

domain software Image. This system allows to display on-line the shape of the electron beam and the angular distribution of the OTR emission. From these images information on the electron energy and the beam emittance are obtained.

Smith-Purcell Effect

An experiment on Smith-Purcell (SP) radiation at optical wavelengths has been carried out using 35-110 MeV electrons. Two types of gratings were used: a holographic sinusoidal grating and a ruled blazed grating, both fabricated in glass with an Al coating and with 1800 lines/mm. No experiments had been done until then with such high-energy electrons. Therefore, one of the main intentions of the experiment was to see (i) if radiation damage to the grating surface can be sufficiently reduced to perform the experiment , (ii) if emission of SP radiation at optical wavelengths by highly relativistic electrons is strong enough to be seen with CCD cameras and (iii) if electron beams of rather moderate beam emittance as they are produced by GELINA can be used for SP experiments.

The gratings were shielded against the electron beam by 20 mm of molybdenum. SP radiation was observed at 90° to the beam axis using the OTR setup. The beam emittance measured with the OTR system was of the order of 10 mm mrad in most cases. At average beam currents of 0.5 or 1 μA the SP radiation was bright enough to be measured with the OTR system. Apart from SP radiation also Cherenkov radiation from electrons hitting the grating was observed. Contrary to SP radiation, the Cherenkov light is less polarized and not monochromatic. The polarization was determined with a commercial linear-polarization filter and the spectral distribution was measured using a set of narrow-band filters ($\Delta\lambda$ = 10 nm). Fig. 33a shows the experimental results observed with a 110 MeV electron beam. In the first graph the intensity observed with the set of narrow-band filters is displayed. For the applied experimental configuration the SP radiation is expected at wavelengths of (559 $\pm$ 10) nm. In the second graph, Fig. 33b, the results of a polarization measurement are shown. The solid line is the theoretically expected polarization curve for a pure H-polarized radiation.

The experiments have proven that electron beams of energies up to 110 MeV and moderate beam emittance can be used to produce SP radiation. However, an analysis of the grating surface using an electron microscope revealed considerable radiation damage. The profile of the holographic grating was destroyed and on the surface of the ruled grating recrystallization of the aluminium coating could be observed. Thus, gratings fabricated in glass and shielded against the electron beam may be used for short SP measurements at low beam currents but solid metallic gratings should be used for long-term measurements at high beam currents.

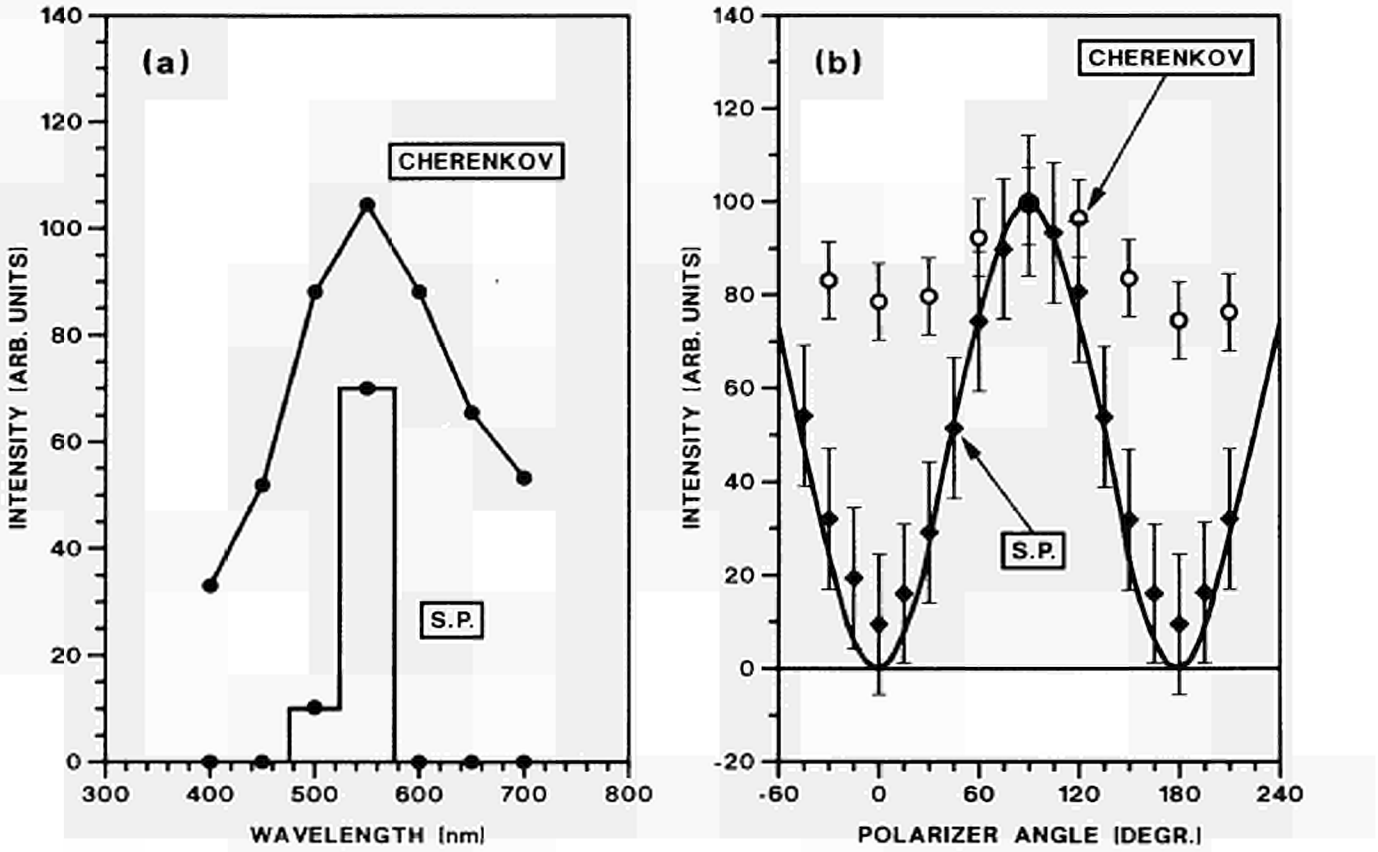

Fig. 33. ***Smith-Purcell radiation generated by a 110 MeV electron beam. (a) Spectral distribution measured with narrow-band filters. Predicted wavelength of SP radiation: (559 ± 10) nm. (b) Measurement of the linear polarization. Solid line: theoretical prediction for a pure H-polarized radiation. Values normalized at 90°***

Van de Graaff Accelerators

A. Crametz, P. Falque, J. Leonard, W. Schubert

The total working time of the two accelerators was 4022 hours. Both accelerators were operated simultaneously during 770 hours. The ratio of neutron to non-neutron activities was 1.42. For 81 % of the total time, the accelerators were used for experiments.

The RF ion source of the CN has been replaced four times, two of which were due to a leak at the welding glass-metal of the radiator after few hours of operation.

During the preparatory tests for the acceleration of a ^{14}N beam, using the RF source, the analyzing magnet ((M × E): $q^2 = 24$), and an intensity in the coils of 210 A, a target current of 0.5 μA for $^{14}N^+$ of 1.0 MeV and of 30 nA for $^{14}N^{++}$ having a quadruple energy has been obtained.

Unfortunately it was not possible to order all the lenses needed for the $^{15}N^+$ beam in the 31 m long tube. However, the third target hall is now ready and starting operation is planned for summer 1994.

Materials Analysis Techniques at the 7 MV VG

G. Giorginis, A. Crametz, M. Conti, P. Misaelides*, P. Courel**

The cross section evaluation programme concerning reactions used in the Nuclear Reaction Analysis (NRA) technique for the determination of light elements (boron, carbon, nitrogen, oxygen) concentrations in advanced materials has been continued. Improved experimental conditions allowed to perform more complete and precise measurements and to derive absolute cross sections of (α,p) nuclear reactions on boron and nitrogen used for the characterization of boron-nitride thin films. The energy spectra of these reactions are characterized by well isolated proton lines (Fig. 34).

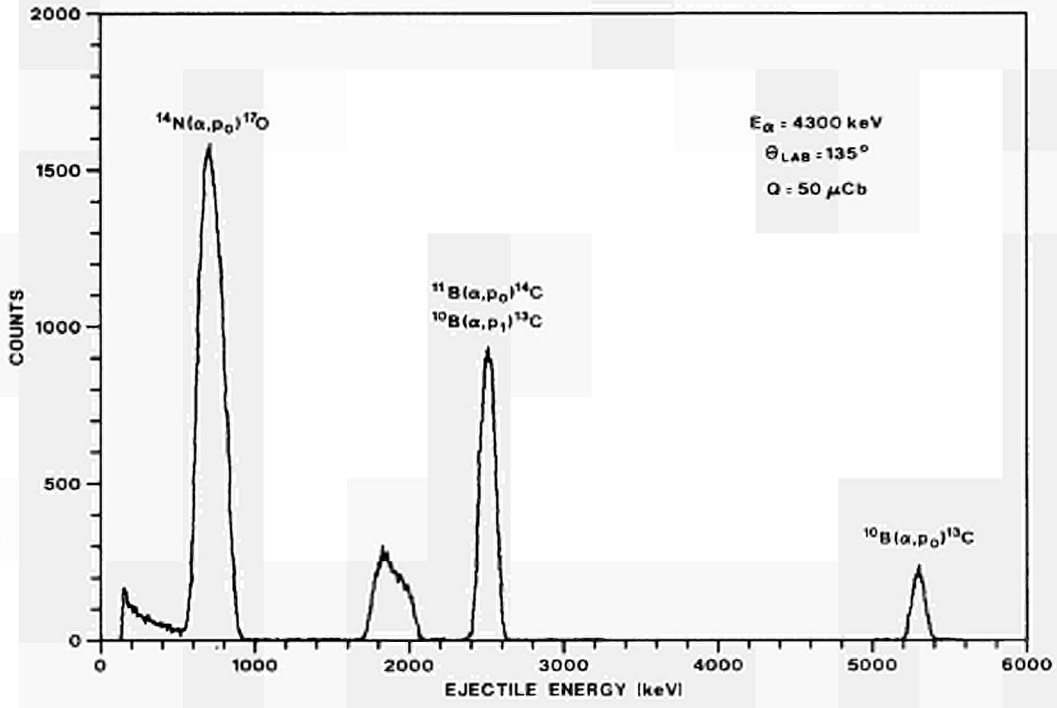

Fig. 34. ***Energy spectrum from the α-particle bombardment of a BN-coating on a stainless steel substrate***

The excitation functions of the $^{14}N(\alpha,p_0)^{17}O$, $^{10}B(\alpha,p_0)^{13}C$, $^{11}B(\alpha,p_0)^{14}C$ and $^{10}B(\alpha,p_1)^{13}C$ reactions measured in the energy range 4-5 MeV and at laboratory scattering angle of 135°, are shown in Fig. 35. The cross section errors, including uncertainties of the target thickness, beam charge collection, solid angle, and statistical errors are of the order of 7 % at the points of low statistics.

The composition of a BN-layer can be deduced from the energy spectra of the ejectile using the measured cross sections. Preliminary results are presented in Fig. 36 for each of the proton lines of Fig. 34. Starting from a rough estimate for the value of the target stoichiometry a simulation programme fits the calculated

* Aristotle University of Thessaloniki, Greece
** EC Fellow from University of Paris, France

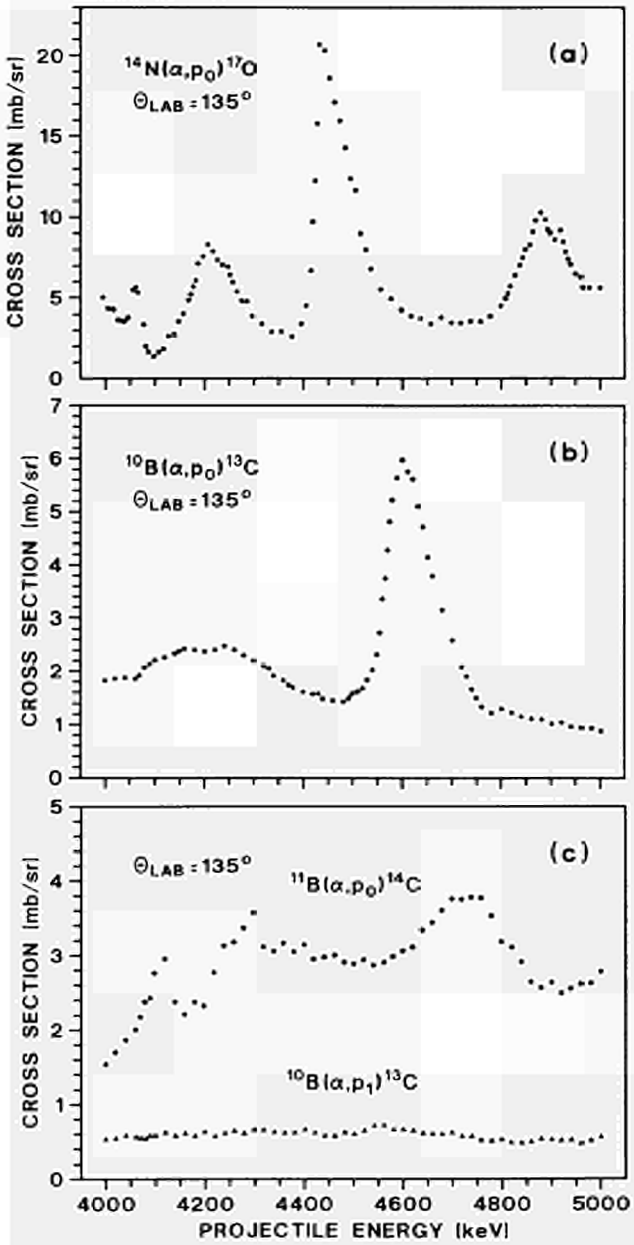

Fig. 35. Excitation functions of (a) the $^{14}N(\alpha,p_0)^{17}O$, (b) the $^{10}B(\alpha,p_0)^{13}C$ and (c) the $^{11}B(\alpha,p_0)^{14}C$ and $^{10}B(\alpha,p_1)^{13}C$ reactions respectively measured at a laboratory scattering angle $\Theta_L = 135°$

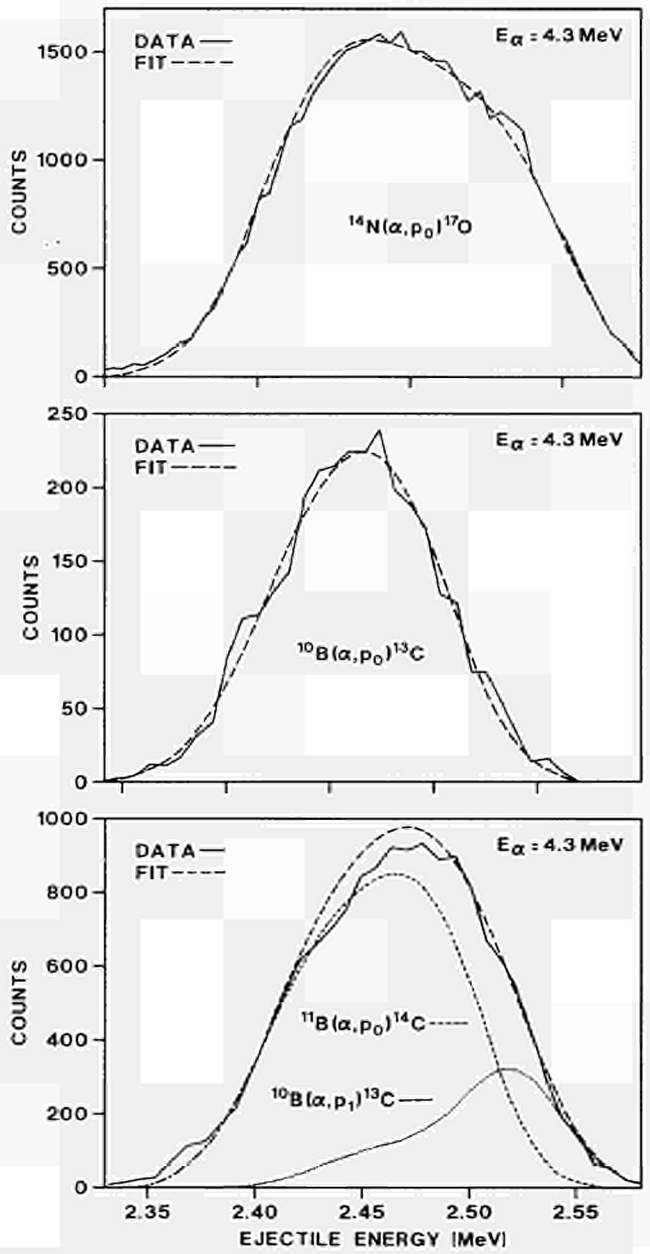

Fig. 36. Simulated (dashed line) and measured (solid line) energy distributions of the proton groups of Fig. 41

energy distribution to the measured one by varying (among other parameters) the elemental concentration. There is a discrepancy of the order of 10 % between the experimental and the calculated results of the stoichiometric composition of the analysed BN-film. The reason for this is under investigation.

Furthermore, the Charged Particle Activation Analysis (CPAA) technique has been installed and tested. Boron and/or carbon in silicon, aluminium and graphite samples were analysed using (d,n) reactions and measuring off-line the decay curve of the residual nuclei (positron emitters). Decomposition of the decay curve

leads, in the absence of interfering reactions, to the elements identification (half lives) and their concentrations (count rates at beam-stop time). Fig. 37 shows the decay curve from a silicon (Si) sample, containing boron (B) and carbon (C), after an irradiation with 2.5 MeV deuterons; it is decomposed by fitting a sum of three exponentials. Silicon, carbon and boron were identified by the half lives of 2.5, 9.96 and 20.3 min, respectively of the residual nuclei produced by the reactions $^{29}Si(d,n)^{30}P$, $^{12}C(d,n)^{13}N$ and $^{10}B(d,n)^{11}C$. Concentrations of about 2 ppm (wt) for ^{12}C and 7 ppm(wt) for ^{10}B were derived. After irradiation and before counting a layer of 9 μm of sample material was removed by chemical etching in order to eliminate surface contamination. Problems associated with the CPAA, such as matrix activation (e.g. silicon activation in this example makes the carbon analysis very difficult) and surface treatment (post-irradiation etching), have to be studied systematically.

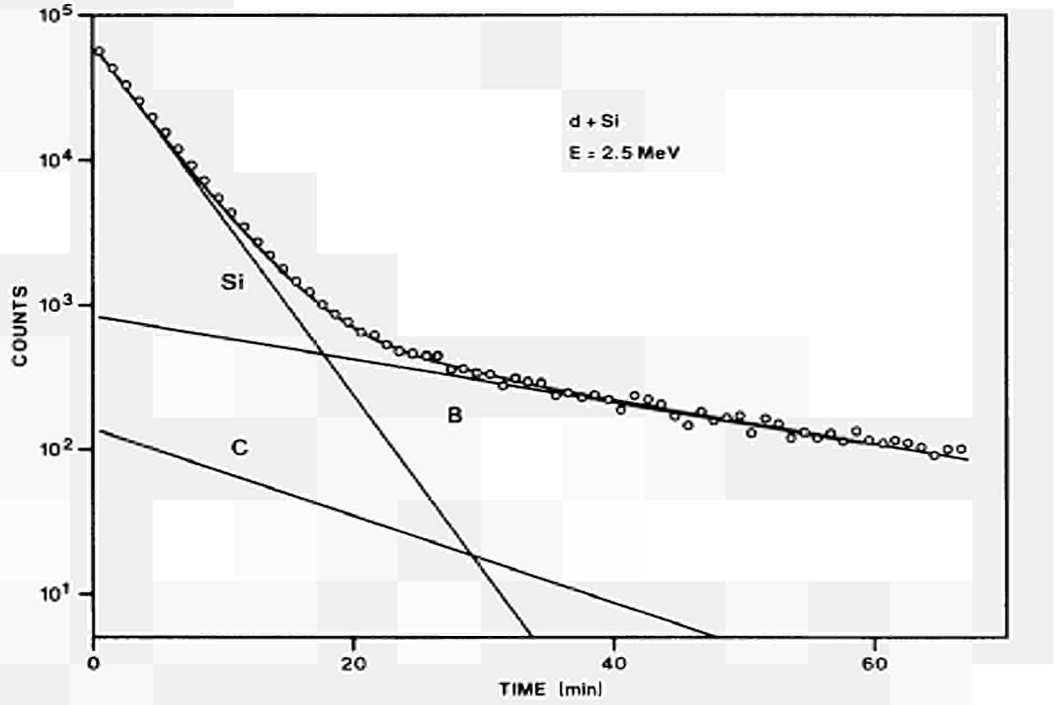

Fig. 37. ***Decay curve from a silicon (Si) sample containing boron (B) and carbon (C) after irradiation with 2.5 MeV deuterons and its decomposition. The circles are measured data, the solid line through them is the fitting function (sum of three exponentials, also shown as solid lines)***

IRMM Computer Network

C. Bernard, C. Cervini, H. Horstmann, C. Van den Broeck*, L. Van Rhee, P. Van Roy

The IBM 4381/P2-16MB CPU has been replaced by an IBM 4381/S91-48MB processor doubling the processing power for most applications. The IBM 3375 disk

* COMPAREX, Brussels

storage system has been replaced by 4 units of type IBM 3380 and all datasets have been moved accordingly.
The network switch MegaPack VME 21 has been installed which among others provides the connection of IRMM to EuropaNET at 64 kbps.
A study of PC networks has been made for TCP/IP as communication protocol and servers which can support DOS, OS/2, UNIX and MAC workstations.
The file service of the XEROX office automation system has been modernized by the installation of a SUN server with 4.6 GB of disk capacity and a more powerful version of the file server software. The presentation of user names in the XEROX system has been harmonized.
The AIX operating system for the RS/6000 computers has been upgraded to version 3.2.3. E and the X Window system to version X11R5 which includes support for 3D graphics, compressed and dynamic fonts, NFS and NIS. A HP Laser Jet 4 printer supporting Postscript outputs is now available on the network.

Multiparametric Event Acquisition with Transputers
C. Bastian, S. de Jonge, J. Gonzalez

The acquisition system as described in the Annual Report 92 was applied to a 6-parameter measurement of ternary fission of ^{235}U.
The transputer network software as well as the corresponding programs on the host (microVAX 4000) were further developed to allow automatic, cyclic acquisition of histogrammed as well as list mode event data. The improved features will be needed for neutron capture cross-section measurements in the near future.
A programmable SCSI Interface was designed to connect our transputer event coders (multiplexers) directly to a standard SCSI bus. It consists of 2 Transputer Modules (TRAM's): a SCSI TRAM for the interface and a Flash-ROM TRAM holding the multiplexer software.

Spectrum Transfer and Analysis with the TGS / AGS File System
C. Bastian

The program package associated with the TGS/AGS formats was further developed in parallel under the UNIX, VMS and DOS operating systems. New developments in AGS include e.g. user-programmable operations, import of evaluated data from ENDF, comparison of evaluated with measured data, graphic display.

Every AGS option is available as an executable command of the operating system hence it may be combined with others to a shell file (.COM in VMS or .BAT in DOS). A shell file for total neutron cross-section data was designed as a test case and successfully applied to measurements on ^{56}Fe and ^{31}P.

The Macintosh Computer Subnetwork

P. ter Meer, F. Gunsing*, O. Haeberlé**

A set of seven Macintosh computers is currently operational at IRMM. They are all connected to the Ethernet , making them fully transparent to each other and providing access facilities to the VAX and RS6000 stations and the IBM-mainframe. Also PC-data files are directly exchangeable and MS DOS and MS Windows programs can be emulated.
Apart from that the computers are used for traditional desktop purposes, data acquisition and data analysis. Two Macs are used for imaging and processing electron beam experiments and one can be used for acquisition and display of single or multi-parameter data. The sorting and analysis of large amounts (gigabytes) of listmode data can be done in combination with an Exabyte storage unit. Data analysis is performed with commercial standard packages as well as with in-house developed computer codes.
Several simulation programs were developed. Modelling of the interaction of the electron beam of GELINA with different kinds of radiators (foil, grating) has been performed. The radiative decay of excited nuclei can be simulated with a modified version of the code "Dicebox".
A backup system has been installed for regular unattended backups of the remote stations over the network.

Downsizing of IBM 4381 Applications to a UNIX Workstation

C. Cervini

The data base IFSPEC for measured spectra from neutron experiments has been ported to a RS/6000-340 workstation and a set of FORTRAN routines has been writen which allows the handling of these spectra. APL2/6000 has been installed for AIX 3.2 and some graphics applications have been downloaded to the RS/6000. A graphical statistical system (AGSS) is also available on the RS/6000. First tests with downloaded neutron data analysis programs have been performed.

---

* EC Fellow from Technical University of Delft, The Netherlands
** EC Fellow from University of Strasbourg, France

Special Electronic Equipment for Laboratory Use

J. Gonzalez, H. Mensch, H. Nerb, W. Stüber

A NIM video distribution unit, a digital ADC multiplexer, a time-of-flight test pulser, an interface for a LeCroy time coder, and a 0.5 ns time coder have been built during the reporting period.

A picoampere current source was improved by using a self-made vacuum capacitor. A unit for absolute calibration of quartz oscillators has been developed (hardware and software) and a corresponding paper has been submitted for publication. The control program of a constant current coulometry systems was adapted to various user requests.

LIST OF PUBLICATIONS

CONTRIBUTION TO CONFERENCES

BASTIAN, C., DE JONGE, S., GONZALEZ, J.
Transputers in acquisition front-ends, performance vs flexibility issues.
Symposium ICS-NET 93, St. Petersbourg, September 13-18, 1993

BEER, H., CORVI, F., ATHANASOPOULOS, K.
The stellar neutron capture rate of the s-process monitor ^{138}Ba.
8th International Symposium on Capture Gamma-Ray Spectroscopy and Related Topics, Fribourg, September, 20-24 1993

COCEVA, C.
M1 transitions from p-wave neutron resonances of ^{53}Cr.
8th International Symposium on Capture Gamma-Ray Spectroscopy and Related Topics, Fribourg, September 20-24, 1993

CORVI, F., GUNSING, F., POSTMA, H., ATHANASOPOULOS, K., MAURI, A.
The spin of the ^{238}U p-wave resonances.
International Workshop on Time Reversal Invariance and Parity Violation in Neutron Reactions, Dubna, May 4-7, 1993

CRAMETZ, A., ROLLIN, G., SCHUBERT, W., TSABARIS, C., WATTECAMPS, E.
Fast neutron cross section measurement techniques at the 7 MV Van de Graaff Laboratory of the IRMM (CBNM).
Int. Workshop on Nuclear Data for Fusion Reactor Technology, San Diego, May 3-6, 1993

DENECKE, B.
Absolute activity measurement with the windowless 4p-CsI(Tl)-sandwich spectrometer.
ICRM '93, Teddington, June 7-11, 1993

GIORGINIS, G., CONTI, N., MISAELIDIS, P.
Characterization of boron-nitride thin films using (alpha,p) nuclear reactions.
3rd European Conference on Accelerators in Applied Research and Technology, Orléans, August 31 - September 4, 1993

HAMBSCH, F.J.
Experimental determination of corrections for fission fragment investigations using a Frisch gridded ionization chamber.
High Resolution Spectroscopy of Fission Fragments, Neutrons and Gamma-Rays, Dresden, February 1-2, 1993

HAMBSCH, F.-J
Modern trends in nuclear fission.
XII Meeting on Physics of Nuclear Fission, Obninsk, September 27-30, 1993

HAMBSCH, F.-J., SIEGLER, P., THEOBALD, J.P., VAN AARLE, J.
Recent fission investigations at IRMM.
2nd International Conference on Dynamical Aspects of Nuclear Fission, Smolenice, June 14-18, 1993

INGELBRECHT, C., PEETERMANS, F., DE CORTE, F.
IRMM reference materials for k_0-activation analysis.
Nuclear Analytical Methods in the Life Sciences, Prague, September 13-17, 1993

INGELBRECHT, C., PEETERMANS, F., PALMERI, S., ROBOUCH, P.
Materials prepared at IRMM for reactor dosimetry applications.
8th ASTM Euratom Symposium on Reactor Dosimetry, Vail, Colorado, August 29 - September 3, 1993

MOUCHEL, D., WORDEL, R.
Investigation of natural and anthropogenic radionuclides in soil and river sediment.
3rd. International Summer School on Low-Level Measurements of Radioactivity in the Environment, Huelva, Spain, September 20 - October 2, 1993

OBERSTEDT, A., HAMBSCH, F.-J.
LISA - a LIstmode and Spectral data Analysis system.
Frühjahrstagung Deutsche Physikalische Gesellschaft, Mainz, March 22-26, 1993

OBERSTEDT, S., WEIGMANN, H., WARTENA, H., BÜRKHOLZ, C., THEOBALD, J.P.
Shape isomerism in light actinide nuclei.
Frühjahrstagung Deutsche Physikalische Gesellschaft, Mainz, March 22-26, 1993

POSTMA, H.
Possibilities to improve the fission fragment experiment with oriented nuclei.
International Workshop on Time Reversal Invariance and Parity Violation in Neutron Reactions, Dubna, May 4-7, 1993

REHER, D.F.G., AALBERS, A.H.L., BJERKE, H., DRUGGE, N., GENKA, T., ROSSITER, M.J., SANTRY, D., SEPHTON, J.P., SIBBENS, G., THIERENS, H., VERHAEGEN, F., WILLIAMS, T.T., WOODS, M.J.
Second EUROMET comparison of air-kerma rate and activity measurements of ^{192}Ir brachytherapy wires.
ICRM '93, Teddington, June 7-11, 1993 - ORA 37532

REHER, D.F.G., DENECKE, B., DE ROOST, E., VAN DER MEER, K.
Standardization of 50 GBq 152,154Eu extended volume source.
ICRM '93, Teddington, June 7-11, 1993

ROHR, G.
Regular spacings of neutron resonances indicate vibration-quanta of a multiple oscillator.
8th International Symposium on Capture Gamma-Ray Spectroscopy and Related Topics, Fribourg, September 20-24, 1993

SHARAPOV, E., CORVI, F., WEIGMANN, H.
IREN and GELINA, complementary sources.
Intern. Workshop on Time Reversal Invariance and Parity Violation in Neutron Reactions, Dubna, May 4-7, 1993

SIEGLER, P., HAMBSCH, F.-J., THEOBALD, J.P.
Fission modes investigations in 237Np(n,f).
Frühjahrstagung Deutsche Physikalische Geseelschaft, Mainz, March 22-26, 1993

STEINBAUER, E., BORTELS, G., BAUER, P., BIERSACK, J.P., BURGER, P., AHMAD, I.
A survey of the physical processes which determine the response function of silicon detectors to alpha particles.
ICRM '93 , Teddington, June 7-11, 1993

URITANI, A., GENKA, T., MORI, C., REHER, D.F.G.
Analytical calculations on radioactivity measurements of ^{192}Ir metallic sources with a calibrated ionization chamber.
ICRM '93, Teddington, June 7 - 11, 1993

WAGEMANS, C., DEMATTE, L., D'HONDT, P., POMMÉ, S., SCHILLEBEECKX, P., DERUYTTER, A.
New results on fission fragment energy and mass characteristics in spontaneous and thermal neutron induced fission.
2nd Int. Conf. on Dynamical Aspects of Nuclear Fission, Smolenice, June 14-18, 1993

WAGEMANS, C., SCHILLEBEECKX, P., WEIGMANN, H., DRUYTS, S.
Study of the ^{41}Ca(n,gamma alpha) reaction.
8th International Symposium on Capture-Gamma-Ray Spectroscopy and Related Topics, Fribourg, September 20-24, 1993

WEIGMANN, H.
Experimental work at the Geel Linac.
International Workshop on Nuclear Data for Fusion Reactor Technology, San Diego, May 3-6, 1993

WORDEL, R., MOUCHEL, D., BONNE, A., MEYNENDONCKX, P., VANMARCKE, H.
Low level gamma-ray measurements in a 225 m deep underground laboratory.
3rd. International Summer School on Low-Level Measurements of Radioactivity in the Environment, Huelva, September 20 - October 2, 1993

WORDEL, R., MOUCHEL, D., SOLÉ, V.A., HOOGEWERFF, J., HERTOGEN, J.
Investigation of the natural radioactivity in volcanic rock samples using a low background gamma-ray spectrometer.
ICRM '93, Teddington, June 7-11, 1993

SCIENTIFIC OR TECHNICAL ARTICLES

BASTIAN, C.
General procedures and computational methods for generating covariance matrices.
In: Nuclear Data Evaluation Methodology, Charles L. Dunford (ed.), World Scientific Singapore, 1993, p. 642

COCEVA, C.
Radiative transitions from neutron capture in ^{53}Cr resonances.
Nuovo Cim. (to be published)

DRUYTS, S., WAGEMANS, C., GELTENBORT, P.
Determination of the ^{35}Cl(n,p)^{35}S reaction cross section and its astrophysical implications.
Nucl. Phys. A (to be published)

DRUYTS, S., WAGEMANS, C., POMMÉ, S., GELTENBORT, P., TRAUTVETTER, H.P.
Measurement of the ^{14}N(nth,p)^{14}C reaction cross-section.
In: Nuclear Astrophysics, IOP Publishing Ltd., 1993, p. 243

GARCIA-TORAÑO, E., ACEÑA, M.L., BORTELS, G., MOUCHEL, D.
Alpha-particle emission probabilities in the decay of ^{239}Pu.
Nucl. Instrum. Methods, Phys. Res., A334(1993)477

GUNSING, F., TER MEER, P., CERVINI, C.
A multiparameter data sorting application for large data amounts.
Software and abstract on CD-ROM (to be published)

HAEBERLÉ, O., RULLHUSEN, P., SALOMÉ, J.M., MAENE, N.
Calculations of Smith-Purcell radiation generated by electrons of 1-100 MeV.
Phys. Rev. E (to be published)

HAMBSCH, F.-J., KNITTER, H.-H., BUDTZ-JÖRGENSEN, C.
The positive odd-even effects observed in cold fragmentation - are they real?
Nucl. Phys., A554(1993)209

INGELBRECHT, C., LIEVENS, F., PAUWELS, J.
Certification of a copper metal reference material for neutron dosimetry.
EUR 14645 EN (1993)

INGELBRECHT, C., LIEVENS, F., PAUWELS, J.
Certification of an iron metal reference material for neutron dosimetry
EUR 14646 EN (1993)

MARTIN, P.W., SURONO, D., HAMBSCH, F.-J., POSTMA, H., RIETVELD, P.
TDPAD measurements with highly oriented pyrolytic graphite using the $^{19}F(p,p')^{19}F^*$ and $^{19}F(alpha,n)^{22}Na^*$ reactions.
Hyperfine Interactions, 77(1993)315

OBERSTEDT, A., HAMBSCH, F.-J.
LISA - A powerful program package for LIstmode and Spectral data Analysis.
Nucl. Instrum. Methods, Phys. Res. A (to be published)

OBERSTEDT, S., THEOBALD, J.P., WEIGMANN, H., WARTENA, J.A. BÜRKHOLZ, C.
Intermediate structure and the shape isomer in ^{233}Th.
Nucl. Phys. A (to be published)

SIEGLER, P., HAMBSCH, F.-J., THEOBALD, J.P.
Messung der Massen-, Energie- und Winkelverteilung der Spaltfragmente bei der Reaktion 237Np(n,f) als Funktion der Neutroneneinschussenergie.
In: 11. Jahresbericht '91-'92 der Technische Hochschule Darmstadt, 1993

SOLÉ, A.V., DENECKE, B., GROSSE, G., BAMBYNEK, W.
Measurement of the K-shell fluorescence yield of Ca and K with a windowless Si(Li) detector.
Nucl. Instrum. Methods, Phys. Res., A329(1993)418

SOLÉ, A.V., DENECKE, B., MOUCHEL, D., BAMBYNEK, W.
Measurement of $P_k\omega_k$ in the decay of ^{56}Zn and the K-shell fluorescence yield of copper.
Appl. Radiat. Isot., Int. J. Radiat. Appl. Instrum. A (to be published)

STEINBAUER, E., BAUER, P., GERETSCHLÄGER, M., BORTELS, G., BIERSACK, J.P., BURGER, P.
Energy resolution of silicon detectors: approaching the physical limit.
Nucl. Instrum. Methods, Phys. Res. (to be published)

STÜBER, W.
Eine einfache Eichanordnung für Oszillatoren.
Elektronik (to be published)

WAGEMANS, C., VAN UFFELEN, P., DERUYTTER, A., BARTHÉLÉMY, R., VAN GILS, J.
Normalization of the ^{239}Pu fission cross-section.
Nucl. Sci. Eng., 115(1993)173

SPECIAL PUBLICATIONS

HANSEN, H.H. (ed.)
Annual Report 92.; EUR 15029 EN (1993)

HANSEN, H.H. (ed.)
Annual Progress Report on Nuclear Data 1992.
NEA/NSC/DOC(93)11; INDC (EUR) 027/G; EUR 15155 EN (1993)

GLOSSARY

AERE	Atomic Energy Research Establishment, Harwell (UK)
ANL	Argonne National Laboratory, Argonne (USA)
BIPM	Bureau International des Poids et Mesures, Sèvres (F)
CBNM	Central Bureau for Nuclear Measurements (now IRMM)
CEA	Commissariat à l'Energie Atomique, Paris (F)
CEC	Commission of the European Communities
CERN	Centre Européen pour la Recherche Nucléaire
CIEMAT	Centro de Investigación Energética, Medio Ambiental y Tecnología
CCD	Charge Coupled Device
CRNS	Centre National de la Recherche Scientifique
CRP	Coordinated Research Programme
DFN	Deutsches Forschungsnetz
DG	Direction Générale
DPhN/ STAS	Département de Physique Nucléaire / Services des Techniques d'Accélération Supraconductrice, Saclay (F)
EFF	European Fusion File
ENDF	Evaluated Nuclear Data File
ENEA	Comitato Nazionale: Energia Nucleare e Energia Alternative
ETL	Electrotechnical Laboratory, Ibaraki (Japan)
EWGRD	European Working Group on Reactor Dosimetry
FWHM	Full Width at Half Maximum
GELINA	Geel Electron Linear Accelerator
HPGe	High Purity Germanium
IAEA	International Atomic Energy Agency, Vienna (A)
ICRM	International Committee for Radionuclide Metrology
ILL	Institut Laue-Langevin, Grenoble (F)
INAA	Instrumental Neutron Activation Analysis
INDC	International Nuclear Data Committee
IPN	Institut de Physique Nucléaire, Lyon (F)
IRK	Institut für Radiumforschung und Kernphysik, Wien (A)
IRMM	Institute for Reference Materials and Measurements, Geel (B)
JAERI	Japan Atomic Energy Research Institute, Tokai-Mura (Japan)
JEF	Joint European File
JENDL	Japanese Evaluated Data Library
JRC	Joint Research Centre
KFA	Kernforschungsanlage, Jülich (D)
KFK	Kernforschungszentrum Karlsruhe, Karlsruhe (D)

K U	Katholieke Universiteit, Leuven (B)
L P R I	Laboratoire Primaire des Rayonnements Ionisants (F)
N E A	Nuclear Energy Agency, Paris (F)
N E A N D C	Nuclear Energy Agency's Nuclear Data Committee
N I R H	National Institute of Radiation Hygene, Osteras (N)
N I R P	National Institute of Radioprotection (S)
N I S T	National Institute of Standards and Technology, Gaithersburg (USA)
N P L	National Physical Laboratory, Teddington (UK)
N R A	Nuclear Reaction Analysis
N R C	National Research Council, Ottawa (CAN)
N R P A	Norwegian Radiation Protection Authority (N)
O T R	Optical Transition Radiation
P T B	Physikalisch-Technische Bundesanstalt, Braunschweig (D)
R P L	Radiation Physics Laboratory
R U G	Rijksuniversiteit Gent, Gent (B)
S C K/ C E N	Studiecentrum voor Kernenergie/ Centre d'Etudes Nucléaires, Mol (B)
S I R	Système International de Référence
S S I - N I R P	Statens Strålskyddinstitut - National Institute for Radiation Protection, Göteborg (S)
T H	Technische Hochschule
T O F	Time of Flight
T R	Transition Radiation
U H V	Ultra High Vacuum
V T T	Technical Research Centre of Finland
W R E N D A	World Request List for Neutron Data Measurements

CINDA ENTRIES LIST

ELEMENT		QUANTITY	TYPE	ENERGY		DOCUMENTATION		LAB	COMMENTS
S	A			MIN	MAX	REF VOL PAGE	DATE		
U	235	NF	EXP	30 + 4	20 + 5	INDC(EUR)028-03	94	GEL	HAMBSCH RATIO TO H(N,N)
Cf	252	SF	EXP			INDC(EUR)028-06	94	GEL	HAMBSCH ENERGY CALIBR.
B	10	NT	EXP	80 + 0	10 + 4	INDC(EUR)028-08	94	GEL	BRUSEGAN TRANSMISSION
Np	237	NF	EXP	30 + 4	55 + 5	INDC(EUR)028-11	94	GEL	SIEGLER FISS. FR. ENERGY
Pu	242	SF	EXP			INDC(EUR)028-15	94	GEL	WAGEMANS FISS. FR. M,E DISTR.
Pu	244	SF	EXP			INDC(EUR)028-15	94	GEL	WAGEMANS FISS. FR. M,E DISTR.
U	235	NF	EXP	20-3	10 + 2	INDC(EUR)028-17	94	GEL	WAGEMANS TERNARY FISSION
Fe	0	NT	EXP	20 + 4	20 + 6	INDC(EUR)028-18	94	GEL	BERTHOLD WEIGMANN HIGH RESOL.
Ni	58	NT	EXP	14 + 0	30 + 6	INDC(EUR)028-20	94	GEL	ROHR SHELLEY HIGH RESOL.
Ni	60	NT	EXP	14 + 0	30 + 6	INDC(EUR)028-20	94	GEL	ROHR SHELLEY HIGH RESOL.
Ni	58	NG	EXP	32 + 1	10 + 4	INDC(EUR)028-21	94	GEL	BRUSEGAN GAMMA RAY SP.
C	12	NT	EXP	15 + 5	18 + 6	INDC(EUR)028-24	94	GEL	CRAMETZ WAGEMANS
Th	232	NT	EXP	15 + 5	18 + 6	INDC(EUR)028-24	94	GEL	CRAMETZ WAGEMANS
B	10	NT	EXP	15 + 5	18 + 6	INDC(EUR)028-24	94	GEL	CRAMETZ WAGEMANS
Al	27	NT	EXP	17 + 4	25 + 6	INDC(EUR)028-24	94	GEL	SHELLEY ROHR HIGH RESOL.
V	0	NT	EXP	17 + 4	25 + 6	INDC(EUR)028-26	94	GEL	SHELLEY ROHR PRELIM.
Ni	58	NX	EXP	65 + 5	16 + 6	INDC(EUR)028-26	94	GEL	WATTECAMPS Ni58/Al27
Cu	63	NX	EXP	80 + 5	80 + 5	INDC(EUR)028-28	94	GEL	TSABARIS Cu63/Ni58 PRELIM
U	238	NG	EXP	10 + 0	60 + 4	INDC(EUR)028-29	94	GEL	CORVI SPIN ASSIGNMENT
Ba	138	NT	EXP	80 + 0	20 + 4	INDC(EUR)028-32	94	GEL	BRUSEGAN RES. PAR. ANAL.
Ba	138	NG	EXP	50 + 2	10 + 4	INDC(EUR)028-33	94	GEL	BEER CORVI NUCLEOSYNTH.
Pd	110	NNG	EXP	20 + 4	33 + 5	INDC(EUR)028-35	94	GEL	WATTECAMPS MEISTER
Cl	35	NP	EXP	10 + 1	10 + 4	INDC(EUR)028-38	94	GEL	WAGEMANS NUCLEOSYNTH.
Cl	36	NP	EXP	10 + 1	10 + 4	INDC(EUR)028-38	94	GEL	WAGEMANS NUCLEOSYNTH.
Cl	36	NA	EXP	10 + 1	10 + 4	INDC(EUR)028-38	94	GEL	WAGEMANS NUCLEOSYNTH.
Ca	41	NX	EXP	10 + 2	10 + 5	INDC(EUR)028-40	94	GEL	WAGEMANS RESONANCES

European Communities - Commission

EUR 15822 EN - ANNUAL PROGRESS REPORT ON
NUCLEAR DATA 1993

Institute for Reference Materials and Measurements

H.H. Hansen (ed.)

Luxembourg: Office for Official Publications of the European Communities

1994 - pag. 66 - 21.0 x 29.7 cm

EN

ISBN 92-826-8432-6

NOTICE TO THE READER

All scientific and technical reports published by the European Commission are announced in the monthly periodical '**euro abstracts**'. For subscription (1 year: ECU 60) please write to the address below.

ISBN 92-826-8432-6

OFFICE FOR OFFICIAL PUBLICATIONS
OF THE EUROPEAN COMMUNITIES

L-2985 Luxembourg